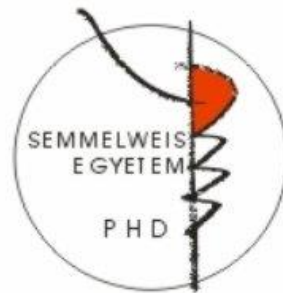


# Molecular regulation of thyroid hormone activation

Ph.D. Thesis

**Péter Egri**

Semmelweis University  
János Szentágotthai Ph.D. School of Neuroscience



Tutor: Dr. Balázs Gereben, D.Sc.

Opponents: Dr. Endre Nagy, D.Sc.  
Dr. Árpád Dobolyi, D.Sc.

Chairman of committee: Dr. Miklós Tóth, D.Sc.  
Members of committee: Dr. Krisztina Kovács, D.Sc.  
Dr. Andrea Tamás, Ph.D.

Budapest  
2016

# 1. TABLE OF CONTENTS

<b>1. TABLE OF CONTENTS .....</b>	<b>2</b>
<b>2. LIST OF ABBREVIATIONS.....</b>	<b>3</b>
<b>3. INTRODUCTION .....</b>	<b>5</b>
3.1. Significance and action of thyroid hormones .....	5
3.2. Deiodinase enzyme family.....	16
3.3. The ubiquitin-proteasome system .....	28
<b>4. SPECIFIC AIMS .....</b>	<b>35</b>
<b>5. MATERIALS AND METHODS.....</b>	<b>36</b>
5.1. DNA constructs and RT-PCR.....	36
5.2. Cell culture and transfection .....	39
5.3. Reagents and treatments .....	40
5.4. Luciferase promoter assay .....	41
5.5. Quantitative PCR .....	41
5.6. Western blot.....	42
5.7. Deiodinase assay.....	42
5.8. Secreted alkaline phosphatase (SEAP) assay .....	43
5.9. Fluorescent resonance energy transfer (FRET) .....	44
5.10. Animals and surgery .....	45
5.11. Thyroid hormone measurement .....	46
5.12. TSH bioactivity measurement.....	46
5.13. Immunohistochemistry .....	46
5.14. Statistical analysis.....	47
<b>6. RESULTS.....</b>	<b>48</b>
6.1. Interaction between PACAP and thyroid hormone signaling.....	48
6.2. Characterization of MARCH6 as D2 ubiquitin ligase .....	56
6.3. Structural background of the ubiquitination of deiodinases .....	66
<b>7. DISCUSSION .....</b>	<b>73</b>
7.1. Interaction between PACAP and thyroid hormone signaling.....	73
7.2. Characterization of MARCH6 as D2 ubiquitin ligase .....	77
7.3. Structural background of the ubiquitination of deiodinases .....	84
<b>8. CONCLUSIONS .....</b>	<b>90</b>
<b>9. SUMMARY.....</b>	<b>92</b>
<b>10. ÖSSZEFOGLALÁS.....</b>	<b>93</b>
<b>11. REFERENCES .....</b>	<b>94</b>
<b>12. PUBLICATION LIST .....</b>	<b>118</b>
12.1. List of publications the thesis is based on.....	118
12.2. Other publications .....	118
<b>13. ACKNOWLEDGMENTS .....</b>	<b>120</b>

## 2. LIST OF ABBREVIATIONS

In accordance with HUGO Gene Nomenclature Committee and Mouse Genome Database guidelines, proteins are written in upper case, human gene symbols and transcripts are indicated upper case and italicized while rodent gene symbols and transcripts are indicated first-letter upper case and italicized.

(a)CSF	(artificial) cerebrospinal fluid
BAT	brown adipose tissue
CDS	coding DNA sequence
CRE	cAMP response element
CREB	cAMP response element-binding protein
D1	type 1 iodothyronine deiodinase protein
D2	type 2 iodothyronine deiodinase protein
D3	type 3 iodothyronine deiodinase protein
<i>DIO1/Dio1</i>	gene or mRNA of human/rodent type 1 iodothyronine deiodinase
<i>DIO2/Dio2</i>	gene or mRNA of human/rodent type 2 iodothyronine deiodinase
<i>DIO3/Dio3</i>	gene or mRNA of human/rodent type 3 iodothyronine deiodinase
E1	ubiquitin activating enzyme
E2	ubiquitin conjugating enzyme
E3	ubiquitin ligase enzyme
ECFP	enhanced cyan fluorescent protein
EERI	Eeyarestatin I
ERAD	endoplasmic-reticulum-associated degradation
EYFP	enhanced yellow fluorescent protein
FRET	fluorescence (Förster) resonance energy transfer
HPT axis	hypothalamo-pituitary-thyroid axis
$K_M$	Michaelis-Menten constant
LPS	lipopolysaccharide
MARCH6	Membrane-Associated Ring Finger (C3HC4) 6

mCherry	monomeric modified red fluorescent protein
MG132	proteasome inhibitor (carbobenzoxy-L-leucyl-L-leucyl-L-leucinal)
NF- $\kappa$ B	nuclear factor $\kappa$ -light-chain-enhancer of activated B cells
p65	subunit of the NF- $\kappa$ B transcription factor
PACAP	pituitary adenylate cyclase-activating polypeptide
PKA	protein kinase A
PVN	paraventricular nucleus
Sec	selenocysteine
SHH	Sonic hedgehog
SP1	specificity protein 1
T <sub>3</sub>	3,3',5-triiodo-L-thyronine
rT <sub>3</sub>	3,3',5'-triiodo-L-thyronine
T <sub>4</sub>	thyroxine, 3,3',5,5'-tetraiodo-L-thyronine
TH	thyroid hormone
TR	thyroid hormone nuclear receptor
TRE	thyroid hormone response element
TSS	transcriptional start site
Ub	ubiquitin
UPS	ubiquitin-proteasome system
UTR	untranslated region
WSB1	WD40 SOCS-box containing protein

## 3. INTRODUCTION

### 3.1. SIGNIFICANCE AND ACTION OF THYROID HORMONES

#### 3.1.1. General aspects of thyroid hormone action in the brain

Thyroid hormones (THs) play essential role in the regulation of a wide range of biological phenomena and fundamentally affect the metabolic and developmental processes. THs exert a major impact on brain development and function, discussed in section [3.1.3](#) in more detail [1]. Furthermore, the level of TH in specific brain regions has far-reaching consequences on various peripheral organ systems [2]. Thus, understanding cellular and molecular mechanisms regulating TH levels in the brain is a great importance both for brain-related and peripheral processes.

Specific features of multiple regulatory levels need to be taken into account when the complex framework of TH economy is discussed. First, the primary product of human thyroid gland is the stable prohormone thyroxine ( $T_4$ ) that cannot be efficiently bound by the thyroid hormone nuclear receptors (TRs) on the canonical ligand-binding pocket [3]. Therefore  $T_4$  is not able to modulate gene expression via the canonical, TR-mediated pathway of TH action [4]. The regulatory capacity of hypothalamo-pituitary-thyroid (HPT) axis is restricted predominantly to the synthesis and release of the  $T_4$  prohormone. Second, mostly  $T_4$  can be transported via the blood-brain and CSF-brain barrier while the transcriptionally active, circulating serum  $T_3$  has poor access to most of the areas of the central nervous system due to the selective affinity of TH transporters (**Fig. 1**) [5]. Taken together, the HPT axis has obvious limitations and is insufficient to control TH action in the brain. Third, and as a consequence, TH action in the brain requires the local conversion of  $T_4$  to  $T_3$  that is critical in the TH-dependent modulation of gene expression. The metabolism of THs is catalyzed by members of the deiodinase enzyme family allowing both the activation and inactivation of THs. Exclusively the type 2 deiodinase (D2) is expressed as activating deiodinase in the human brain and D2 is the main source of the  $T_3$  in the central nervous system [6, 7].

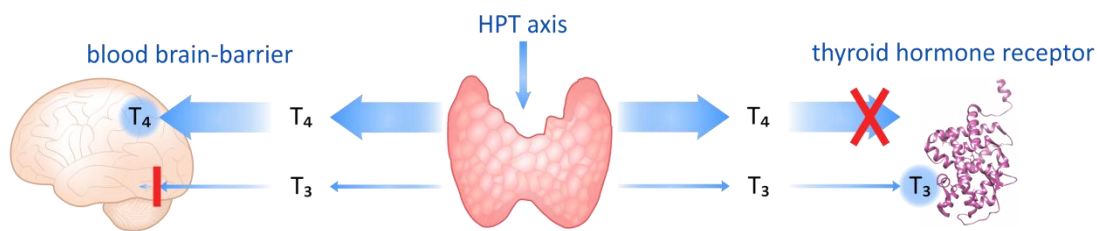


**Figure 1. Limitations of the HPT axis in the regulation of local thyroid hormone action**

The thyroid hormone receptor binds T<sub>3</sub> with high affinity but thyroid hormone transporters of the blood-brain barrier have low permeability for T<sub>3</sub> that makes local activation essential for thyroid hormone action in the brain.

Importantly, TH metabolism in the brain is highly compartmentalized. While D2 is expressed exclusively in glial cells – in astrocytes and hypothalamic tanycytes – the neurons are not able to activate THs, the glial-derived T<sub>3</sub> affects the neuronal transcriptome on a paracrine manner. However, neurons are able to modulate their intracellular TH level via type 3 deiodinase (D3) catalyzed inactivation [8]. Therefore the control of TH mediated gene expression in the brain requires the coordinated actions of TH transport and deiodinase-mediated TH metabolism (**Fig. 2**). These processes are especially significant in the regulation of the HPT axis as they result not only in local but also systemic changes in TH economy via the control of negative feedback of TRH neurons, see in section 3.1.4.

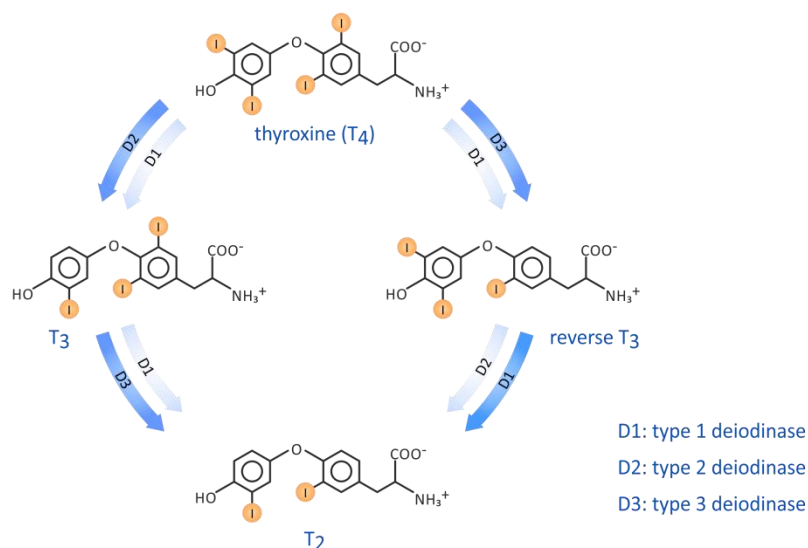


**Figure 2. Thyroid hormone metabolism**

Activation and inactivation pathways are catalyzed by the members of deiodinase enzyme family via removal of iodine from the outer or inner ring of thyroid hormone derivatives, respectively.

In conclusion, the interaction between deiodinase-mediated TH activation in the brain and the HPT axis represents a core mechanism of controlling TH economy through the body. Thus, we focused our studies to better understand the molecular regulation of TH activation and its impact on the HPT axis. The following sections provide a brief overview on different regulatory levels of TH action including the mechanism of TH transport and TRs followed by the introduction of the role THs in the central nervous system (CNS) and the periphery. The second part will focus on the deiodinase-mediated metabolism of THs – especially the activation by D2 – and the regulation of the D2 enzyme.

### 3.1.2. Mechanism of thyroid hormone action: transporters and receptors

TRs – exerting the canonical TH effect – selectively bind  $T_3$  as ligand therefore the precise control of intracellular availability of  $T_3$  directly affects the exerted effects of TH. This regulation requires the contribution of thyroid hormone transporters (both at the blood- brain barrier and at paracrine transport between glial and neuronal cells) and thyroid hormone metabolizing enzymes, deiodinases. The coordinated action of transporters and deiodinases also provides the opportunity of fine-tuning of  $T_3$  availability at the cellular level and determining the liganded state of TRs (**Fig. 3**) [9].

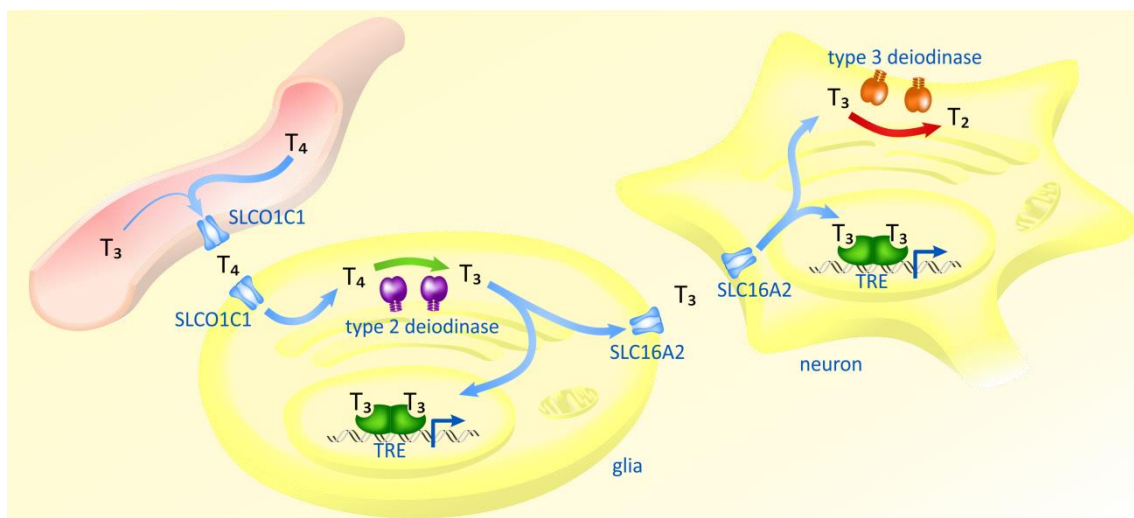


**Figure 3. Thyroid hormone metabolism in the brain**

Schematic depiction of the thyroid hormone availability in the brain based on the neuro-glial compartmentalization of thyroid hormone transport and metabolism.

According to the old dogma, THs as lipophilic molecules were thought to undergo passive membrane transport upon their passage through the plasmamembrane into the cytosol without the involvement of active transport. However, this idea was disproved by the identification of different types of thyroid hormone transporters that allowed the specific transport of TH through the plasmamembrane [10, 11]. The importance of active TH transport is clearly demonstrated in the Allan-Herndon-Dudley syndrome (AHDS) leads to a mixed thyroid phenotype with mental retardation, central hypotonia and impaired auditory development [12]. AHDS is caused by mutations in thyroid hormone transporter SLC16A2 (MCT8) belongs to the monocarboxylate transporter (MCT) family along with SLC16A10 (MCT10). SLC16A2 is capable to transport both T<sub>4</sub> and T<sub>3</sub> while SLC16A10 has selective binding for T<sub>3</sub> [5]. SLC16A2 is widely expressed in the CNS including neurons, glial cells and capillaries [13].

The second class of thyroid hormone transporters is the large family of organic anion-transporting polypeptides (OATPs). The selectivity of SLCO1C1 for T<sub>4</sub> over T<sub>3</sub> and its enriched expression in endothelial cells of capillaries could underline the unequal permeability of the blood-brain barrier for TH derivatives [13]. Additionally, while the SLCO1C1 knock-out mouse has a mild phenotype [14], its combined deletion with SLC16A2 resembles the developmental abnormalities of AHDS in human [15]. L-amino acid transporter (LAT) family is also capable for TH transport SLC7A2 (LAT1) and SLC7A8 (LAT2) are identified as TH transporters however their *in vivo* importance in TH transport are much less characterized compared to the above mentioned transporters [5].

The canonical and most studied pathway of TH action is mediated by transcriptional events via the TRs [4]. In contrast to other nuclear receptors, e.g. the estrogen receptor and glucocorticoid receptor, TRs are located predominantly in the nucleus even in unliganded form. The general TR structure contains the following domains in order from N-terminus to C-terminus: N-terminal activator (A/B), DNA-binding (C), hinge region (D), ligand-binding and dimerization (E), C-terminal activator (F) (**Fig. 4**) [16]. Two TR encoding genes were identified (*THRA* and *THRB*) each of these has three transcript variants [17]. TR $\alpha$ 1, TR $\alpha$ 2 and TR $\alpha$ 3 are transcribed from *THRA* gene however only TR $\alpha$ 1 has classical receptor functions while TR $\alpha$ 2 and TR $\alpha$ 3 lack the T<sub>3</sub>-binding ability due its alternatively spliced C-terminus and abolished T<sub>3</sub>-

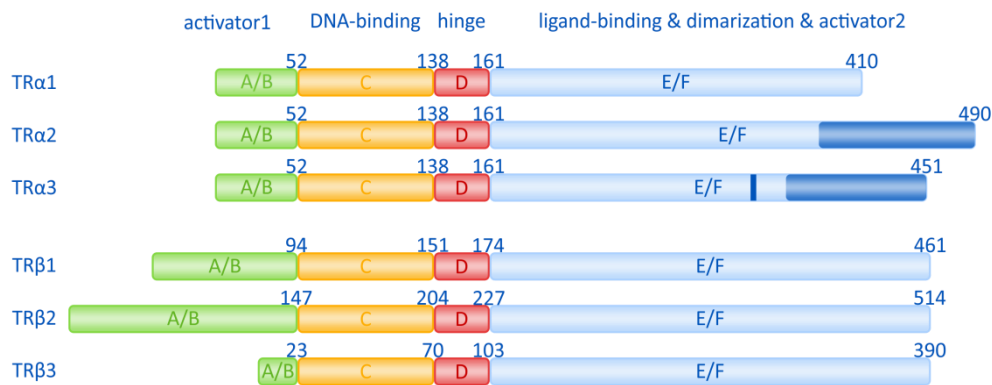


**Figure 4. Schematic structure of thyroid hormone nuclear receptors**  
 Amino acid position refers for human orthologues; note the alternative splicing of the C-terminus of TR $\alpha$ 2 and TR $\alpha$ 3 results in abolished ligand binding.

binding pocket [17, 18]. Additionally, a downstream alternative transcriptional start site within *THRA* gene results in a truncated transcripts similarly to TR $\alpha$ 2 lacking the T<sub>3</sub>-binding capacity. TRs bind one T<sub>3</sub> molecule prior to activation. While a recent study indicated an additional ligand-binding surface within TR $\alpha$ 1 that shows selectivity for T<sub>4</sub> however the importance of this site is remained to be confirmed [19]. The *THRB* gene has three transcript variants: TR $\beta$ 1, TR $\beta$ 2 and TR $\beta$ 3. Based on crystal structure data a second ligand binding surface could be formed by TR $\beta$  at least for the TR $\beta$ -specific T<sub>3</sub>-analogue GC-24 [20]. Beside the canonical genomic effects of TRs TR $\beta$  was demonstrated to modulate the phosphatidylinositol-3-kinase (PI3K) pathway and affect HIF-1 $\alpha$  level via non-translational manner. The importance of this pathway is poorly understood yet.

The model of TH action suggests that TR-mediated regulation of gene expression is based on the altered interaction profile for cofactors upon T<sub>3</sub>-binding. This current model is based on the activation of well conserved positive thyroid hormone response elements (TREs) in the genome while the negative action of TH's is much less understood. The prediction of the TR binding sites for negative regulation is not conclusive. In the absence of T<sub>3</sub>, TRs bind to TRE and recruit histone deacetylases e.g. nuclear receptor corepressor (NCoR1) and silencing mediator of retinoic acid and thyroid hormone receptors (SMRT, NCoR2) [21]. The binding of T<sub>3</sub> alters the equilibrium between the monomeric-dimeric states and allows the heterodimerization with retinoid X-receptor (RXR). This transition leads to the release of repressor complex and harboring activator proteins including histone acetyltransferases (steroid receptor coactivator-1 and 2, SRC1, SRC2 or NCoA1/2) and p300 (**Fig. 5**) [22]. In case of a negative TRE the T<sub>3</sub>

induced binding of TR represses promoter activity however the precise mechanism of action of THs on negative TRE is poorly characterized.

TR $\alpha$  is expressed in most tissues including the brain, cardiac and skeletal muscle, intestine and bone. TR $\beta$ 1 has also wide expression profile e.g. in the brain and liver while TR $\beta$ 2 is the predominant isoform in the hypothalamus and pituitary, consequently plays a crucial in the TH-feedback of HPT axis [23]. The differential expression has also clinical significance providing the opportunity of tissue-specific targeting of TH action using TR $\alpha$ - or TR $\beta$ -selective agonists or antagonists. Mutations in TR proteins can lead to the manifestation of the Resistance to thyroid hormone (RTH) syndrome hallmarked by altered TH-binding capacity causing symptoms of hyperactivity, emotional alterations and mental deficit on different levels of severity. Most known cases involve mutation(s) in TR $\beta$  [24] but recently TR $\alpha$  mutant patients have been also revealed [25-27].

Extranuclear, non-canonical TRs have been also discovered. Mitochondrial processes are major target of TH action and the p43 protein was identified as a mitochondrial TR [28, 29]. Under specific conditions the kinetics and the cell permeability independent nature of TH action suggested the existence of thyroid hormone membrane receptors that could govern genome-independent action. Integrin  $\alpha$ v $\beta$ 3 was identified as a cell membrane located receptor showing specific binding for T<sub>4</sub> [30]. This cascade activates the MAPK signaling that results in phosphorylation of TR $\beta$  and increasing its transcriptional activity [31].

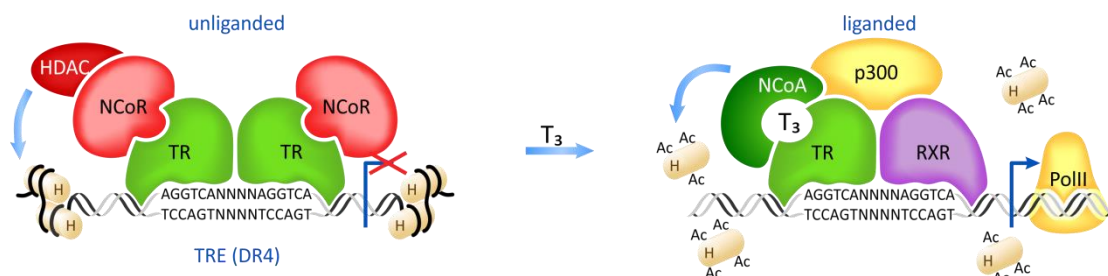


**Figure 5. Schematic model of the activation of thyroid hormone receptors by ligand binding**  
 TR: thyroid hormone receptor; TRE: thyroid hormone response element (DR4 type); HDAC: histone deacetylase; NCoR: nuclear corepressor; NCoA: nuclear coactivator; H: histone; Ac: acetyl group.

### **3.1.3. The biological significance of thyroid hormones**

#### *3.1.3.1. Brain*

THs are crucial regulators of developmental programs and their role in neural development is clearly demonstrated by symptoms caused by various defects of different events of TH action. Congenital hypothyroidism requires on-time TH supplementation to avoid irreversible developmental brain deficits. Promoting the exit from cell cycle and affecting differentiation programs THs are major regulators of progenitor cell development. Altered TH synthesis, metabolism or transport result in dramatic effects on neuronal differentiation and maturation manifested in significant loss in cognitive functions [1, 32]. Numerous genes with specific roles played in brain development are regulated by THs. Expression of crucial factors that organize the migration and survive of precursor cells like reelin, brain-derived neurotropic factor (BDNF) and nerve growth factor (NGF) are under the regulation of THs [33-35]. Oligodendrocyte differentiation, myelination and axonal growth are proved to be sensitive to TH status via the involvement of crucial genes like myelin basic protein (MBP) and myelin-associated glycoprotein (MAG) that are transcriptionally upregulated by THs [36, 37]. Expression of synaptotagmin – a protein involved in the docking and fusion of synaptic vesicles – is also affected by THs [38] suggesting a general mechanism how THs are able to influence neural communication.

Cerebellar development, foliation, maturation and migration of cerebellar neurons are strongly affected by THs via TR $\alpha$  [39, 40]. Dendritic arborization of Purkinje cells is also controlled by THs [39]. Delayed maturation and abnormal migration of granular cells was observed while the maturation of Bergmann glia and GABAergic interneurons were also affected in TR $\alpha$  dominant negative mutant mice [41]. These developmental processes reflect to the mechanistic background of impacted motoric phenotype in hypothyroidism observed both in human and animal models with deficiencies on different levels of TH signaling [40]. Normal cerebellar development requires the rapid supplementation of TH in congenital hypothyroidism.

Decreased mental capacity by hypothyroidism is associated with impaired learning and memory as broad range of hippocampal functions are controlled by THs. Synaptic remodeling, excitability, associative learning and inhibitory inputs for hippocampal cells

are also affected by THs [42]. Timing of the developmental phases of new-born neurons is controlled by coordinated TR expression [43]. Affected mood and behavior in patients with altered TH state is underlined by the connection between THs and the molecular elements of serotonergic system [44]. THs are in tight interaction with other neurosecretory systems both in the hypothalamus and the pituitary. Reproductive functions are targeted by local TH metabolism in the hypothalamus by the regulation of seasonal activity [45, 46] and lactation [47, 48]. TH levels also affect stress response and anxiety, CRH expression is stimulated by THs [49-51].

Proper TH signaling is also essential in the sensory system. THs are crucial in the development of auditory system as found in congenital hypothyroidism or in Allan-Herndon-Dudley syndrome with severe deficits or complete loss of hearing [12]. Both the morphogenesis and function of the auditory system requires precise control of local TH transport and metabolism [52-55]. Improper TH level results in delayed program of eye development, eye opening and retina morphogenesis probably via altered mitochondrial biogenesis [56]. THs are also important regulators of opsin expression and patterning, defects in TH signaling results in reprogramming of M-opsin cones to S type [57, 58].

### 3.1.3.2. *Peripheral organs*

THs increase mitochondrial activity and elevate the metabolic rate both on cellular and systemic level [59, 60]. Alterations in TH actions directly affect energy homeostasis and could serve as a source of several clinical symptoms. In hypothyroidism, the basal metabolism is decreased and consequently energy consumption is reduced that can be manifested in weight gain while hyperthyroidism has the opposite effect on energy homeostasis. Liver has crucial function in chemical energy storage, conversion and transport therefore hepatic transcriptome is a major target of TH actions. THs are also crucial factors in the central regulation of energy balance. Genes involved in lipolysis, lipogenesis, fatty acid transport and gluconeogenesis were shown to be under TH control. The clinical significance of this regulation is demonstrated by impaired liver metabolism in altered TH status [61]. THs also affect the cardiovascular system and cardiac metabolism increasing heart rate and volume while hyperthyroidism leads to cardiac muscle hypertrophy. THs contribute to the regulation of skeletal muscle metabolism and

substrate preference of chemical energy production while hypothyroidism manifested in decreased muscle tone [62].

The brown adipose tissue (BAT) is a well-documented target of THs involved in the maintenance of body temperature in hypothermic condition, especially in rodents [63]. While this function is also important in human neonates, until the last decade it was thought that thermogenesis by BAT is absent in human adults due to the documented regression of BAT depositions. However, a few years ago the presence of functionally active BAT islands was identified in the skeletal muscle by PET imaging [64-66]. Recent studies suggest that these depots belong to the beige adipose tissue derived from different progenitors compared to BAT [67-69]. Human BAT or beige fat could have clinical significance since experimental data demonstrated the induction of beige adipose tissue by drugs used for treatment of type 2 diabetes [68]. Therefore in adult humans these cells could play an important role in maintaining body energy balance rather than protecting body temperature.

The thermogenesis is an alternative route in mitochondria to use the electrochemical energy of proton gradient between the two sides of the inner membrane. In this process the protons are not transferred through the ATP synthase but carried by the uncoupling protein 1 (UCP1 or thermogenin) into the mitochondrial matrix. Therefore the electrochemical energy generated by oxidative phosphorylation is converted to thermal energy instead of storage in chemical energy by ATP. After the discovery of UCP1 homologue proteins have been also identified and shown to be expressed in several tissues including the hypothalamus however the exact function and uncoupling capacity of these UCP's are remained to be clarified similarly to the exact mechanism of heat generation by shuffling H<sup>+</sup>-ions into the mitochondrial matrix.

The BAT is under the control of the sympathetic nervous system by noradrenergic stimulation predominantly via  $\beta_3$ -adrenergic receptor [70]. The selective agonists of this receptor evoke the activation of BAT and induction of the differentiation of beige cells in white adipose tissue [71]. Induction of heat production is controlled by the noradrenergic stimulus-driven activation of cAMP second messenger system resulting in upregulation of *Ucp1* transcription and lipolytic enzymes. The release of fatty acids by lipoprotein lipase from triglycerides is also increased by elevation of intracellular cAMP and serves both as fuel and also as cofactor for UCP1. TH contributes to elevated UCP1 level and T<sub>3</sub>

production is elevated by the cAMP-mediated induction of the *Dio2* gene, see also in [3.2.2.1](#). As a consequence, hypothyroidism results in severe deficits in adaptive thermogenesis. [72].

#### **3.1.4. The hypothalamo-pituitary-thyroid (HPT) axis**

The synthesis and release of THs are controlled by the HPT axis. The HPT axis consists of hypophysiotropic TRH neurons of the paraventricular nucleus, thyroid-stimulating hormone (TSH) secreting cells of the adenohypophysis and the thyroid gland itself. The precise control is supported by multilevel negative feedback of the axis (**Fig. 6**).

Hypophysiotropic TRH neurons are located in the paraventricular nucleus (PVN) of the hypothalamus sending axon terminals to the portal vessels of the median eminence and regulating the TSH synthesis and secretion of the adenohypophysis. We summarize below how THs are able to modulate TRH expression along with distinct peptidergic inputs on TRH neurons. TRH gene encodes a precursor protein (preproTRH) containing five copies of TRH. The precursor is processed by endopeptidases (prohormone convertase, PC) cleaving the three amino acid-long TRH peptide. TRH contains N-terminal pyroglutamate and its C-terminus is amidated (pGlu-His-Pro-NH<sub>2</sub>). These modifications are obligatory for the active peptide. PC1 expression and pyroglutamyl peptidase (PPII) – cleaves the pyroglutamate at the N-terminus – is regulated by THs [73-76]. The TRH gene contains several TREs therefore directly responsive to TH via TRβ2 receptors [77-80].

Hypothalamic T<sub>3</sub> concentration is controlled by local activation and inactivation of TH but TH economy in this brain region is more complex than in the rest of the brain. The reason is that the blood-brain barrier in the median eminence – the region below the floor of the third ventricle – is incomplete. Therefore hypothalamic TH levels are affected both by local TH metabolism, tanycytic D2, neuronal D3 and by circulating T<sub>3</sub> (**Fig. 6**). Thus T<sub>3</sub> input of TRH neurons are coming from both local and peripheral sources. The balance between these two T<sub>3</sub> sources can be shifted towards locally generated T<sub>3</sub> by tanycytic D2 under specific circumstances as clearly demonstrated in the infection-evoked rodent model of non-thyroidal illness. In this model, despite falling

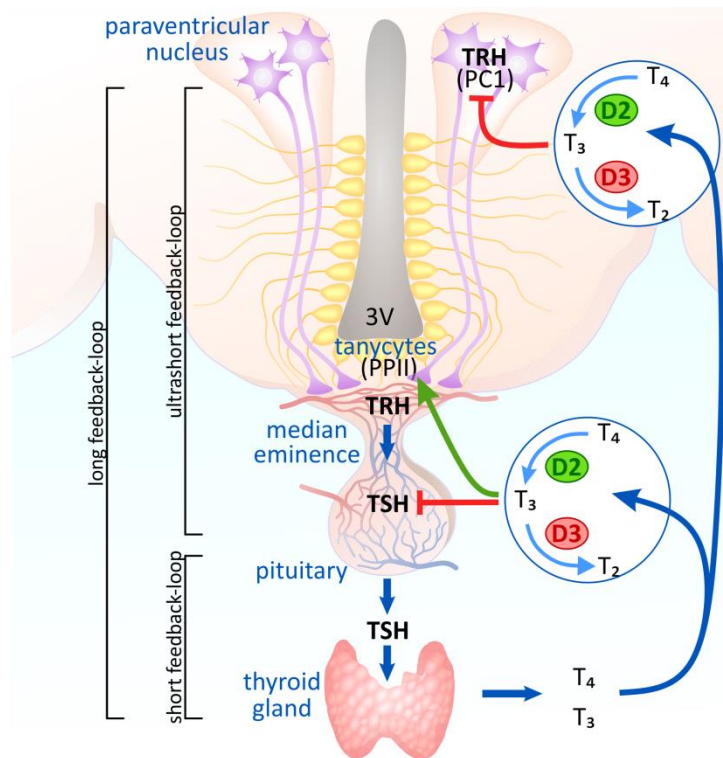


**Figure 6. Schematic depiction of thyroid hormone feedback of the HPT axis**  
 Involvement of thyroid hormone metabolism in the regulation of HPT axis.

serum TH levels, the upregulated tanycytic D2 activity results in local hypothalamic hyperthyroidism that leads to the suppression of HPT axis and hypothyroid peripheral status [81]. Therefore D2 activity in tanycytes is under strict control that includes the posttranslational ubiquitin-proteasome system (UPS), see in section 3.3. Factors that modulate tanycytic D2 activity have the potential to directly affect the HPT axis [82]. Beside their crucial role of T<sub>3</sub>-production tanycytes are capable to affect TRH neurons by several ways. As mentioned above PPII inactivates TRH and tanycytes express PPII that is regulated by THs [75, 76]. Tanycyte processes terminate on the capillaries of the median eminence and form a dynamic barrier for the axon terminals that release hormone-secreting neurons as observed in case of TRH [83] and GnRH neurons [84].

The TRH promoter cAMP-response element (CRE), glucocorticoid response element (GRE), STAT3 and SP1 binding sites [85, 86]. These pathways transmit crucial peptidergic signals involved in the regulation of energy homeostasis. TRH cells receive information from the orexigenic NPY/AgRP- and anorectic  $\alpha$ MSH/CART-containing neurons in the arcuate nucleus sensing humoral signals including insulin, leptin, glucose and ghrelin [87]. Recent studies revealed that cells coexpressing TRH and pituitary

adenylate cyclase-activating peptide (PACAP) in the PVN send stimulatory inputs to the inhibitory AgRP cells of the arcuate nucleus providing a short feedback loop for TRH cells [88]. TRH neurons are innervated by the hypothalamic dorsomedial nucleus and the adrenergic nuclei of the brainstem; afferents from the last region contain CART, NPY and PACAP peptides [89-91].

The axons of TRH neurons project to the median eminence where release to the portal system and stimulate the TSH expression and secretion of thyrotropic cells in the adenohypophysis (**Fig. 6**). This occurs via the type I TRH receptor [92] and by the involvement of the activation of phospholipase C pathway inducing  $Ca^{2+}$ -release and activation of CAMK-mediated CREB phosphorylation [93]. TSH is a heterodimer of thyrotropin-specific TSH $\beta$  and TSH $\alpha$  (CGA) that is a common subunit of chorionic gonadotropin (CG), luteinizing hormone (LH), follicle-stimulating hormone (FSH) and TSH. Both  $\alpha$  and  $\beta$  subunit expression are stimulated by TRH via CRE sites and inhibited by TH via negative TREs that results in a short feedback-loop [94, 95]. Importantly, these hormones are glycoproteins and the amount and pattern of carbohydrates highly affects their stability and bioactivity that posttranslational modifications are sensitive for TRH [96, 97]. TSH glycosylation was also shown to be sensitive for  $T_3$  and its secretion and bioactivity is also affected by deletion of *Dio2* gene [98, 99] indicating that the short feedback loop of HPT axis also requires the local  $T_3$  generation via D2.

In the thyroid gland the activated TSH receptor (TSHR) induces cAMP production and PI3K activation [100, 101] stimulating the transcription of genes involved in TH synthesis including  $I^-$  uptake by  $Na^+/I^-$  symporter (NIS) [102], thyroglobulin [103] thyroid peroxidase (TPO) [104] and  $I^-$ -recycling by iodotyrosine dehalogenase (DEHAL1) [105].

## **3.2. DEIODINASE ENZYME FAMILY**

### **3.2.1. Structure and biochemistry of deiodinases**

THs are metabolized by a specialized oxidoreductase enzyme family called iodothyronine deiodinases. Deiodinases are different both in structure, catalytic mechanism and function from iodotyrosine deiodinases involved in the recirculation of iodine in the thyroid gland. As a common feature, deiodinases contain a rare amino acid; selenocysteine (Sec), often referred as 21th amino acid. While the exact catalytic

mechanism is not completely understood it has been established that based on larger atomic radius, Sec is much more efficiently ionized at physiological pH than cysteine that represents a major advantage to catalyze oxidoreductive processes, like deiodination. As a result, the presence of Sec increases the affinity for substrate robustly. Its replacement with Cys results in a ~1000-fold elevated  $K_M$  of D2 for  $T_4$  along with a highly increased translation [106]. Thus the presence of Sec in deiodinases results in high substrate affinity and low protein level. Deiodinases has the ability to catalyze the loss of iodine both of the outer and inner ring of thyronine backbone (**Fig 2.**). The incorporation of Sec is carried out by a complex apparatus during the translation (**Fig. 7**) [107]. Unlike the common 20 amino acids, Sec is encoded by the UGA STOP codon that is subjected to read-through in selenoproteins. This process requires the presence of a specific mRNA secondary loop structure called selenocysteine insertion sequence (SECIS) element in the 3'-untranslated region of the selenoprotein encoding mRNA. The SECIS-loop is bound by SECIS binding protein 2 (SBP2) that interacts with the special elongation factor  $eEF_{Sec}$  allowing the recruitment of the tRNA specific for Sec. In contrast to the common amino acids Sec is synthesized on its transfer RNA ( $tRNA^{Sec}$ ). The  $tRNA^{Sec}$  is loaded with a serine then the hydroxyl-group of serine is edited to selenol-group by enzymatic cascade [108]. Available clinical data demonstrated that mutations in SBP2 affects the TH metabolism and reported impaired response for  $T_4$  but not for  $T_3$  [109]. In summary, this sophisticated system allows the cotranslational incorporation of a special amino acid Sec into selenoproteins by a complex and energy-dependent manner.

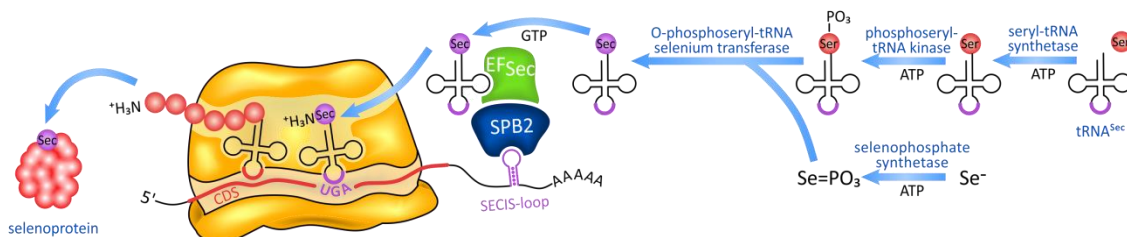


**Figure 7. Synthesis and cotranslational insertion of selenocysteine into selenoproteins**  
 $EF_{Sec}$ : Selenocysteine-specific elongation factor; SBP2: SECIS-binding protein 2.

### 3.2.1.1. Type 1 iodothyronine deiodinase (D1)

D1 is encoded by the *DIO1* gene located on the chromosome 1p32 in human and by the homologous *Dio1* gene in mouse on the chromosome 4. *DIO1* gene contains 4

exons; exon 1 contains the translational start ATG codon after a short, 25 nucleotide-lengths 5'-untranslated region (UTR) [110]. Exon 2 encodes the catalytic selenocysteine and exon 4 carries the SECIS region within the 3'-UTR which is crucial in the insertion of selenocysteine amino acid during the translation.

The product of the *DIO1* gene is a 249 amino acid-lengths type I membrane protein located in the plasmamembrane, with 26-30 kDa molecular weight. As a common feature of deiodinases D1 forms dimer which is obligatory for active conformation. The three dimensional structure of D1 has not been resolved yet therefore the domain structure and catalytic mechanism are based on predictions and sequence homologies. D1 shows highly conserved amino acid sequence between species. The N-terminus of D1 contains a short extracellular-tail composed from approximately the first 10 amino acids followed by the transmembrane helix located between amino acid position 10 and 40. Despite of the fact that D1 is highly conserved between species the first region of the cytosolic globular domain between amino acid position 40 and 70 shows variability (**Fig. 8**) [111]. Importantly, within this region there is a short deletion in feline and canine D1, two species where the biochemical properties of D1 are slightly different compared to other mammals [112, 113]. The globular domain contains the active center and the catalytic selenocysteine in the amino acid position 126. The region spans the active center is highly conserved between homologues and orthologue deiodinases.

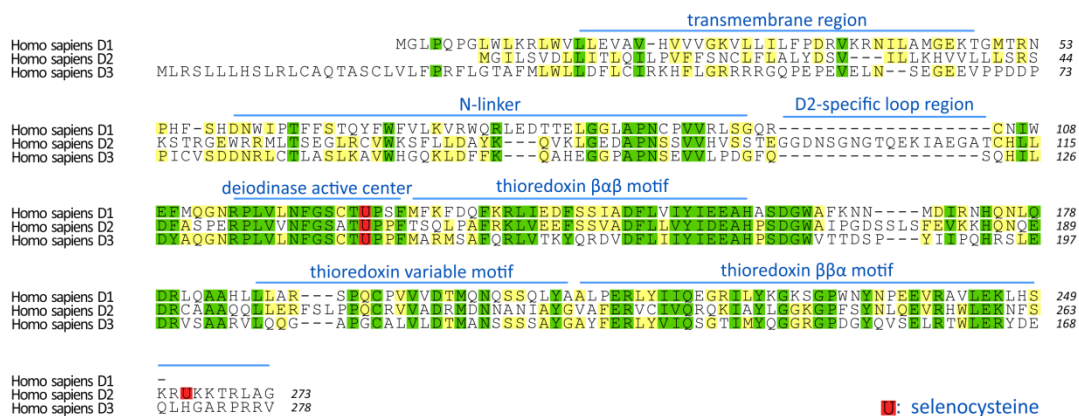


**Figure 8. Alignment of human D1, D2 and D3 proteins and the predicted domain structure**

D1 has the ability to catalyze both outer- (ORD) and inner-ring deiodination (IRD) that is unique compared to the other members of deiodinase enzyme family. Therefore both the activation and inactivation of thyroxine (ORD and IRD of  $T_4$ ) are catalyzed by D1 with the affinity for substrate  $K_M \approx 10^{-6}$  M in both cases which is slightly higher compared to the same values of D1 for the IRD of  $T_3$ . However the affinity for IRD of  $rT_3$  is one

order of magnitude lower ( $K_M \approx 10^{-7}$  M) suggesting this derivative is the preferred substrate of D1. While the catalytic mechanism of deiodinases is poorly understood, interestingly the conserved deletion in case of feline and canine D1 revealed the importance of this region in the IRD of rT<sub>3</sub>. In case of this species the  $K_M$  is elevated to  $\sim 10^{-5}$  M. 6-n-propyl-2-thiouracil (PTU) competes with the reducing agent of D1 while has a minimal effect on the other two deiodinases this effect has both clinical and methodological importance.

D1 is expressed in various tissues and cell types but importantly not in the human central nervous system. The most abundant D1 expression was found in liver, kidney and intestine while its activity is also present in the thyroid gland, pituitary and other tissues depending on the developmental stage. It is important to note that in contrast to the other two deiodinases D1 is not restricted to either the activation or inactivation of HTs therefore its expression and activity has to be evaluated in accordance with thyroid status and the available substrates. Hepatic D1 contributes to circulating T<sub>3</sub> in hyperthyroidism while under euthyroid conditions D1 deiodinates predominantly rT<sub>3</sub> as demonstrated in the *Dio1* KO mice that shows slightly elevated T<sub>4</sub> level while rT<sub>3</sub> level is increased 3-fold [114].

Available data are limited on the regulation of the *DIO1* gene however it was demonstrated that its transcription is positively regulated by T<sub>3</sub> [115]. This attribute of D1 explains the relatively larger contribution of liver D1 to the circulating T<sub>3</sub> in hyperthyroid conditions which is sensitive to PTU. Thyroidal but not the liver D1 was shown to be modulated by TSH-driven cAMP however it is unlikely that this effect is driven by the cAMP-sensitivity of *DIO1* gene [116]. Similar asymmetry was observed in case of selenium-deficiency which results in decreased hepatic and renal D1 activity while thyroidal and pituitary D1 is slightly affected [117]. The energy balance, steroids and circadian rhythm are also showed to affect D1 activity however it is unlikely to be a specific and direct effect on *DIO1* gene. There is no evidence to have posttranslational modification on D1 protein. In contrast with D2 that is targeted by the ubiquitin-proteasome system D1 is not ubiquitinated and has longer half-life [118].

### 3.2.1.2. Type 2 iodothyronine deiodinase (D2)

Type 2 deiodinase (D2) is encoded by the *DIO2* gene in human and located on chromosome 14q24 while *Dio2* gene on chromosome 12 in mouse. *DIO2* gene contains two exons separated by a ~7.4 kb intron. Three transcription start sites (TSS) [119] were found in *DIO2* gene affecting the unusually long 5'-UTR of the mRNA. Five splice variants of human *DIO2* gene were identified that show differences in the insertion of two portions of the intron and the termination of translation. The alternatively spliced mRNA forms encode four different putative proteins [120]. The 5'-UTR of *DIO2* mRNA contains upstream/short open reading frames (uORF or sORF) in different species, and not their number (3-5) but their existence is conserved between species (**Fig. 9**). The uORF-A affects the translation efficiency of the *DIO2* coding sequence (CDS) and helps to keep D2 protein level low due to represent a translational roadblock during ribosomal scanning [121]. The *DIO2* mRNA has a 5 kb 3'-UTR containing the SECIS-loop at the 3'-end. The 3'-UTR segment between the D2 CDS and SECIS-loop contributes to the instability of the *DIO2* mRNA [121] however the accurate mechanism of this phenomenon is not yet resolved.

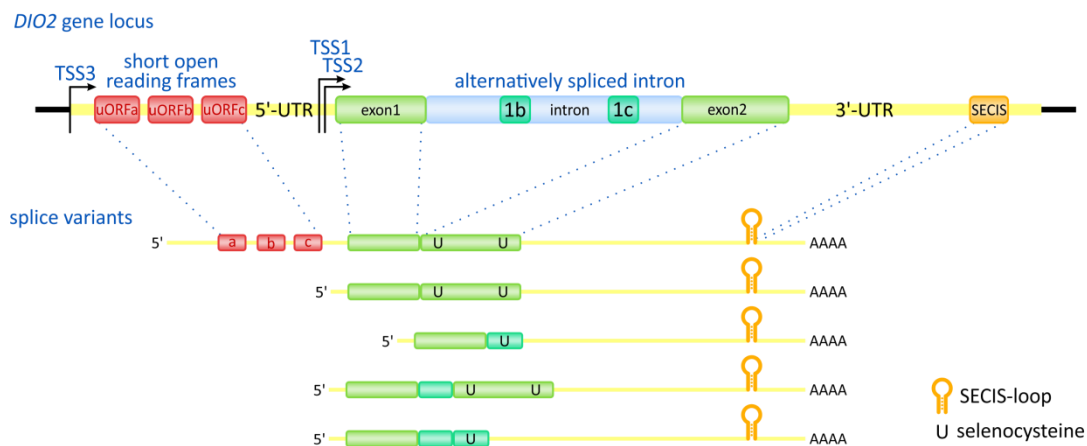


**Figure 9. Structure of *DIO2* gene and splice variants**

uORF: upstream open reading frame; UTR: untranslated region; TSS: transcription start site; SECIS: selenocysteine insertion sequence.

Despite the unusual length of the *DIO2* mRNA (6-7.5 kb in vertebrates) the D2 protein is encoded by an only ~800 kb long coding region generating a 31 kDa type I membrane protein, localized in the ER in stable retention. Similarly to the other members of deiodinase family, D2 also forms homodimers and this structure is obligatory for the

active conformation of the enzyme. D2 has a short ER-lumen localized N-terminal tail followed by the transmembrane domain between amino acid position 20 and 40. The transmembrane domain plays an important role in the dimerization of D2 via ionic interaction between helices. Based on homology and hydrophobicity predictions the TM domain is followed by a cytosolic linker region and thioredoxin-fold  $\beta\alpha\beta$  motif between amino acid 122 and 163 [122]. The catalytic selenocysteine amino acid is localized within this domain in position 133 of human D2 which is followed by iodothyronine-deiodinase active center motif localized between amino acid 164 and 192. The C-terminus of the protein contains a variable and  $\beta\beta\alpha$  thioredoxin motif between 193-224 and 225-273 amino acids, respectively. Unlike D1 and D3, D2 contains a second UGA close to its C-terminus at codon position 266, however the second Sec residue is not required for catalytic activity of the enzyme (**Fig. 8**) [123].

Point mutations that alter amino acid in the D2 protein were identified but their significance is still poorly understood [124-126]. These polymorphisms include L4H, T92A and T102I amino acid changes. L4H and T102 seem to have identical properties compared to abundant allele of D2 [125]. Interestingly, T92A is suggested to be in correlation with numerous symptoms e.g. type 2 diabetes mellitus, Graves' disease, mental abnormalities, affected bone and muscle metabolism etc. however most of these studies are controversial and restricted to clinical data [124]. It is also remained to be clarified whether the statistical correlation is underlined by the effect of T92A polymorphism via modified biochemical characteristics of D2 or this polymorphism is a linked genetic marker of other mutations in same region of chromosome [124, 127-130]. While the precise background of the effect T92A polymorphism is poorly understood it is important to note that the 92th amino acid position is within the previously identified instability-loop of D2 involved in its posttranslational regulation by ubiquitin-proteasome system.

In contrast to D1, the catalytic activity of D2 is restricted to ORD of TH derivatives. The mechanism of deiodination and the structural basis of the difference between D2 and D1 are incompletely understood. However, there are major differences between the biochemical properties between the two  $T_4$  activating deiodinases, D2 and D1. First, the primary substrate of D2 is  $T_4$  and has three orders of magnitude lower,  $\sim 10^{-9}$  M in vitro  $K_M$  for this molecule, than that of D1. D2 is also effective in the deiodination of  $rT_3$

indicating that the structural differences between D1 and D2 result in higher catalytic efficiency. The importance of selenocysteine played in the catalytic mechanism of deiodinases was demonstrated clearly for D2; the mutation of this residue to cysteine results three orders of magnitude higher  $K_M$  for  $T_4$  [106]. The homologue mutation in D1 leads to only one order of magnitude increase in  $K_M$  for the preferred substrate  $rT_3$  [131]. Importantly, the studies targeting the biochemical characteristics of deiodinases were performed in cell lysates not using purified enzymes therefore the comparisons between different studies should be read carefully.

D2 is widely distributed in different tissues and its function is primarily the local  $T_3$  generation compared to D1. Importantly, D2 is the activating deiodinase in central nervous tissue and its expression is confined to glial cell types. High D2 activity was described in pituitary [98] while high *DIO2* mRNA level in thyroid [132]. Another important target organ is the brown adipose tissue (BAT) where the D2-driven  $T_3$  increases the noradrenergic signal stimulated UCP1 expression. Probably due the common lineage, similarly to BAT, D2 refers for  $T_3$  generation in skeletal muscle, and seems to be important in tissue regeneration after injury [133]. D2 was also found in cardiac muscle, lung [134], perinatal liver and skin.

The complex regulation of D2 is summarized in section [3.2.2](#).

### 3.2.1.3. Type 3 iodothyronine deiodinase (D3)

D3 is encoded by the *DIO3* gene located on chromosome 14q32 in human. The homologue chromosome region belongs to the *Dlk1-Dio3* imprinted locus in mouse on chromosome 12 and D3 is preferentially expressed from the paternal allele [135], at least at the periphery, while in the brain *Dio3* imprinting is region specific [136]. *DIO3* gene contains one exon and the predominant *DIO3* transcript is 2.1 kb however there were identified alternative transcription start sites that result in different transcript sizes [137-139]. These forms do not affect the coding sequence however in low abundance an alternative translation initiation methionine containing transcript was identified resulting 26 amino acid elongation of the N-terminal extracellular tail. The abundance of alternative transcripts is dependent on thyroid status. Additionally, the *DIO3* locus is also transcribed in antisense orientation named as *DIO3OS* pseudogene however its translation to protein is controversial [139].

D3 is a 32 kDa type I membrane protein located in the plasma membrane with its C-terminus in the cytosol forming homodimers [140, 141]. Similarly to D1 and D2, D3 has a short N-terminal tail followed by transmembrane region that was suggested between amino acids 29 and 49. The predicted domain structure of D3 shows high similarity to the other two member of the enzyme family. The first crystallized data on deiodinase structure was recently obtained on the D3 globular domain fragment [142]. These results confirm the thioredoxin- and peroxiredoxin-fold homology and the insertion of iodothyronine deiodinase-specific helix-loop- $\beta$ -sheet organization with critical function in the TH binding. D3, similarly to D1, contains one selenocysteine residue in amino acid position 162 of human D3 (**Fig. 8**). Posttranslational modification of D3 is not indicated by the presently available data.

The catalytic action of D3 is restricted to IRD therefore the inactivation of THs. D3 has nearly equal affinity for T<sub>3</sub> and T<sub>4</sub> (K<sub>M</sub>=1-2 nM and 4-5 nM, respectively) therefore it has the ability to reduce directly the thyroid prohormone compound without its activation [122]. The recently obtained structural data allowed to constitute the model of catalytic mechanism of D3 and – based on the conserved structure of deiodinases – also helped to better understand the principle of deiodination catalyzed by D1 or D2. This study revealed the presence of conserved amino acids with a predicted proton-shuttle function and importance in the protonation of carbonyl atom after elimination of iodonium by selenate. It has been suggested that the regeneration of active center requires a two-step mechanism: in the first phase it is reduced by the formation of an intramolecular disulfide-bond which is reduced by the endogenous cofactor of deiodinases remained to be identified. This mechanism seems to be non-functional for D2 since this enzyme lacks the required C-terminal cysteine [142]. D3 is also insensitive for PTU [110].

D3 is expressed in neurons in the CNS cells where it inactivates T<sub>3</sub> generated by glial D2. In *Dio3* KO mice the abolished clearance of T<sub>3</sub> by D3 results in severe thyrotoxicosis in perinatal life leading to central hypothyroidism via suppressed HPT axis [143]. Placental and uterine D3 is crucial in supporting the independent thyroid state of embryos from the maternal environment [144]. D3 is also expressed in liver and intestine especially in the embryonic days involved in the control of fetal TH environment. High D3 activity could be detected in skin and reproductive organs [145].

In the CNS the *DIO3* transcription shows high sensitivity for the thyroid state which serves as a negative feedback toward the transcriptionally active TH [138]. In the placenta and uterus *DIO3* is strongly correlated with estrogen and progesterone levels these hormones have a synergistic effect on *DIO3* translation at least within this region [146]. The *DIO3* is directly upregulated by HIF-1 $\alpha$  in response of hypoxic condition to locally decrease the energy and oxygen consumption via inactivating T<sub>3</sub> [147].

### 3.2.2. Regulation of type 2 deiodinase (D2)

#### 3.2.2.1. Transcriptional regulation of D2

The regulation of D2 is the best characterized among deiodinases (**Fig. 10**). D2 is sensitive to intracellular cAMP level and a functional CRE was identified within the 5' flanking region (5' FR) of both the human *DIO2*, and the rat and mouse *Dio2* genes showing that D2 expression is directly targeted by cAMP-driven CREB phosphorylation (**Fig. 11**) [119, 148, 149]. Beside the induction of *DIO2* promoter, the cAMP/PKA pathway is also an important regulator of the basal promoter activity of *DIO2* gene demonstrated by the mutation of cAMP response element (CRE) that resulted in decreased basal promoter activity by one order of magnitude [119]. Despite the crucial role of cAMP/PKA pathway in the regulation of *DIO2* transcription only a few upstream factors have been revealed elevating D2 activity via this pathway. During the induction of adaptive thermogenesis in brown adipose tissue (BAT) the noradrenergic stimulus via  $\beta$ 3 adrenergic receptors promotes intracellular cAMP production and increases D2 expression. The elevated T<sub>3</sub> generation contributes to the induction and increase of UCP1 level [150]. The adrenergic stimulus also targets D2 in the pineal gland regulating the photoperiodic alterations in TH activation [151]. In birds

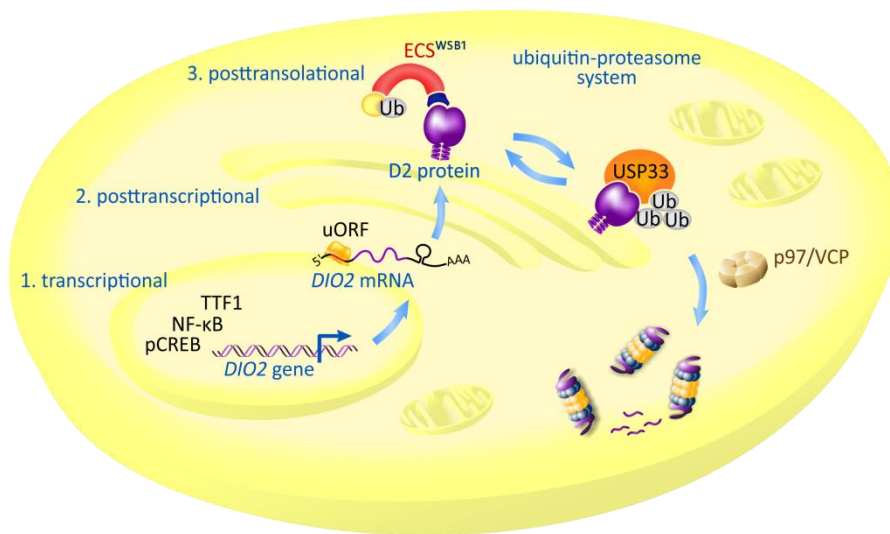


**Figure 10. Regulatory levels of D2 activity**

Schematic depiction of elements involved in the transcriptional, posttranscriptional and posttranslational regulation of D2 activity.

and mammals, the hypothalamic TH metabolism is in tight correlation with the seasonal regulation of gonads and reproductive axis and D2 expression is under the control of TSH $\beta$  derived from pars tuberalis [152-154]. However, the importance of cAMP-mediated regulation of D2 in tanycytes is poorly understood especially in aspects of HPT axis.

The human *DIO2* gene was shown to be a positive target for NF- $\kappa$ B pathway as the overexpression of p65 subunit of NF- $\kappa$ B results robust increase of *DIO2* promoter activity (**Fig. 11**) [155]. This pathway plays a major role in the bacterial lipopolysaccharide (LPS) infection-induced suppression of the HPT axis via the induction of D2 activity in tanycytes that results in the inhibition of TRH neurons. This mechanism generates local hypothalamic hyperthyroidism and uncouples local TH levels from the peripheral TH economy in non-thyroidal illness [81, 156]. In cultured tanycytes LPS was able to induce D2 and the inhibition of the NF- $\kappa$ B pathway completely abolished this effect [157].

In contrast to the conserved responsiveness to cAMP and NF- $\kappa$ B, the *DIO2* promoter shows species-specific response to other factors e.g. the human *DIO2* but not the rat *Dio2* gene was found to be responsive to TTF1 (Nkx2.1) [149] and this could underline the strikingly different D2 levels in the human vs rat thyroid gland (**Fig. 11**). A similar phenomenon was observed regarding GATA-4 and Nkx2.5. Human *DIO2* is

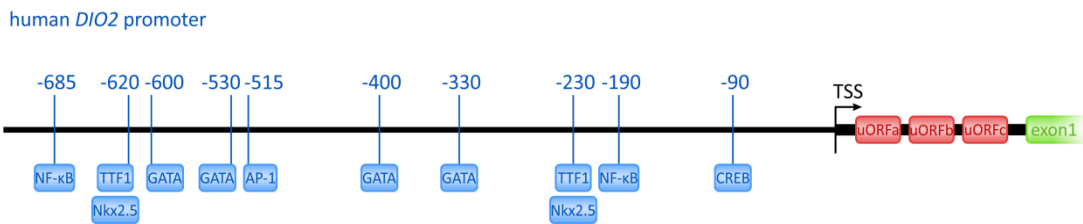


**Figure 11. Transcriptional regulation of D2**  
Transcription factor binding sites in the promoter of the human *DIO2* gene.

affected by these factors while rat *Dio2* is not sensitive. This mechanism is suggested to explain the difference in D2 expression in case of cardiac muscle of these two species [158].

D2 expression was showed to be inversely regulated by THs in the cortex however direct transcriptional effect is remained to be elucidated because the lack of evidences for negative TRE in the promoter region of *DIO2* gene [159].

These examples reveal the complex transcriptional regulation of the *DIO2* gene encoding D2 that is affected by several pathways. However little known how these signaling cascades and factors affect D2 *in vivo*, especially in hypothalamus where the local T<sub>3</sub> generation has crucial impact on the HPT axis.

### 3.2.2.2. Posttranscriptional regulation of D2

The 5'-UTR of *DIO2* mRNA contains uORFs and these are able to decrease the efficiency of D2 translation that allows keeping D2 protein at low level that contributes to the tight regulation of D2 activity (**Fig. 10**) [121]. The 5'-UTR structure can be subjected to alternative splicing that provides an additional mechanism to regulate the efficiency of *DIO2* translation but the physiological significance of this mechanism remains to be understood (**Fig. 9**) [119]. The *DIO2* mRNA has very long 3'-UTR (4-5 kb) and contains RNA instability motifs that contribute to the short half-life of *DIO2* mRNA [121].

### 3.2.2.3. Posttranslational regulation of D2

As a unique feature among deiodinases, D2 activity is subjected to complex posttranslational control by the ubiquitin-proteasome system. The mechanism of this regulatory pathway is summarized in section 3.3. The short half-life of D2 protein is caused by ubiquitin-mediated proteasomal degradation (**Fig. 10**) [118]. The D2 is processed by an E3 ligase complex organized by the Cullin5 E3 ligase backbone and Elongin B and C adaptor proteins. The WSB1 SOCS-box protein binds to Elongin B and C and refers for the recognition of D2 by this complex ( $ECS^{WSB1}$ ). The ubiquitin is carried by the UBE2J (Ubc6) and UBE2G (Ubc7) E2 enzymes [160, 161]. This machinery is strongly associated to D2 homodimers on the cytosolic surface of ER and allows a precise control of D2 activity on  $T_4$ -dependent manner therefore the D2 is also targeted by TH control on the posttranslational level (**Fig. 12**). The substrate induced ubiquitination of D2 represented the first example of this type of regulation of hormonal activity via an ER resident enzyme [118].

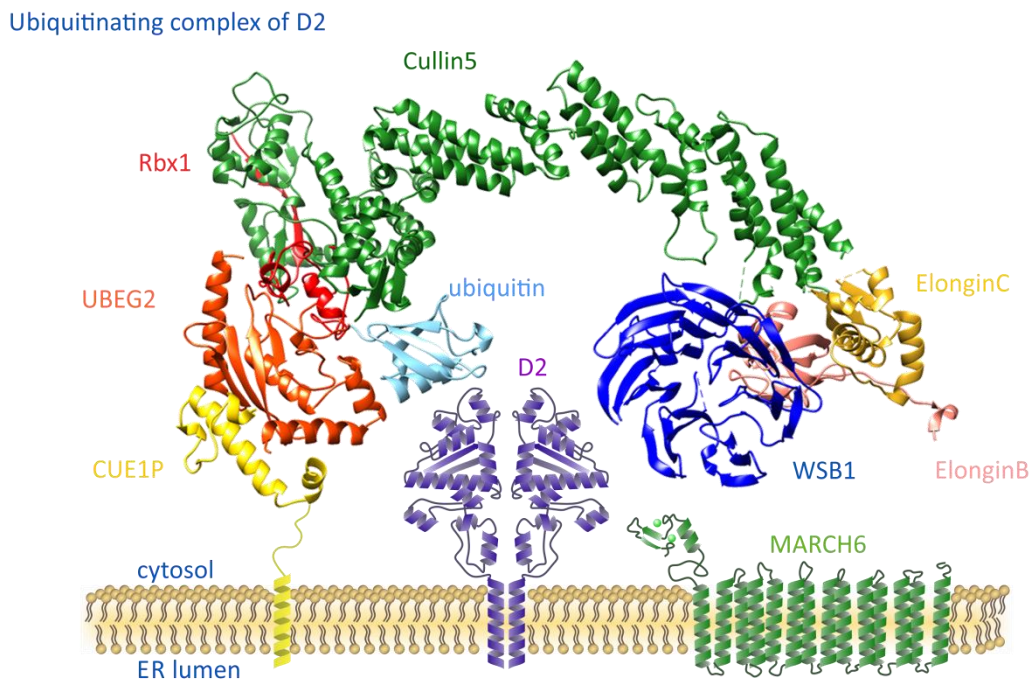


**Figure 12. Schematic model of ubiquitinating apparatus in close association with D2 in the ER**  
Cullin5: scaffold protein; Rbx1, Elongin B and C: adaptors; WSB1: SOCS-box substrate-binding subunit; UBE2G (Ubc7): E2 ubiquitin conjugating enzyme; CUE1P: anchoring and activator protein of UBE2G.

Importantly, this system is capable to downregulate the D2 activity without degradation of the protein which is favorable in case of a selenoprotein that requires an energy-dependent insertion of the rare amino acid selenocysteine. The ubiquitination of D2 protein results a conformational change that abolishes the enzyme activity [162]. The ubiquitinated inactive state of D2 could be reversed by deubiquitinating enzymes via the cleavage of ubiquitin chain resulting regained activity. Previous studies identified the USP33 (VDU1) and USP20 (VDU2) proteins with the capability to deubiquitinate the D2 [163]. The recognition of D2 by ECS<sup>WSB1</sup> is facilitated by T<sub>4</sub>, the substrate of D2, demonstrating a unique regulation of enzyme activity. Moreover the T<sub>4</sub>-dependent reversible inactivation of D2 allows a rapid and efficient way to fine-tune the TH activation capacity. Beside the ECS<sup>WSB1</sup> complex, recent studies based on yeast two hybrid screen identified the MARCH6 (TEB4, mammalian orthologue of Doa10 in yeast) ERAD ubiquitin ligase as potential E3 enzyme for D2 [164].

As previously mentioned, the ubiquitination is a unique feature of D2 among deiodinases however the background of the difference is not clearly understood. Previous studies identified critical elements involved in the short half-life and ubiquitination of D2 protein. It is also remained to be elucidated how ubiquitin ligases contributes to the regulation of D2. Specific features of D2 ubiquitination has been suggested in the hypothalamus with major impact on TH replacement therapy [82, 165]. Therefore detailed molecular characterization of D2 ubiquitination is essential to better understand the regulation of hypothalamic TH activation. The crucial components of the ubiquitin-proteasome system will be summarized below.

### **3.3. THE UBIQUITIN-PROTEASOME SYSTEM**

#### **3.3.1. Mechanism of ubiquitin-conjugation**

The ubiquitin-proteasome system (UPS) was discovered as a complex machinery dedicated to targeted intracellular proteolysis that impacts a wide range of cellular processes e.g. cell division, signal transduction, gene regulation and ER quality control (endoplasmic reticulum-associated degradation, ERAD) [166]. Further studies on the UPS revealed that it is more accurate to distinguish between the ubiquitin tagging and proteasomal degradation since only a subclass of ubiquitinated proteins is degraded by

proteasome. The ubiquitin is an evolutionary conserved small, 8.5 kDa protein containing 76 amino acid residues containing seven lysines and C-terminal glycine-glycine residues. It is important to note these features serve as the structural basics of the diversity of ubiquitin signal as described below.

In the first step the ubiquitin-activating enzyme (E1) catalyzes the formation of an ester linkage between adenosine-monophosphate from ATP and the C-terminal glycine of ubiquitin followed by direct conjugation of ubiquitin to a cysteine residue of the E1 enzyme by thioester linkage resulting a high-energy reactive bound (**Fig. 13**). In the most of the species only a single gene encodes E1 suggesting that the role of the E1 enzyme is restricted to the universal activation step of the ubiquitin moiety and has a limited effect on its further processing or target selection [167].

The action of E1 is followed by the transfer of ubiquitin to a cysteine residue of ubiquitin-conjugating enzyme (E2) via formation of a thioester linkage. In contrast to E1 there are multiple E2 enzymes with specific expression, localization and different mechanisms of action (**Fig. 13**). The core catalytic domain of E2's is highly conserved but some of them contain N- or C- terminal extension that affects their localization or interaction with E3 ligases [167]. While the function of E1 enzymes is restricted to supporting the energetic background of ubiquitin conjugation some of E2 sterically determinates or restricts the ubiquitin conjugation process.

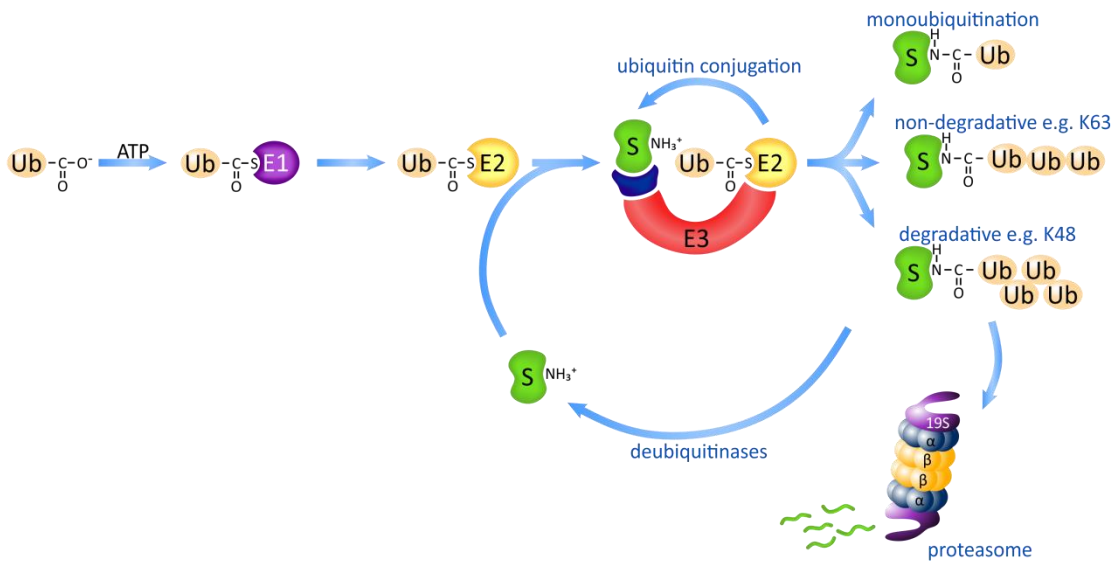


**Figure 13. Mechanism of ubiquitin conjugation**

Ub: ubiquitin; E1: ubiquitin activating enzyme; E2: ubiquitin conjugating enzyme; E3: ubiquitin ligase (complex); S: substrate protein.

The most diverse component of the ubiquitinating apparatus consists of E3 ligases; there are hundreds of proteins with ubiquitin ligase function. E3 enzymes catalyze the formation of isopeptide-bond between the C-terminal carboxyl-group of ubiquitin moiety and  $\epsilon$ -amino-group on one or more lysine residues of target protein, the second often referred as multiubiquitination. Importantly, the E3 ligases have the ability to extend the initial ubiquitin by the addition of further ubiquitin moieties result polyubiquitin chain formation. The quantity and quality of these chains substantially determinate the way of downstream processing of the target protein (**Fig. 13**).

The E3 ligases can be grouped into three classes based on the mechanism of ubiquitin-transfer and structural properties. HECT-type (homologue to E6-AP carboxyl-terminus) ligases form a covalent bond between one of their cysteine residue and ubiquitin therefore the ubiquitin is not directly attached to the target protein. The other two groups similarly bind the ubiquitin-carrier E2 and transfer ubiquitin directly to the substrate protein. The vast majority of E3 enzymes is RING-type (homologue to the Zn-finger of “really interesting new gene”) coordinating two  $Zn^{2+}$ -ion which are involved in the stabilization of RING-domain. In contrast, the U-box E3 ligases have a structurally similar domain to RING but lack the metal-binding ability.

Most of the RING-finger E3 ligases have modular multiprotein structure splitting the major functions (scaffolding the complex, binding E2 and recognizing substrate) between different protein chains [168]. In case of Cullin-based ligases these functions are carried out separately. The core unit of the complex is the Cullin lacking the ability to bind to ubiquitin-loaded E2 that is carried out by Rbx proteins. Another part of the complex refers for the substrate recognition e.g. F-box and SOCS-proteins which are connected to the Cullin-organized complex via Skp1 or Elongin B and C adaptor proteins [169]. This modular scheme allows the precise combination of target selection with the type of conjugated ubiquitin chain.

The fused ubiquitin or ubiquitin chain determinate the fate of the substrate protein and its degradation in the proteasome represents only one possibility. The exact understanding of ubiquitin code is one of the most important issues related to the UPS function. The single ubiquitin or ubiquitin chain and in the last case the structure of the chain result a major difference in the acceptability for ubiquitin-binding proteins which stands in the structural background of the linkage between ubiquitin signal synthesis and

function. Other theories raised the possibility that the difference is based on molecular dynamic aspects which are determined by the orientation of proximal and distal ubiquitin within the ubiquitin chain [170].

While the soluble proteins in the cytosol could reach the proteasome directly after tagged by degradative ubiquitin signal, the ER membrane proteins have to undergo a complex process to access to the proteasome. This includes the cleavage of degradative ubiquitin signal partial unfolding and transport to the cytosol where new degradative signal is synthesized for these proteins. The core member to organize this machinery is the p97/VCP complex. The importance of this system is to support the accessibility of proteasome for ER-proteins [171].

### **3.3.2. Cleavage of ubiquitin: the deubiquitinases**

The ubiquitin chain synthesizing apparatus allows the selective labelling of proteins resulting precise targeting of their action that is fine-tuned by the reversibility of ubiquitin-mediated modification. This system allows a reversible posttranslational modification of protein function, localization, stability and importantly the recircularization of ubiquitin. The latter is critical within the cell demonstrated by the inhibition of the proteasome (e.g. by MG132) that contains subunits with deubiquitinase activity for cleavage of polyubiquitin chain from substrates. Inhibition of this process leads to ubiquitin “depletion” and interferes with ubiquitin-conjugation [172]. Because *de novo* ubiquitin synthesis is not able to compensate the inhibition of ubiquitin recycling this condition has severe toxicity for the cell. Importantly, *de novo* ubiquitin synthesis is also requires the cleavage of ubiquitin because the four genes encode ubiquitin in repeated copies of ubiquitin or ubiquitin is translated in fusion to other proteins and in all of the cases ubiquitin moiety is released after cleavage [173, 174]. Deubiquitination is also involved in the extraction of ER-localized proteins to the cytosol ensuring the unfolding of target proteins which are reubiquitinated after reaching the cytosol.

Deubiquitinases (ubiquitin-specific proteases, USPs) are cysteine- or metalloproteases with the ability to cleave ubiquitin or ubiquitin chain at different sites. The cleavage site could be determined by the docking surface on deubiquitinases, linkage type of ubiquitin chain and also by the substrate [175]. These capabilities allow a broad

range of action of deubiquitinases including the rescue from degradation, allowing chain-editing or transport.

### **3.3.3. Importance of ubiquitin-ubiquitin linkage**

All of the seven lysine residues of ubiquitin and also the N-terminal amino-group could be involved in the formation of a polyubiquitin chain but only the K48- and K63-linked chains are well characterized. The following section briefly addresses the diversities of protein processing by different ubiquitin linkages.

Despite of lacking evidences on the exact role of K6 ubiquitination this type of ubiquitin chain seems to exert non-degradative functions. K6-linked polyubiquitin chain synthesis is involved in the recognition of DNA damage and the recruitment of repair machinery recognized by Werner helicase interacting protein 1 (WRNIP1) [176, 177]. Cytoskeletal dynamics and remodeling are affected by K6-mediated ubiquitination of  $\alpha$ -tubulin [178].

K11-linked ubiquitin chain possesses proteolytic functions and its essential role was demonstrated in endoplasmic reticulum associated degradation (ERAD). In other cases, K11 ubiquitin chain formation interferes with K48-linked ubiquitination rescuing the target protein from degradation [179] or resulting partial proteolysis as in the case of Ci (insect orthologue of mammalian Gli proteins involved in Sonic hedgehog signalization). K11 ubiquitin chain synthesis is demonstrated in signaling pathways and cell cycle [180, 181] Interestingly, Doa10 – the yeast orthologue of mammalian MARCH6 – is suggested to be involved in K11-linkage formation in combination with Ubc6 E2 enzyme [182]. Importantly, both of them are involved in the regulation of D2.

The K27-linked polyubiquitin chain is predominantly a non-degradative tag, involved in DNA damage response, histone-modification [183]. K27-linked ubiquitin chain is synthesized by Parkin ubiquitin ligase and shown to be involved in the turnover of mitochondria [184].

Recently, only very limited data are available on processes modulated by K29-linked ubiquitin chain exclusively and this type of action is often reported in mixed or not characterized ubiquitin chains. K29-chain is involved in the activation and regulation of the stability of  $\beta$ -catenin transcription factor modulator in Wnt pathway [185, 186].

The function of K33-linked chains is also poorly characterized but it was suggested to work as a non-degradative signal. The K33 signal affects actin assembling and cellular trafficking in trans-Golgi [187] and has a role in the regulation of TCR- $\zeta$  phosphorylation [188].

There is no doubt that the K48-linked ubiquitin chain is the most characterized and understood linkage type. While other linkage types also can target proteins for proteasomal degradation, the K48-chain is the major functional linker of ubiquitin conjugation to proteasomal degradation, referred together as the ubiquitin-proteasome system [166, 189].

The K63-linked ubiquitin chain is the canonical example of non-degradative ubiquitin signals. The activation of NF- $\kappa$ B pathway requires K63-linked ubiquitin chain formation involved in IKK activation [190, 191]. This chain type is also involved in the response for double-strand break of DNA by the recruitment of the repair machinery [192] and play a role in intracellular trafficking and endocytosis [193].

#### **3.3.4. The proteasome**

The proteasome is a multicatalytic protease complex with a fundamental role in several cellular functions. The subunits are organized into 4 rings forming a barrel structure. While the potential ancestral prokaryotic proteasome the HslU–HslV complex show hexameric symmetry [194] the eukaryotic proteasomes are common in the formation of heptameric rings [195]. The 20S core proteasome is built up by two outer rings formed by the  $\alpha$ -subunits and two inner rings which are constituted by the  $\beta$ -subunits. The  $\alpha$ -rings have a gate keeper function – especially  $\alpha$ 3-subunit is critical in this aspect – and contribute to the conveying of unfolded proteins [196]. The  $\beta$ -rings carry the protease activities:  $\beta$ 1 shows caspase-like,  $\beta$ 2 trypsin-like and  $\beta$ 5 chymotrypsin-like substrate preference. The proteasome has an important role in the process of antigen presentation by MHCI proteins via the generation of short oligopeptides. In case of immunoproteasome, the catalytic subunits are changed to  $\beta$ 1i (LMP2),  $\beta$ 2i (MECL) and  $\beta$ 5i (LMP7) therefore the generated oligopeptides are optimized in the critical amino acid positions for binding into antigen pocket of MHCI [197]. Interestingly, genes encoding

$\beta$ 1i and  $\beta$ 5i subunits are located in the MHC locus and deletion of these three immunoproteasome subunits leads to severely altered antigen presentation [198].

The 20S core proteasome carries the catalytic activity however the mature proteasome usually contains additional cap complexes. The most abundant lid structure is the 19S (PA700) subunit incorporating multiple functions. Similarly to 20S complex the 19S regulator has also ring-shape structure and it contains multiple subunits that can be divided into two major subclasses: ATPase (RPT) and non-ATPase (RPN) proteins. 19S complex refers for the recognition and docking of polyubiquitin chain on target protein, unfolds the protein, and involved in the gating mechanism of 20S core proteasome. The complex of 19S and 20S is referred as 26S proteasome.

The 11S (PA28) subunit increases proteasomal activity although it restricts its acceptability to unfolded substrates. It is suggested that the 11S subunit is involved in MCHI antigen presentation by forming hybrid proteasomes with 19S subunit and docking it to the TAP1/2 proteins in the ER.

## 4. SPECIFIC AIMS

1. Novel mechanisms regulating the HPT axis via D2-mediated thyroid hormone activation in the hypothalamus
  - a) regulation of D2 transcription in the hypothalamus
  - b) interaction between thyroid hormone and pituitary adenylate cyclase-activating polypeptide (PACAP) signaling
  
2. Involvement of MARCH6 ubiquitin ligase in the regulation of thyroid hormone activation
  - a) tissue distribution and transcriptional regulation of *MARCH6* gene
  - b) characterization of D2-MARCH6 interaction
  
3. Structural aspects of the ubiquitination of D2 protein
  - a) combination of molecular elements required for the ubiquitin-mediated regulation of deiodinases
  - b) structural background of the recognition of D2 by ubiquitin ligases
  - c) importance of ER-membrane extraction in the reversible ubiquitin-mediated regulation of D2

## 5. MATERIALS AND METHODS

### 5.1. DNA constructs and RT-PCR

#### 5.1.1. Luciferase promoter constructs

DNA construct containing the human 7 kb *DIO2* promoter in pGL3-basic vector (*wtDIO2-Luc*) expressing Firefly luciferase reporter was described earlier [155]. In order to generate cAMP-insensitive reporter construct site-directed mutagenesis was performed on the region containing CRE using overlap-extension PCR and primers indicated in **Table 1**. PCR fragment was inserted into *wtDIO2-Luc* construct using PacI-NheI sites resulting in CREmut-*DIO2-Luc* construct. Expression vector encoding mouse thyroid hormone receptor  $\alpha$  (TR $\alpha$ ) was described in [199].

Plasmid encoding mouse *Adcyap1* (PACAP) promoter driving luciferase reporter was a kind gift of Dr. Hashimoto (Osaka University) [200]. Plasmids containing constitutive active Gli2 (Gli2 $\Delta$ N2) and octamer Gli-binding sites driving luciferase reporter used as positive control (8 $\times$ Gli-BS) were kind gifts of Dr. Sasaki (Osaka University) [201]. The  $\beta$ -catenin containing expression vector and the human *WSB* promoter-luciferase reporter were kind gifts of Dr. Dentice [202].

**Table 1. Primers designed for CRE mutation in the 7 kb 5'FR human *DIO2* gene**

<i>hDIO2</i>	FW	5'-GCACCTACTGCTTAGCTTATG-3'
<i>hDIO2-mutCRE</i>	R	5'-AAGATCTTGtCGaCtTTGAGAAAGAGGGC-3'
<i>hDIO2-mutCRE</i>	FW	5'-TTCTCAAaGtCGaCAAGATCTTTACCAAG-3'
<i>pGL3-basic</i>	R	5'-TTCCATCTTCCAGCGGATAGA-3'

#### 5.1.2. Tissue distribution of *March6*

Tissue samples were collected from adult male Wistar rats and total RNA was isolated using TRIzol reagent (Thermo, Waltham USA) following the manufacturer's instructions. Reverse transcription to cDNA was performed using SuperScript II Reverse Transcriptase kit (Thermo, Waltham USA) and oligo dT. Intron-spanning primers were designed to amplify *March6*, *Wsb1* and *Ppia* (Cyclophilin A) (**Table 2**) transcripts using Taq polymerase (Thermo, Waltham USA). PCR products were run in 1 % agarose gel and documented by Kodak Gel Logic 2200 Imaging System.

**Table 2. Primers designed for detection of *March6*, *Wsb1* and *Ppia* in rat tissue samples**

<i>March6</i>	FW	5'-GTGTCGGTCAGAAGGAACACCTGA-3'
<i>March6</i>	R	5'-AGTGATCCATCAAGTCCAAGCAT-3'
<i>Wsb1</i>	FW	5'-CGAGGGTCAACGAGAAAGAGAT-3'
<i>Wsb1</i>	R	5'-GACGCAGTAGCTAGTAATGCT-3'
<i>Ppia</i>	FW	5'-TGACTTCACACGCCATAATG-3'
<i>Ppia</i>	R	5'-CCACAATGCTCATGCCTTC-3'

### 5.1.3. Cloning of human *MARCH6* 5' flanking region

Genomic DNA was isolated from human HEK-293T cells using DNeasy Blood & Tissue Kit (Qiagen, Hilden Germany) and the 3.5 kb flanking region 5' to the transcription start site (TSS) of *MARCH6* gene was amplified using the primers indicated in **Table 3** and Expand Long Range dNTPack (Roche, Basel Switzerland) following the manufacturer's instructions. The generated amplicon was inserted between the MluI-XhoI sites of pGL3-basic vector (Promega, Madison USA) that resulted in the *MARCH6*-Luc construct. For deletion of the predicted SP1 binding site-containing 130 bp-length region the previously described construct was cut with SacII-XhoI, blunted and religated to generate the *MARCH6-Δ130*-Luc plasmid. The protein kinase A (PKA)  $\alpha$ -catalytic subunit and the NF- $\kappa$ B subunit p65 encoding vectors were described previously in [119] and [155], respectively.

**Table 3. Primers designed for cloning the 3.5 kb 5' FR of human *MARCH6* gene**

<i>MluI-hMARCH6 5' FR</i>	FW	5'-tcgacgcgtGGAACAAGCTTCAGACCTGAGTCCACGTTAC-3'
<i>XhoI-hMARCH6 5' FR</i>	R	5'-ccgctcgagGGAGAGAGGCTGACAGAAAGCGAGCGACA-3'

### 5.1.4. FRET constructs

The human *MARCH6* CDS-containing plasmid (pcDNA3.1-GFP-*MARCH6*) was used as a template (kind gift of Dr. M. Hochstrasser Yale University) for the generation of fusion proteins as follows. The EYFP-*MARCH6* and ECFP-*MARCH6* constructs were generated by the amplification of *MARCH6* by Vent PCR (New England Biolabs) using the primers indicated in **Table 4**. Amplicon was inserted between the EcoRI-BamHI sites of pEYFP-C1 or pECFP-C1 vectors (Clontech, Mountain View USA), respectively. The *MARCH6*-EYFP construct was generated by exchanging GFP in pcDNA3.1-GFP-*MARCH6* plasmid to EYFP using primers depicted in **Table 4** and NheI-EcoRI sites.

**Table 4. Primers used for cloning MARCH6 constructs for FRET measurements**

<i>EcoRI-MARCH6</i>	FW	5'-ggaattctattATGGACACCCGCGGAGGAAGACATATGTAGA-3'
<i>BamHI-MARCH6</i>	R	5'-cgggatccTTATTCTTGGGATGACTGTGGAGGTGGTGGA-3'
<i>NheI-EYFP</i>	FW	5'-ctagctagcATGGTGAGCAAGGGCGAGGAGCT-3'
<i>EcoRI-EYFP</i>	R	5'-gaattccTTCGAA TTA <del>CTT</del> GTACAGCTCGTCCATG-3'

The WSB1-mCherry-SOCS fusion was generated by mutating STOP codon at the end of mCherry coding sequence (CDS) and inserting MluI site into pmCherry-N1 (Clontech, Mountain View USA) vector. Full length CDS and SOCS-box region of mouse WSB1 was amplified by Vent PCR. Mouse WSB1 was inserted to the 5'-end of mCherry using EcoRI-KpnI sites while the SOCS-box region was cloned after the 3'-end of STOP-codon mutant pmCherry-N1 between MluI-NotI sites. The used primers are summarized in **Table 5**.

**Table 5. Primers used for cloning WSB1 constructs for FRET measurements**

<i>mCherry</i>	FW	5'-GAGCTGTACAAGTCACGCGTGCGGCCGCGACT-3'
<i>mCherry</i>	R	5'-AGTCGCGGCCGCACGCGTGACTTGTACAGCTC-3'
<i>EcoRI-Wsb1</i>	FW	5'-ggaattcattATGGCCAGCTTTCCCCGAGGGTTA-3'
<i>KpnI-Wsb1</i>	R	5'-ggggtaccgtACCGCGGTAGGAGAGAAACG-3'
<i>MluI-Wsb1-SOCS</i>	FW	5'-tctacgcgtgtacAGGATTGTCCGGTAC-3'
<i>NotI-Wsb1-SOCS</i>	R	5'-gcggccgcaCTA <del>ACC</del> GCGGTAGGAGAG-3'

D2-EYFP, D2-ECFP, ECFP-D2, WSB1-ECFP and EYFP-USP33 constructs were described in [162]. For FRET experiments applied to test the interactions between chimeric deiodinases and ubiquitin ligases the chimeras were subcloned into pEYFP-N1 to generate C-terminal EYFP-fusion. Generation of chimeric deiodinases was described below. D2-T92A-EYFP construct was generated by overlap extension PCR on human D2 using the primers depicted in **Table 6** and cassette between internal AccI sites was exchanged in D2-EYFP construct resulting D2-T92A-EYFP, mutations indicated by lower case and underline.

**Table 6. Primers designed for D2-T92A construct for FRET measurements**

<i>hDIO2</i>	FW	5'- ggaattcattATGGGCATCCTCAGCGTAGACTTGCTGATCA -3'
<i>hDIO2-T92A</i>	R	5'- GTCACCTCCTTCTG <u>c</u> ACTGGAGACATGCA -3'
<i>hDIO2-T92A</i>	FW	5'- GTGCATGTCTCCAGT <u>g</u> CAGAAGGAGGTGA -3'
<i>hDIO2</i>	R	5'- cgggatcccgACCAGCTAATCTAGTTTTCT -3'

### 5.1.5. Generation of chimeric D1-D2 constructs

Cysteine-mutant rat D1 and human D2-containing vectors were described earlier [203]. Construction of chimeric deiodinases was based on the modification of cysteine-mutant rat D1 using standard recombinant DNA techniques as described below. All constructs were cloned into a Tet-off system, D10 vector [204] and tagged by N-terminal FLAG-epitope.

D1-K and D1-2K constructs were generated by the insertion of P230K or R223K/P230K mutations into D1 using site-directed mutagenesis PCR using primers indicated in **Table 7** and amplicon was inserted between the NheI and Bsu36I sites of the original rD1 construct.

**Table 7. Primers for generation of D1-D2 chimeras**

<i>NheI-D1</i>	FW	5'-ctagctagccATGGGGCTGTCCCAGCTATG-3'
<i>D1 P230K</i>	R	5'-CGGACTTCCTCAGGATTGTAGTTCCAAGGGCCcttTTTACCCTTGT-3'
<i>D1 R223K/P230K</i>	R	5'-TCGGACTTCCTCAGGATTGTAGTTCCAAGGGCCcttTTTACCCTTG TAGCAGATCtTGCCTTCCT-3'
<i>D2-loop</i>	FW	5'-acagaaggaggtgacaacCAGAAGTGCAACGTCTGGGA-3'
<i>D2-loop</i>	R	5'-gttgtcacctccttctgtTCCTGAGAGGGCGGACCACGGT-3'
<i>D1</i>	R	5'-ttccgcgccgctatggccgacgtcgacCTAGAAGTGAAGGCATGTGTCCAGG TGGGAT-3'
<i>D1</i>	FW	5'-ggaattcCCAGAGAGAGTCAAGCAGAACA-3'
<i>D1</i>	R	5'-ataagaatgcggccgcCTAGAAGTGAAGGCATGTGTCCA-3'

To generate the D1-K-loop and D1-2K-loop constructs the aa. 92-97 region of human D2 was inserted into D1-K and D1-2K constructs – respectively – by overlap-extension PCR followed using AccI-SalI sites and primers indicated in **Table 7**.

The Sec62-D1-2K-loop construct was generated by the insertion of D1-2K-loop construct between the EcoRI-NotI sites of human SEC62-containing plasmid [203] using PCR and the primers indicated in **Table 7**.

All constructs were confirmed by sequencing and the scheme of chimeras was summarized in **Fig. 27B**.

## 5.2. Cell culture and transfection

HEK-293T and HeLa cells were grown in Dulbecco's Modified Eagle Medium (Gibco, Gaithersburg USA) supplemented with 10 % Fetal Bovine Serum (Gibco,

Gaithersburg USA, PAA Laboratories, Dartmouth USA) and 1 % penicillin-streptomycin (Sigma, St. Louis USA). Briefly, for transient transfection cells were suspended in trypsin-EDTA solution and split into 6-well plate (Greiner, Kremsmünster Austria) or 35 mm diameter glass-bottom dish (MatTek, Ashland USA) at a concentration of  $2 \times 10^5$  cells/well. For luciferase promoter assay cells were plated into 24-well plate in  $0.7 \times 10^5$  cells/well concentration. Lipofectamine 2000 (Invitrogen) or Xtremegene HP (Roche, Basel Switzerland) reagents were used for cell transfection following the manufacturer's instruction.

### **5.3. Reagents and treatments**

3,3',5-triiodo-thyronine ( $T_3$ ) and thyroxine ( $T_4$ ) were purchase form Sigma Co. and dissolved in 40 mM NaOH, the appropriate concentration was determined by photometry. In treatments hormones were diluted in charcoal-stripped serum and used against NaOH vehicle. In brief, charcoal-stripped serum was generated as described in the following: 100 mg charcoal (Sigma, St. Louis USA) and 50 mg dextran (Sigma, St. Louis USA) were preincubated overnight in 10 mM Tris buffer (pH=7.6). After centrifugation, 40 ml FBS were added to the pellet and incubated for 1 h on 45 °C. The suspension was centrifuged and the supernatant was added to DMEM in 1:10 dilution followed by membrane filtration.

Tetracycline (Sigma, St. Louis USA) was dissolved in MQ water and used in 1  $\mu$ g/ml as final concentration for 12-hours.

MG132 (Calbiochem, Darmstadt Germany) proteasome inhibitor was dissolved in dimethyl sulfoxide (DMSO, Sigma, St. Louis USA) and used in 2  $\mu$ M final concentration for 4-hours against equivalent volume of DMSO as control.

Eeyarestatin I (Santa Cruz, Dallas USA) was dissolved in DMSO and used in 10  $\mu$ M as final concentration and applied for 4-hours against equivalent volume of DMSO as control.

Forskolin (Santa Cruz, Dallas USA) was dissolved in DMSO and applied in 20 nM as final concentration against equivalent volume of DMSO as control.

Treatments were carried out 48-hours after transfection.

#### 5.4. Luciferase promoter assay

On the second day after transfection cells were washed with ice-cold 1× PBS and collected in 1× Passive Lysis Buffer (Promega, Madison USA). Luciferase assay was carried out by using Dual-Luciferase® Reporter Assay System (Promega, Madison USA) and Luminoskan Ascent equipment (Thermo, Waltham USA) following the manufacturer's instructions.

#### 5.5. Quantitative PCR

Total RNA was isolated with the previously described TRIzol reagent for cell culture samples or with the RNeasy Lipid Tissue Mini Kit (Qiagen, Hilden Germany) for brown adipose tissue and nervous tissue samples. RNA was transcribed to cDNA with the High-Capacity cDNA Reverse Transcription Kit (Thermo, Waltham USA). RNA and cDNA concentrations were quantified using Qubit 2.0 fluorometric assay (Thermo, Waltham USA). TaqMan real-time PCR was applied for quantification of gene expression using TaqMan Fast Universal PCR Master Mix (Thermo, Waltham USA) and TaqMan Gene Expression Assays (Thermo, Waltham USA) listed below in **Table 8**. Reactions were run in ViiA™ 7 Real-Time PCR System (Thermo, Waltham USA). PCR data was normalized by the geometric mean of *Gapdh* and *Hprt1* housekeeping genes [205] in case of mouse samples and by *S18* in case of human cell lines.

Gene expression was calculated by  $2^{-\Delta\Delta C_t}$  method.

**Table 8. List of TaqMan Gene Expression Assays used in this study**

species	gene	Assay ID
mouse	<i>Adcyap1</i>	Mm00437433_m1
mouse	<i>Dio1</i>	Mm00839358_m1
mouse	<i>Dio2</i>	Mm00515664_m1
mouse	<i>Dio3</i>	Mm00548953_s1
mouse	<i>Slc16a2</i>	Mm01232724_m1
mouse	<i>Slco1c1</i>	Mm00451845_m1
mouse	<i>Thrb</i>	Mm00437044_m1
mouse	<i>Tshb</i>	Mm03990915_g1
mouse	<i>Trh</i>	Mm01963590_s1
mouse	<i>March6</i>	Mm00553784_m1
mouse	<i>Wsb1</i>	Mm01303073_m1
mouse	<i>Usp33</i>	Mm01316841_m1
mouse	<i>Ucp1</i>	Mm01244861_m1
mouse	<i>Gapdh</i>	Mm99999915_g1
mouse	<i>Hprt1</i>	Mm01545399_m1
human	<i>MARCH6</i>	Hs00195391_m1
human	<i>PTCH1</i>	Hs00181117_m1
human	<i>18S</i>	Hs99999901_s1

## 5.6. Western blot

Cells were harvested on the second day after transfection in Western lysis buffer containing 50 mM HEPES, 5 mM MgCl<sub>2</sub>, 1 mM EGTA, 100 mM NaCl, 1 % Triton X-100, 0.1 mM dithiothreitol and supplemented with cComplete™ Mini, EDTA-free protease inhibitor (Roche, Basel Switzerland). Protein concentration was determined by Bradford method and using Bio-Rad iMark Microplate Absorbance Reader. Samples were run in 4-20 % gradient (Bio-Rad) or 10 % acrylamide/bis-acrylamide gel. FLAG-epitope was detected by M2 anti-FLAG monoclonal antibody (Sigma, St. Louis USA) using in 1:3000 dilution in 1× PBS and BM Chemiluminescence Western Blotting Kit (Roche, Basel Switzerland) following the manufacturers instruction. Western blots were imaged onto Kodak BioMax MS film (Sigma, St. Louis USA).

## 5.7. Deiodinase assay

Tissue samples or cell pellets were obtained on the second day after transfection and sonicated in deiodinase assay buffer (100 mM potassium-phosphate, 1 mM EDTA, 250 mM sucrose, 10 mM dithiothreitol, pH=7.0) on ice. <sup>125</sup>I-labelled T<sub>4</sub> (PerkinElmer, Waltham USA) was purified on the day of measurement on LH-20 Sephadex column (GE

Healthcare Life Sciences, New Jersey USA). Briefly, for D1 activity assay the following concentrations were used: 10 mM dithiothreitol, 100 000 CPM <sup>125</sup>I-labelled T<sub>4</sub> (Sigma, St. Louis USA), 1 μM T<sub>4</sub> and cell total lysate in 300 μl as final reaction volume. For D2 activity measurement the following concentrations were used: 20 mM dithiothreitol, 1 mM 6-n-propyl-2-thiouracil (PTU), 100 nM T<sub>3</sub>, 100 000 CPM <sup>125</sup>I-labelled T<sub>4</sub>, 100 nM T<sub>4</sub> and cell total lysate in 300 μl as final volume. Assay was terminated by the addition of 200 μl normal horse serum (PAA Laboratories, Dartmouth USA) and 100 μl trichloroacetic acid (Sigma, St. Louis USA) on ice. Samples were centrifuged on 13,000 rpm and supernatants were collected and measured using gamma counter (PerkinElmer, Waltham USA).

Deiodinase activities were calculated by **Eq. 1**.

---


$$Activity = \frac{(CPM_S - CPM_B) * c_{T_4}}{CPM_T * 0.6 * t * m} \quad \text{Equation 1.}$$


---

where:

CPM<sub>S</sub>: <sup>125</sup>I counts of sample

CPM<sub>B</sub>: <sup>125</sup>I counts of background, non-transfected cells

CPM<sub>T</sub>: <sup>125</sup>I counts of tracer mix

cT<sub>4</sub>: T<sub>4</sub> concentration in reaction mix

t: assay time

m: amount of protein in the reaction from the sample

---

### 5.8. Secreted alkaline phosphatase (SEAP) assay

Cells were cotransfected with the pSEAP2-Promoter plasmid containing the SV40 early promoter (Clontech, Mountain View USA). Media were collected on day of cell treatment and stored on -20 °C until measurement. SEAP assay was performed using NovaBright Chemiluminescent SEAP Reporter Gene Assays (Thermo, Waltham USA) and Luminoskan Ascent equipment (Thermo, Waltham USA) according to the manufacturer's instructions.

## 5.9. Fluorescent resonance energy transfer (FRET)

Cells were transfected as described above with the exception of plating into 35-mm glass-bottom dishes (MatTek, Ashland USA). Treatments and FRET measurements were performed on the second day after transfection using Nikon A1R laser scanning microscope equipped with Tokai Hit stage top incubator and Supertech temperature controller allowing the maintenance of constant 37 °C and 5 % CO<sub>2</sub>-level during imaging. Spectral detector was used for FRET measurement in virtual filter mode with the following parameters: 453 nm argon laser for ECFP excitation with 465-500 nm detection range; 514 nm argon laser for EYFP excitation with 515-540 nm detection range; 561 nm DPSS laser for excitation of mCherry with 600-650 nm detection range. Acceptor photobleaching method was applied, in case of 3-FRET experiments mCherry and EYFP were bleached sequentially in this order. Cells with at least 80 % bleach efficiency were involved into analysis.

Calculation of FRET efficiency was based on the increase of donor emission by the disruption of acceptor fluorophore using photobleaching and determined by **Eq. 2 and 3**.

FRET efficiency was normalized by the same value of fusion constructs of fluorophores (ECFP-EYFP and EYFP-mCherry) demonstrating the maximal achievable FRET. The background FRET signal caused by e.g. the oligomerization of fluorescent proteins was determined by the measurement of interaction between monomeric fluorescent proteins. The presence of interaction is defined by significant difference in FRET signal between investigated FRET pairs and the corresponding monomeric fluorescent proteins.

---

$$E_{FRET(ECFP-EYFP)} \% = \frac{ECFP_{postbleach} - ECFP_{prebleach}}{ECFP_{prebleach}} \times 100 \quad \text{Equation 2.}$$

---

---

$$E_{FRET(EYFP-mCherry)} \% = \frac{EYFP_{postbleach} - EYFP_{prebleach}}{EYFP_{prebleach}} \times 100 \quad \text{Equation 3.}$$

---

## 5.10. Animals and surgery

Animal experiments were performed in accordance with the legal requirements of the Animal Care and Use Committees of the Institute of Experimental Medicine (Hungarian Academy of Sciences, Budapest) following the European Communities Council Directive (2010/63/EU).

### 5.10.1. Intracerebroventricular PACAP administration

Stereotaxic surgery was performed using Stereotaxic Instrument (David Kopf Instruments, Tujunga USA) to insert 26-gauge stainless-steel guide cannula (Plastics One, Roanoke USA) into the lateral ventricle of 8-week old male CD1 mice to the following coordinates: anteroposterior -0.2; lateral -1.0 and dorsoventral -2.0 from Bregma. Cannula was fixed by “Krazy Glue” (Electron Microscopy Sciences, Fort Washington USA). After one week recovery 33-gauge stainless-steel internal cannula was connected to the guide cannula and 300 pmol PACAP 1-38 in 2  $\mu$ l artificial CSF (aCSF: 140 mM NaCl; 3.35 mM KCl; 1.15 mM MgCl<sub>2</sub>; 1.26 mM CaCl<sub>2</sub>; 1.2 mM Na<sub>2</sub>HPO<sub>4</sub>; 0.3 mM NaH<sub>2</sub>PO<sub>4</sub>; and 0.05 % BSA, pH 7.4) or 2  $\mu$ l aCSF/BSA was injected into the lateral ventricle. Animals were sacrificed 4-hours after treatment by decapitation, blood and tissue samples were collected. Blood was centrifuged twice at 3000g at 4 °C and sera were stored at -80 °C. The mediobasal hypothalamus was dissected and the remaining parts of brain were frozen, cut to 1 mm thick coronal section, and the region of paraventricular nucleus was isolated using micropunch technique. The samples were stored at -80°C until further processing.

### 5.10.2. Generation of hypo- and hyperthyroid mice

To generate hypothyroid animals 8-week-old CD1 mice were fed with iodide-deficient chow and drinking water was supplemented with 0.1 % sodium perchlorate and 0.5 % methimazole (Sigma, St. Louis USA) for 3 weeks. Hyperthyroid mice were generated by the following protocol: 10 mM T<sub>4</sub> stock was prepared in 40 mM NaOH solution which was diluted in 0.002 % BSA-containing PBS to 75  $\mu$ g/ml as final dilution. 200  $\mu$ l 75  $\mu$ g/ml solution was injected i.p. for 3 days resulting 15  $\mu$ g/day/animal dosage [206].

### 5.11. Thyroid hormone measurement

Serum free T<sub>3</sub> and T<sub>4</sub> levels were measured using AccuLite CLIA microwells assays kit (Monobind, Lake Forest USA) with Luminoskan Ascent Luminometer and LIAISON® fT<sub>3</sub> and fT<sub>4</sub> assays with LIAISON® Analyzer following the manufacturer's instructions.

### 5.12. TSH bioactivity measurement

Chinese hamster ovary cells stably transfected with the human TSH receptor (CHO-TSHR) was described in [207] and were plated 24-hours before the assay in 96-well plate in concentration of  $5 \times 10^4$  cells/well. Cells were preincubated in 90  $\mu$ l stimulation buffer (5 mM HEPES, 0.1 % BSA and 0.5 mM IBMX (Sigma, St. Louis USA) in  $1 \times$  HBSS) for 30 minutes. 10  $\mu$ l serum samples were added to the cells and incubated for 1 hour followed by lysis in ethanol led to evaporate in 37 °C. Cells were collected in 50  $\mu$ l Lysis buffer (5 mM HEPES, 0.1 % BSA and 0.3 % Tween-20 in MQ). Lysates were processed for cAMP measurement using AlphaScreen cAMP Assay Kit and EnSpire® Multimode Plate Reader (PerkinElmer, Waltham USA) following the manufacturer's instructions.

### 5.13. Immunohistochemistry

Mice were perfused transcardially with 40 ml 4 % paraformaldehyde dissolved in 0.1 M PB. The brains were removed and postfixed for 2 hours following by cryoprotective immersion in 30 % sucrose in PBS overnight. 25  $\mu$ m thick coronal sections were cut using freezing microtome (Leica Microsystems, Wetzlar Germany). Slices were permeabilized in 0.5 % Triton X-100 (Sigma, St. Louis USA) and 0.5 % H<sub>2</sub>O<sub>2</sub> in PBS for 15 min and non-specific antibody binding was blocked by treatment in 2 % normal horse serum in PBS. Antibodies and sera were diluted in 2 % normal horse serum-containing PBS. Dilution and source of antibodies and sera are summarized in **Table 9**. The PAC1R antisera from Dr. Shioda was raised C-terminal intracellular domain while P8872 N-terminal extracellular domain. The two antisera produced the same staining pattern (not shown). Imaging was performed using Nikon A1R laser scanning microscope.

---

**Table 9. List of antibodies and reagents used for immunohistochemistry**

---

antigen	primary antibody	secondary antibody		amplification		fluorophore
<b>PAC1</b>	1:100 rabbit anti-PAC1 serum (from Dr. Shioda, Showa University)	1:250 biotin-conjugated anti-rabbit IgG (Jackson)	1:1000 avidin-biotin complex (Vector Lab)	biotinylated tyramide TSA amplification kit (Perkin Elmer)	1:1000 ABC	streptavidin-fluorescein-isothiocyanate (FITC) (Jackson)
<b>PAC1</b>	1:100 rabbit anti-PAC1 antibody (Sigma)		1:1000 avidin-biotin complex (Vector Lab)	biotinylated tyramide TSA amplification kit (Perkin Elmer)	1:1000 ABC	streptavidin-fluorescein-isothiocyanate (FITC) (Jackson)
<b>vimentin</b>	1:1500 goat anti-vimentin antibody (Santa Cruz)	1:500 Alexa555-conjugated IgG (Thermo)		-		Alexa555
<b>GFAP</b>	1:500 goat anti-GFAP antibody (Santa Cruz)	1:500 Alexa555-conjugated IgG (Thermo)		-		Alexa555

#### 5.14. Statistical analysis

Prism 3.0 (GraphPad Software, La Jolla USA) and Statistica 8.0 (StatSoft, Tulsa USA) software's were used for statistical analyzes. In brief, data were visualized as mean  $\pm$  SEM and for indication of significance level the following convention was used: \*:  $p < 0.05$ ; \*\*:  $p < 0.01$ ; \*\*\*:  $p < 0.001$ . In general, two groups was compared by t-test, three or more samples were compared by the appropriate type of ANOVA and *post hoc* test. The applied statistical methods were specified in detail in the legends below figures.

## 6. RESULTS

### 6.1. INTERACTION BETWEEN PACAP AND THYROID HORMONE SIGNALING

#### 6.1.1. PACAP induces D2 expression via cAMP/PKA pathway

Previous studies identified signaling pathways involved in the transcriptional control of D2 including cAMP/PKA, NF- $\kappa$ B and TTF1 [119, 149, 155] however upstream factors regulating D2 via these pathways are poorly characterized. The cAMP/PKA pathway is crucial in the thermal regulation of BAT and photoperiodic alterations of TH action in pineal gland, in both cases D2 is induced by adrenergic control. However the importance of cAMP/PKA pathway in tanycytes is poorly understood. Pituitary adenylate cyclase-activating polypeptide (PACAP) was identified as stimulatory factor of adenylate cyclase increasing intracellular cAMP production. Further studies revealed the broad range of biological action of PACAP and the hypothalamus is one of the major areas of PACAP-mediated processes e.g. control of energy balance, central thermoregulation and regulation of stress axis. Despite the remarkable overlap between PACAP action and TH-mediated processes the interaction of this two major pathway is poorly understood.

The cAMP/PKA is one of the second messenger systems that is both activated by PACAP and was also reported to stimulate D2. This raised the question whether PACAP is able to act on *DIO2* transcription. To test this hypothesis the effect of PACAP treatment on 7 kb 5' flanking region (5' FR) of human *DIO2* gene was measured using dual luciferase promoter assay in HEK-293T cells found to express endogenous PACAP receptor PAC1R protein (**Fig. 14A**). 100 nM PACAP induced 7-fold increase of *DIO2* promoter activity (wtDIO2-Luc) after 4-hours and the induction was still detectable after 24-hours (**Fig. 14B**). To test whether PACAP acts via cAMP/PKA pathway the cAMP response element (CRE) of 5' FR of *DIO2* gene was modified using site-directed mutagenesis to generate cAMP-insensitive *DIO2* promoter region. The mutation is depicted on **Fig. 14C**. The effect and specificity of mutation was tested by the response to coexpression of PKA catalytic subunit  $\alpha$  and NF- $\kappa$ B subunit p65. The CREmut-*DIO2*-Luc construct lost its responsiveness to PKA but remained to be inducible by p65 (**Fig. 14D**).

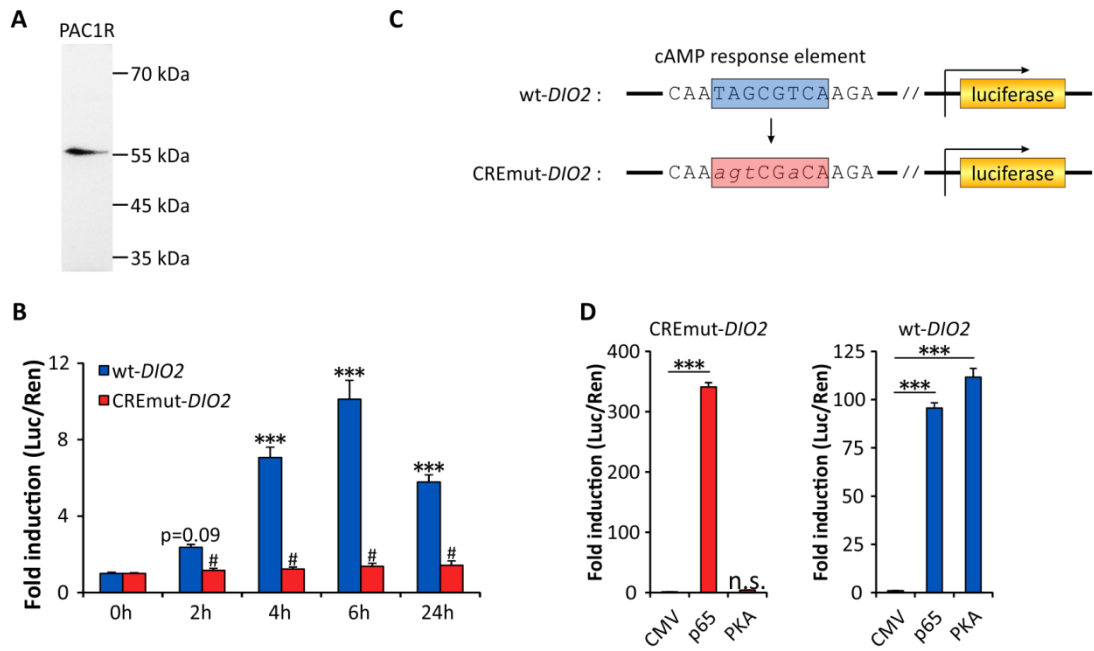


**Figure 14. PACAP induces *DIO2* promoter via cAMP/PKA pathway**  
 (A) PACAP receptor (PAC1R) is expressed in HEK-293T cells detected by Western blot. (B) Time-dependent induction of *DIO2* promoter activity by 100 nM PACAP 1-38 treatment (mean  $\pm$  SEM, n=4 per group). \*\*: p<0.01, p<0.001 by one-way ANOVA followed by Newman-Keuls *post hoc* test vs 0h group; #: p<0.001 by t-test vs the wt-*DIO2* promoter at the corresponding time-point. (C) Schematic draw of wild type (wt-*DIO2*) and cAMP response element mutant (CREmut-*DIO2*) *DIO2* 7 kb promoter luciferase reporter construct; mutations are indicated by lower case. (D) Responsiveness of CREmut-*DIO2* and wt-*DIO2* promoter to the induction by PKA and p65 (mean  $\pm$  SEM, n=3 per group). \*\*\*: p<0.001 by t-test vs non-induced (CMV) group.

The CREmut-*DIO2*-Luc construct was found completely insensitive to treatment with 100 nM PACAP indicating that PACAP-mediated upregulation of *DIO2* 5' FR was carried out exclusively by cAMP/PKA pathway (Fig. 14B).

### 6.1.2. Tanycytes express the PAC1R PACAP receptor

In order to identify cell types and brain regions where PACAP-mediated regulation of D2 could be relevant *in vivo* the expression of PAC1R is studied in D2-expressing cells. In the brain two major D2-expressing cell types are known; astrocytes and hypothalamic tanycytes. Immunohistochemistry was performed to test whether these cells express PAC1R protein. In vimentin positive tanycytes colocalization was observed between vimentin- and PAC1R-immunoreactivity in both of the  $\alpha$ - and  $\beta$ -tanycytes subregion

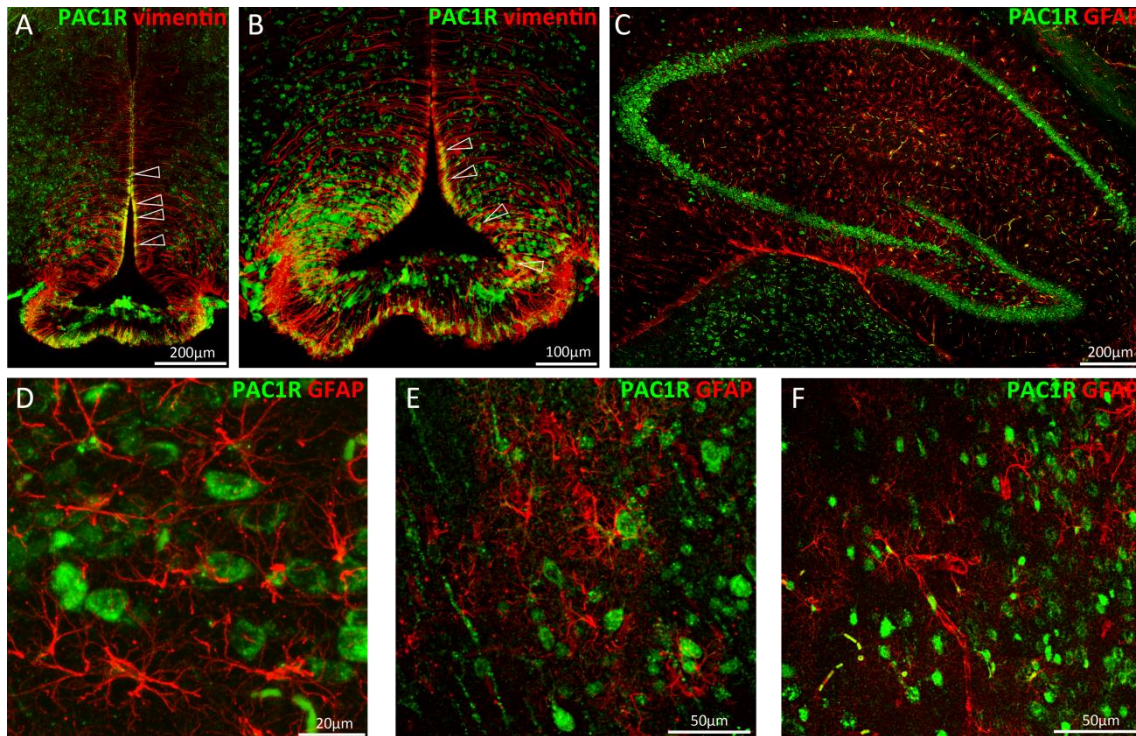


**Figure 15. PAC1R PACAP receptor is expressed in tanyocytes of the mouse hypothalamus**  
 (A) Confocal images of dual immunofluorescence labeling of PAC1R (green) and vimentin (red) as tanyocyte marker in the mouse mediobasal hypothalamus, open arrowheads indicate the colocalization of vimentin and PAC1R. (B) Higher magnification of median eminence region of panel A. (C) PAC1R (green) and the astrocyte marker GFAP (red) immunoreactivity did not colocalize in the mouse hippocampus. (D) Higher magnification from the region of dentate gyrus of panel C. (E) and (F) PAC1R (green) and astrocyte marker GFAP (red) immunoreactivity did not colocalize in the cortex.

(Fig. 15A and B). In contrast, detectable PAC1R-staining was not observed in case of hippocampal and cortical GFAP-positive astrocytes (Fig. 15C and F). These results indicate tanyocytes as cell-type where TH activation could be targeted by PACAP signaling.

### 6.1.3. PACAP affects the feedback and development of HPT axis

Having identified PAC1R receptor expression in tanyocytes asked whether PACAP affects local  $T_3$  generation and regulation of HPT axis *in vivo*. Therefore 300 pmol PACAP was injected intracerebroventrically into male CD1 mice and animals were sacrificed 4 hours after treatment. PACAP resulted 2.4-fold increase of D2 activity in the mediobasal hypothalamus where D2 is expressed exclusively in tanyocytes indicating these cells have functional PACAP signaling (Fig. 16A). The response of TRH neurons to the increased TH activating capacity was tested by the measurement of *Trh*

expression in microdissected samples of the paraventricular nucleus using quantitative PCR. *Trh* mRNA level was decreased by 45.89 % compared to control mice (**Fig. 16B**). *Tshb* (encoding the  $\beta$  subunit of TSH) mRNA was suppressed by 23.30 % in pituitary (**Fig. 16C**) while *Dio2* expression in this region was not changed by PACAP treatment (**Fig. 16D**). Serum TSH bioactivity and free T<sub>4</sub> level were unaffected after 4-hours (**Fig. 16E and F**) however that was expected taking into account the requirement of the series of transcriptional and secretory events in the HPT axis leading to alterations in TH synthesis and secretion and the long half-life of circulating T<sub>4</sub>. The D2 activities in cortex and hippocampus remained unaffected (**Fig. 16G and H**).

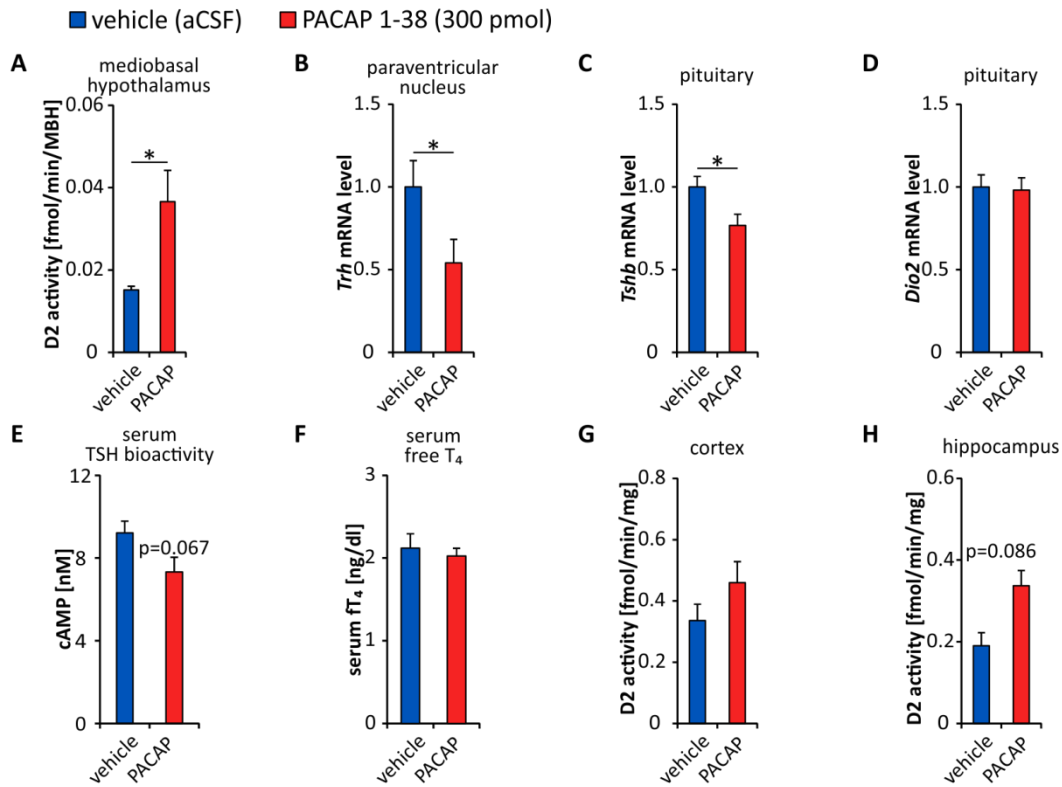


**Figure 16. PACAP induces D2 in tanycytes modulating HPT axis**

Effect of intracerebroventricular administration of 300 pmol PACAP 1-38 for 4-hour on (A) D2 activity in the mediobasal hypothalamus (B) *Trh* expression of the paraventricular nucleus (C) *Tshb* expression in the pituitary (D) *Dio2* expression in the pituitary (E) serum TSH bioactivity (F) serum free T<sub>4</sub> concentration (G) D2 activity in the cortex (H) D2 activity in the hippocampus. Quantitative PCR data were normalized to the geometric mean of *Gapdh* and *Hprt1* housekeeping genes and depicted as fold change compared to control group. (mean  $\pm$  SEM, n=8 in PACAP-treated and n=9 in control group) \*: p<0.05 by t-test.

Acute PACAP treatment resulted remarkable changes in HPT axis therefore we also studied the long term effect of altered PACAP signalization on TH metabolism and the HPT axis using PACAP-deficient mice. Interestingly, these animals were found hypothyroid at the periphery showing decreased serum free T<sub>4</sub> and T<sub>3</sub> levels (**Fig. 17A and B**). TSH bioactivity was also decreased indicating alterations in the central regulation of HPT axis (**Fig. 17C**). As a consequence the hippocampal and cortical D2 activities were elevated compensating the decreased circulating TH availability (**Fig. 17D and E**). Regions where local T<sub>3</sub> production has systemic importance via the modulation of HPT axis, in the mediobasal hypothalamus and pituitary the D2 activities were found to be unaffected (**Fig. 17F and G**).

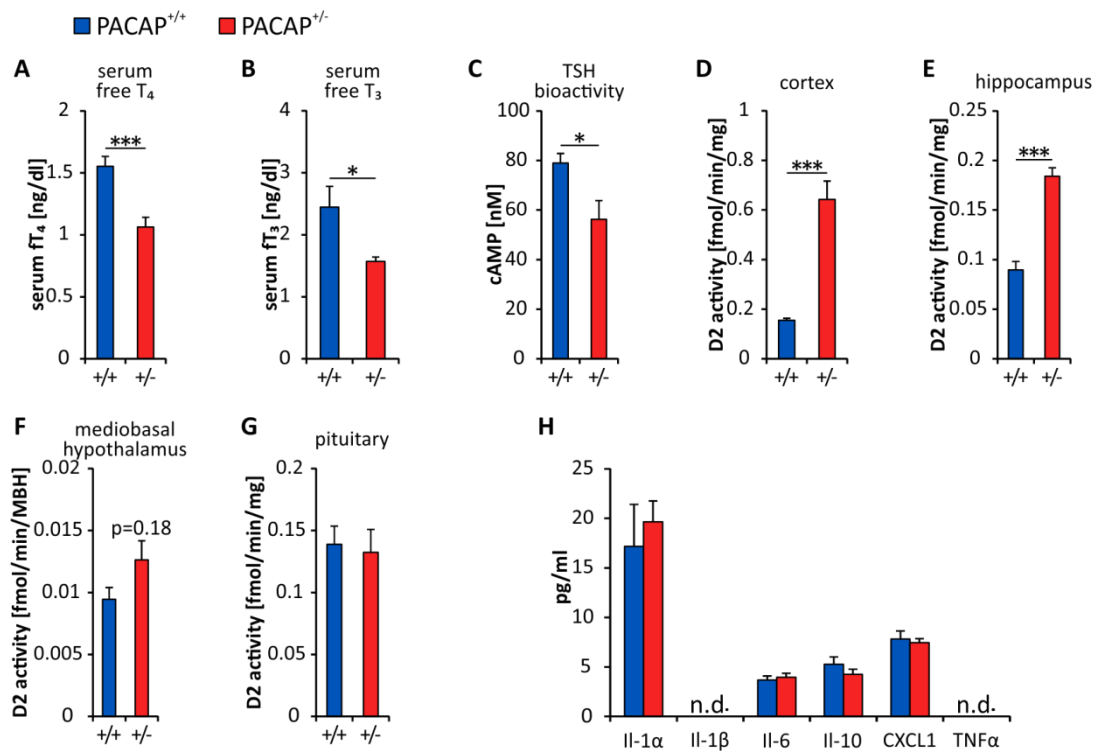


**Figure 17. Thyroid hormone economy in adult PACAP-deficient (PACAP<sup>+/-</sup>) mice**

(A) Serum free T<sub>4</sub> concentration (B) serum free T<sub>3</sub> concentration (C) TSH bioactivity (D) D2 activity in the cortex (E) D2 activity in the hippocampus (F) D2 activity in the mediobasal hypothalamus (G) D2 activity in the pituitary (H) serum inflammatory and antiinflammatory cytokine concentrations of wild-type and PACAP-deficient mice (mean ± SEM, n=5 in PACAP<sup>+/+</sup> and n=9 in PACAP<sup>+/-</sup>). n.d.: not detectable \*: p<0.05; \*\*\*: p<0.001 by t-test.

Signs of central hypothyroidism of the observed phenotype were similar to the situation hallmarking non-thyroidal illness where infection results in suppressed HPT axis. Taking into account the important antiinflammatory effect of PACAP, the cytokine profile reflecting the immune status of PACAP-deficient animals was measured. Concentrations of IL-1 $\alpha$  IL-1 $\beta$  IL-6, IL-10, CXCL1 and TNF $\alpha$  were not different between PACAP<sup>+/+</sup> and PACAP<sup>+/-</sup> genotypes indicating that the affected HPT axis was not caused by a secondary process induced by altered immune state (**Fig. 17H**).

As demonstrated in *Dio3* knock-out mice – that are hypothyroid despite the loss of the inactivating deiodinase – development of the HPT axis has a critical postnatal period when improper local T<sub>3</sub> availability results in altered set point of the axis with consequences persisting also in adults. Therefore we speculated that the development of HPT axis could be the reason of the phenotype of the PACAP-deficient mice. To test this hypothesis the expression of genes involved in local TH metabolism and signalization were compared between 5-days old PACAP<sup>+/+</sup> and PACAP<sup>+/-</sup> pups. Genes involved in measurement included activating and inactivating deiodinases: *Dio2*, *Dio3*; thyroid hormone transporters: *Slco1c1* (*Oatp1c1*) and *Slc16a2* (*Mct8*); thyroid hormone receptor  $\beta$ , *Thrb* and *Trh*. Importantly, *Dio3* mRNA was increased in PACAP-deficient mice indicating increased TH inactivation resulting local hypothyroid conditions during the establishment of proper set point of the feedback of HPT axis (**Fig. 18A**). Other genes were found to be statistically unaffected. The peripheral TH availability was assessed by measuring hepatic *Dio1* and *Thrb* expression well-established markers of thyroid status. *Dio1* was found to be decreased while *Thrb* showed slight elevation indicating hypothyroid periphery (**Fig. 18B**).

#### **6.1.4. Thyroid hormones modulate *Adcyap1* (PACAP) gene transcription**

Having identified the PACAP as a novel central regulator of HPT axis we tested whether the PACAP-TH interaction is bidirectional therefore we investigated whether the THs are able to modulate PACAP synthesis. Therefore the modulatory effect of T<sub>3</sub> was tested on 3 kb 5' FR of mouse *Adcyap1* gene in HEK-293T cells using dual luciferase reporter assay. 5' FR of *Adcyap1* gene was found to be insensitive for 0.1, 1, 10 and 100 nM T<sub>3</sub> treatment that the basal activity of the PACAP promoter is not

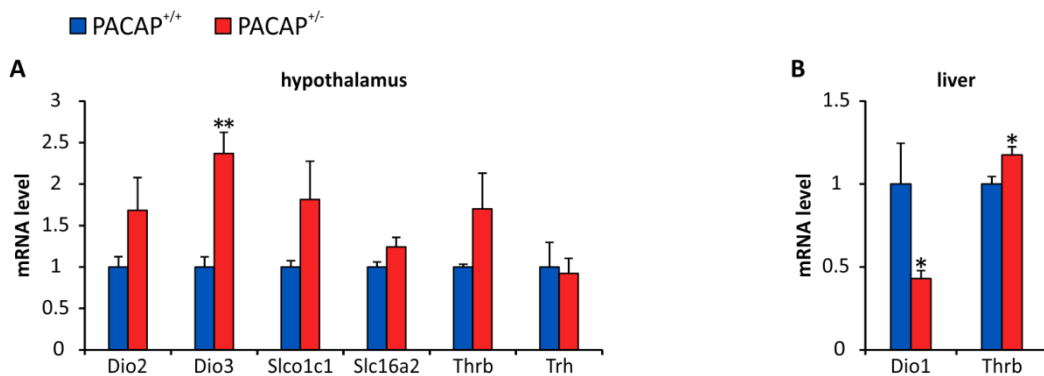


**Figure 18. Regulation of local thyroid availability and action in 5-day old PACAP-deficient mice** (A) Expression of genes involved in thyroid hormone metabolism (*Dio2*, *Dio3*), thyroid hormone transport (*Slco1c1*, *Slc16a2*), thyroid hormone receptor  $\beta$  (*Thrb*) and *Trh*. (B) Expression of *Dio1* and *Thrb* in liver used to assess the peripheral thyroid hormone economy. Quantitative PCR data were normalized to the geometric mean of *Gapdh* and *Hprt1* housekeeping genes and depicted as fold change compared to wild-type (PACAP<sup>+/+</sup>) group (mean  $\pm$  SEM, n=4 per genotype). \*: p<0.05, \*\*: p<0.01 by t-test.

regulated directly by THs (**Fig. 19A**). It was previously shown that *Adcyap1* transcription is upregulated by the cAMP/PKA second messenger system as demonstrated by the presence of catalytically active  $\alpha$  subunit of PKA (**Fig. 19B**). Therefore we tested the effect of THs on the induction of 5' FR of *Adcyap1* by cAMP.

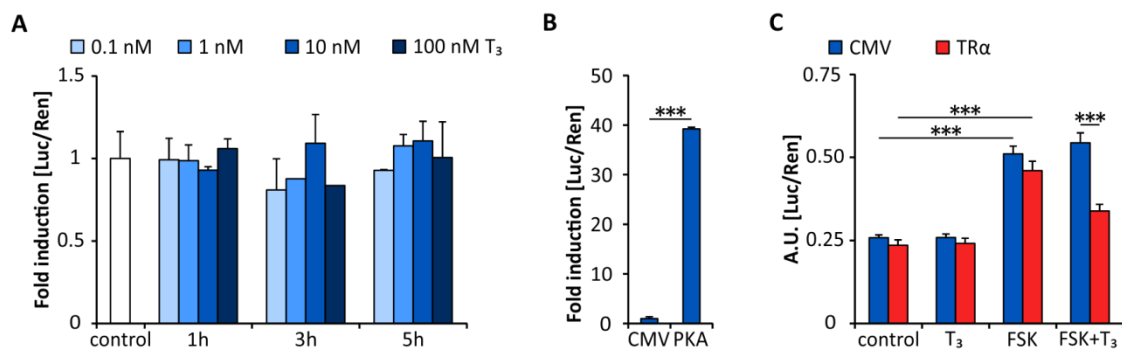


**Figure 19. Thyroid hormones interferes the cAMP/PKA-mediated activation of *Adcyap1* (PACAP) promoter**

(A) Effect of 0.1, 1, 10 and 100 nM T<sub>3</sub> for 1-, 3-, 5-hours on the promoter activity of the 3 kb 5' FR of mouse *Adcyap1* gene in HEK-293T cells (mean  $\pm$  SEM, n=4 per group). (B) Induction of *Adcyap1* gene promoter to constitutive active PKA signal (mean  $\pm$  SEM, n=4 per group) \*\*\*: p<0.001 by t-test. (C) Effect of 100 nM T<sub>3</sub> and mouse thyroid hormone receptor  $\alpha$  (TR $\alpha$ ) to the cAMP/PKA-mediated induction of the *Adcyap1* promoter by 20 nM Forskolin (FSK) mean  $\pm$  SEM, n=6 per group). A.U.: arbitrary unit (Firefly/Renilla luciferase) \*\*\*: p<0.001 by factorial ANOVA indicated interaction between T<sub>3</sub>, FSK treatment and presence of TR $\alpha$  and followed by Tukey *post hoc* test.

In the presence of TR and T<sub>3</sub> the inductive effect of adenylate cyclase activator Forskolin (20 nM) was significantly decreased indicating that THs are able to antagonize the induction of *Adcyap1* transcription by cAMP/PKA pathway (**Fig. 19C**).

To test the *in vivo* significance of THs in the regulation of PACAP synthesis hypo- and hyperthyroid mice were generated and expression of *Adcyap1* gene was measured on microdissected regions with identified role in the hypothalamic regulation of energy homeostasis using quantitative PCR. *Adcyap1* mRNA level was decreased in the parabrachial nucleus by hyperthyroid conditions (**Fig. 20B**), while in pituitary the *Adcyap1* expression was decreased under hypothyroid conditions (**Fig. 20H**). However, in general, *Adcyap1* transcription was not affected by altered TH level (**Fig. 20**).

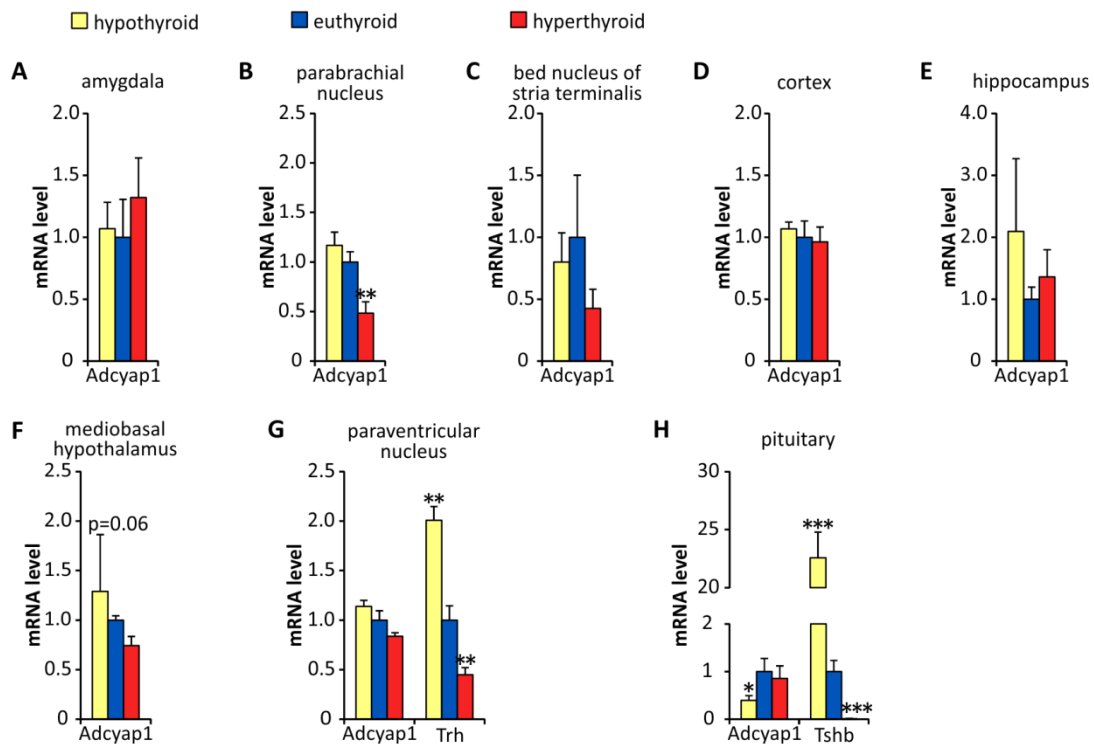


**Figure 20. *Adcyap1* gene expression in hypo-, eu- and hyperthyroid mice**

Expression of *Adcyap1* gene in microdissected brain samples of hypo-, eu- and hyperthyroid mice. The qPCR data were normalized to the geometric mean of *Gapdh* and *Hprt1* housekeeping genes and depicted as fold change compared to euthyroid levels (mean  $\pm$  SEM, n>4 per group) \*: p<0.05; \*\*: p<0.01 and \*\*\*: p<0.001 by one-way ANOVA followed by Newman-Keuls *post hoc* test vs euthyroid group.

## 6.2. CHARACTERIZATION OF MARCH6 AS D2 UBIQUITIN LIGASE

### 6.2.1. Expression profile of *March6*

*March6* was earlier shown to be coexpressed with D2 in tanycytes. First we aimed to identify extrahypothalamic target tissues where MARCH6 could be involved in the posttranslational control of TH activation via the ubiquitination of D2. Therefore the expression of the *March6* gene was studied in different organs known to be important in D2-mediated T<sub>3</sub> generation. Total mRNA was isolated from the cerebral cortex, pituitary, liver, kidney, muscle, heart, brown adipose tissue, and thyroid gland of Wistar rats and processed for semiquantitative RT-PCR. Intron-spanning primers were designed to detect *March6*, *Wsb1* and *Cyclophilin A* as housekeeping gene. Strong *March6* expression was detected in the cerebral cortex, pituitary, kidney, muscle and heart while lower level of *March6* mRNA could be detected in the liver (**Fig. 21**). *Wsb1*, the substrate binding subunit of the firstly described ECS<sup>WSB1</sup> D2 ubiquitin ligase was also expressed in the studied tissues. *March6* mRNA was much less intense in the brown adipose tissue while *Wsb1* showed solid expression in this tissue. Interestingly, *March6* and *Wsb1* transcripts could not be detected in the thyroid gland (**Fig. 21**). These data identified several tissues where MARCH6 could be potentially involved in the regulation of D2 e.g. the cerebral cortex, pituitary, muscle, heart where D2 is the exclusive or predominant activating deiodinase enzyme. It needs to be noted that other substrates targeted by MARCH6-mediated ubiquitination are identified e.g. squalene monooxygenase (SM), 3-hydroxy-3-methyl-glutaryl coenzyme A reductase (HMGCR) involved in cholesterol biosynthesis [208, 209] and regulator of G protein signaling 2 (RGS2) stimulating the hydrolysis of GTP by G<sub>α</sub> subunit of G-protein complexes [210] therefore the action of MARCH6 is not obviously restricted to D2 in these tissues. Additionally, MARCH6 has identified role as ERAD ubiquitin ligase thus beyond the posttranslational control of steroid biosynthesis, G-protein signaling and TH activation it also plays a crucial role in the quality control of protein translation.

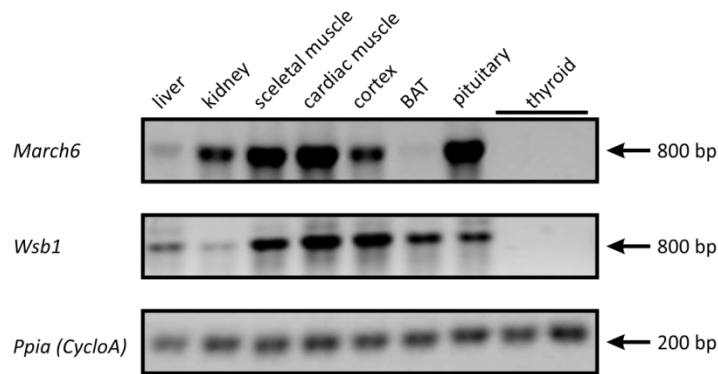


**Figure 21. Expression of *March6* and *Wsb1* differ between rat tissues**  
 Results of semiquantitative RT-PCR on tissue samples from adult Wistar rats. *Ppia* (Peptidylprolyl isomerase A, Cyclophilin A) was used as housekeeping gene to control initial amount of RNA.

### 6.2.2. Characterization of the human *MARCH6* promoter

Having identified tissues where *MARCH6* could be involved in the regulation of TH activation we aimed to study signaling pathways that could potentially modulate  $T_3$  generation via the *MARCH6*-driven ubiquitination of D2. Since the promoter region of *MARCH6* gene is poorly characterized we aimed to identify transcriptional factors that are involved in the regulation of *MARCH6* expression. At first, potential transcription factor binding sites were predicted by *in silico* analysis of the 5' flanking region (5' FR) of human *MARCH6* gene using TRANSFAC database (Biobase GmbH., Germany). The 5' FR analysis focused mainly on the known regulators of TH metabolism and important modulators of development. In this manner potential NF- $\kappa$ B and CREB binding sites were identified. The core promoter of the *MARCH6* gene contains GC-rich region several potential SP1 sites were located within the 130 bp-length region 5' to the transcriptional start site (TSS). *MARCH6* 5' FR was summarized on **Fig. 22A**.

To test the impact of these potential regulators on the transcription of *MARCH6* gene, first we cloned the 3.5 kb fragment of 5' flanking region of the human *MARCH6* gene into pGL3-basic Firefly luciferase-expressing vector. The pGL3-*MARCH6* construct was used in dual luciferase assay allowing the measurement of promoter activity in presence of active transcriptional factors. This approach also allows the mutagenesis- or deletion-based characterization of regions with anticipated role in gene regulation. HEK-293T cells were used to coexpress promoter constructs with transcription factors. First the NF- $\kappa$ B and cAMP/CREB pathways were tested by overexpressing p65 and

protein kinase A catalytic subunit  $\alpha$  (PKA), respectively. The 3.5 kb 5' flanking region of *MARCH6* gene was downregulated by both NF- $\kappa$ B and cAMP signals (**Fig. 22B**).

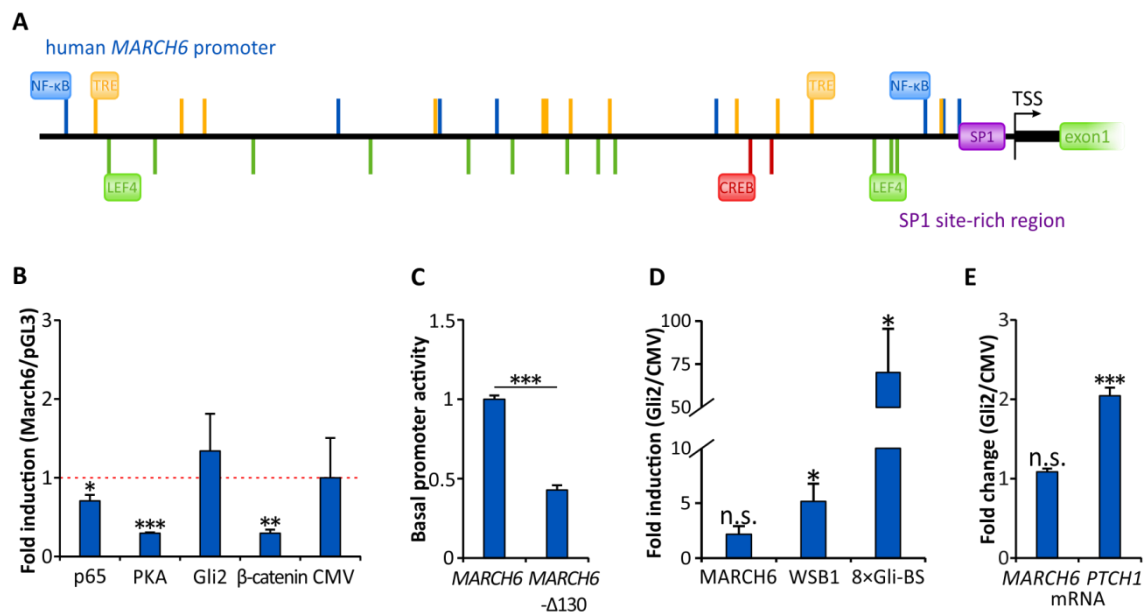
Additional experiments were performed to test the functional significance of the putative SP1 binding sites. For this purpose, the 130 bp-length region up from TSS containing the predicted SP1 sites was deleted. The truncation resulted a ~50 % decrease in the basal promoter activity demonstrating the functional role of SP1 sites in the regulation of *MARCH6* transcription (**Fig. 22C**).

It is known that Sonic hedgehog (SHH) signaling antagonizes TH activation via stimulating the ubiquitination of D2 [161]. It was shown that expression of WSB1 subunit of the ECS<sup>WSB1</sup> ubiquitin ligase of D2 is upregulated by the transcription factor Gli2, the main effector of SHH signalization. This mechanism allows a cross-talk between the two important morphological signals but it is not clarified whether the *MARCH6* is also involved in the SHH-mediated downregulation of TH activating capacity. Therefore the transcriptional regulation of the 3.5 kb 5' flanking region of *MARCH6* gene upon SHH induction was tested. Experiments were performed in HeLa cells which were previously shown to be more appropriate to study of SHH-related effects. To mimic the SHH signal expression plasmid containing the N-terminal truncated constitutive active fragment of Gli2 (Gli2- $\Delta$ N2) transcription factor was cotransfected with the pGL3-*MARCH6* reporter construct. While the Gli2 reporter positive control (8 $\times$ Gli-BS) and *WSB1* promoter were induced in this experimental setup *MARCH6* was not upregulated (**Fig. 22D**).

This finding was also supported by measuring the alterations of endogenous *MARCH6* mRNA. HeLa cells were transfected with Gli2- $\Delta$ N2 or empty expression vector and processed for TaqMan real-time PCR measuring. The *MARCH6* mRNA level was not changed in the presence of active SHH-signalization while the *PTCH1* expression – used as positive control for active SHH-signalization – was readily induced (**Fig. 22E**).

The Wnt signalization is also a fundamental regulator of development. However, in contrast to the SHH pathway which acts in the determination of ventral structures, Wnt is expressed in the dorsal part of developing neural tube. To address the question whether this important morphogenic signal could affect the TH metabolism via *MARCH6* the effect of  $\beta$ -catenin the transcriptional coregulator of Wnt signalization was tested on *MARCH6* 5' FR. The *MARCH6* promoter region was showed 3-fold suppression by  $\beta$ -catenin (**Fig. 22B**).

In conclusion, these data indicate the opposite regulation of *DIO2* and *MARCH6* by PKA and NF- $\kappa$ B signaling pathways and revealed an important difference between the two ubiquitin ligases of D2: while the WSB1 is a positive target the SHH signaling pathway, *MARCH6* remains to be unaffected and regulated independently. Therefore the ubiquitin-conjugating machinery could serve as an integrator of different signals involved in the downregulation of TH activating capacity.



### 6.2.3. Contribution of ubiquitination to the regulation of D2 in brown adipose tissue (BAT)

In BAT, adrenergic stimuli act via  $\beta$ 3-adrenergic receptor activating cAMP production that transcriptionally induces *Dio2* expression. Our *in vitro* data suggested that the activity of the *March6* promoter is downregulated by the cAMP/PKA pathway. This

prompted us to study whether the upregulation of T<sub>3</sub> generation in the cold induced BAT could be also affected by a novel posttranslational mechanism based on cAMP/PKA mediated decrease of D2 ubiquitination. To test this hypothesis we measured in the BAT the expressional response of D2 ubiquitination associated genes to cold stress, a condition known to evoke cAMP generation via adrenergic signaling.

In the first set of experiments mice were transferred from thermoneutral temperature (30 °C) to 4 °C for 1, 2, 4, 6 or 9 hours. Samples from interscapular BAT were processed for qPCR and D2 activity measurements. *March6* expression was not affected in BAT by cold stress (**Fig. 23A**). Interestingly, *Wsb1*, the substrate recognition subunit of the ECS<sup>WSB1</sup> complex showed elevated mRNA level from the first hour of cold stress during the whole period of experiment (**Fig. 23B**). *Usp33* deubiquitinase

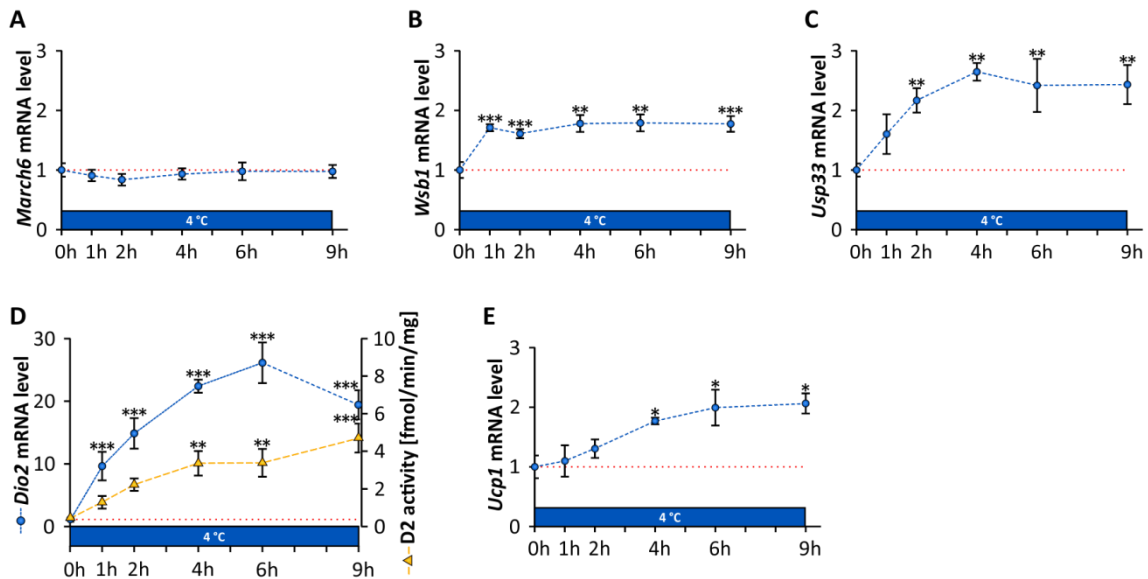


**Figure 23. Expression of genes involved in ubiquitin-mediated regulation of D2 in cold induced BAT of CD1 mice**

Expression of (A) *March6* (B) *Wsb1* ubiquitin ligases and (C) *Usp33* deubiquitinase (D) *Dio2* mRNA level and D2 activity (E) *Ucp1* expression. The qPCR data were normalized to the geometric mean of *Gapdh* and *Hprt1* housekeeping genes and gene expression was depicted as fold change compared to group kept on thermoneutrality at 30°C (0h group) (mean ± SEM, n=4 per group). \*: p<0.05, \*\*: p<0.01, \*\*\*: p<0.001 by one-way ANOVA followed by Newman-Keuls *post hoc* test vs 0-hour group.

expression was induced 2-hours after the transfer of mice to 4 °C (**Fig. 23C**). *Dio2* mRNA level was increased after 1h at 4 °C while elevated D2 activity could be measured after 4-hours of cold stress (**Fig. 23D**). The uncoupling protein 1 (*Ucp1*) mRNA was found to be elevated from 4-hours after the start of the cold stress (**Fig. 23E**).

To test whether the ubiquitin-mediated regulation could be involved in the reduction of elevated T<sub>3</sub>-activating capacity under cold induction, we performed reversed

experimental design transferring mice kept at 4 °C for 8-hours to the thermoneutral 30 °C where non-shivering thermogenesis is absent in rodents. Mice were sacrificed 1, 2, 4, 6 or 8 hours after the end of cold stress and processed for the similar measurements as described above. Similarly to the previous experiment *March6* expression was not affected by the induced state of BAT (**Fig. 24A**). *Wsb1* expression was also showed similar pattern and found to be highly sensitive for adrenergic activation of the BAT and its mRNA level returned to the non-induced level after the transfer of animals to 30 °C (**Fig. 24B**). *Usp33* deubiquitinase showed elevated mRNA level with slow decrease during the whole period after the end of cold stress (**Fig. 24C**).

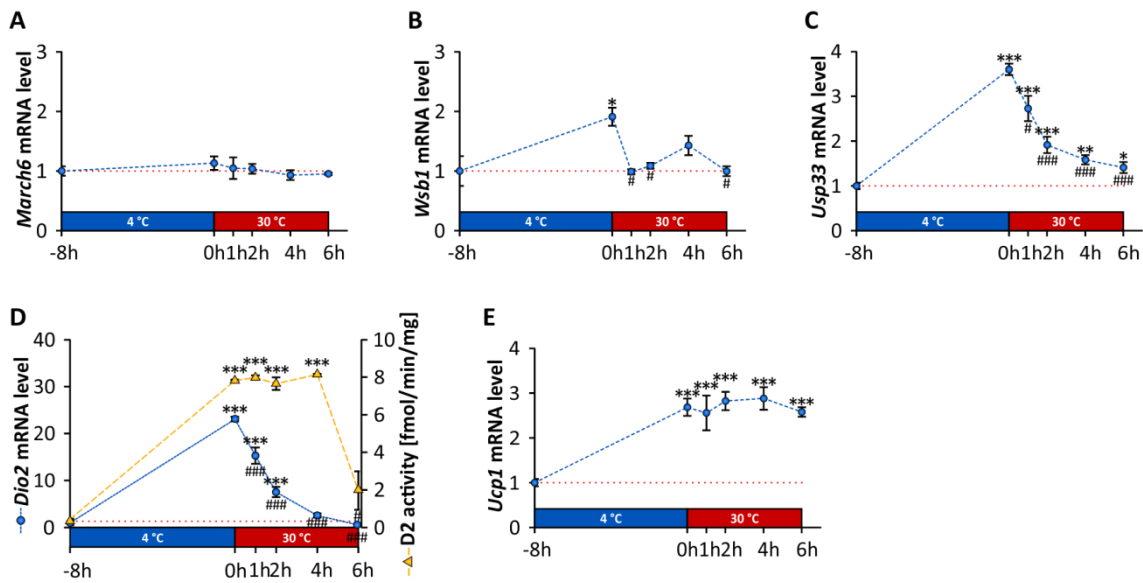


**Figure 24. Expression of genes involved in ubiquitin-mediated regulation of D2 in BAT after 8-hours cold stress of CD1 mice**

Expression of (A) *March6* (B) *Wsb1* ubiquitin ligases and (C) *Usp33* deubiquitinase (D) *Dio2* mRNA level and D2 activity (E) *Ucp1* expression. The qPCR data were normalized to the geometric mean of *Gapdh* and *Hprt1* housekeeping genes and gene expression was depicted as fold change compared to group kept on thermoneutral temperature at 30 °C (-8h group) (mean  $\pm$  SEM, n=3 per group). \*: p<0.05, \*\*: p<0.01, \*\*\*: p<0.001 by one-way ANOVA followed by Newman-Keuls *post hoc* test vs group kept on thermoneutral temperature (-8h group); #: p<0.05, ###: p<0.001 by one-way ANOVA followed by Newman-Keuls *post hoc* test vs 0-hour group.

*Dio2* mRNA was elevated for 2-hours after the end of cold stimulus compared to the control group kept constantly at 30 °C however showed a remarkably rapid decrease after the first hour at 30 °C. In contrast after 6-hours of the transfer from 4 °C the D2 activity was still elevated and decrease could be detected only at 6-hours compared to the induced state (**Fig. 24D**). *Ucp1* mRNA level was found to be stable and its expression was not decreased even after 6-hours at 30 °C (**Fig. 24E**).

#### 6.2.4. Topology of D2-MARCH6 interaction

Previously Doa10 the yeast orthologue of MARCH6 ubiquitin ligase was identified by yeast-two hybrid screen as a potential interaction partner for D2. Other studies demonstrated that silencing of MARCH6 led to increased stability of D2 protein in mammalian cells indicating that MARCH6 is involved in the regulation of D2 enzyme. However, crucial pre-requisites of a functional ubiquitin D2 ligase remained to be established, i.e. the protein-protein interaction between D2 and MARCH6 and the interacting domains remained to be determined.

To address this question we performed fluorescent resonance energy transfer (FRET) studies. ECFP-EYFP FRET pairs were used in the acceptor photobleaching method to detect FRET signal. The EYFP-MARCH6 and MARCH6-EYFP (EYFP on the N- or C-terminus of MARCH6, respectively) constructs were generated by standard recombinant DNA techniques. The interactions were measured between these proteins and ECFP-tagged D2 either on its N- or C-terminus in living HEK-293T cells. The exact membrane topology of the Doa10/MARCH6 protein was unresolved and the localization of its C-terminus was controversial. Therefore we investigated both possibilities whether i) the C-terminus of MARCH6 is localized in the cytosol allowing the interaction with the C-terminus of D2 or ii) expressed in the ER lumen providing access for the N-terminus of D2 (**Fig. 25A**).

Measurable FRET signal was detected between the cytosolic C-terminus of D2 and the N-terminus of MARCH6 (D2-ECFP *vs* EYFP-MARCH6;  $E_{\text{FRET}} = 20.04 \pm 1.02 \%$ ) that was significantly different from the same value of monomeric fluorescent proteins (ECFP and EYFP) used for detection of non-specific background ( $8.03 \pm 2.87 \%$ ) (**Fig. 25B**). In contrast, FRET signal could not be detected between the C-terminus

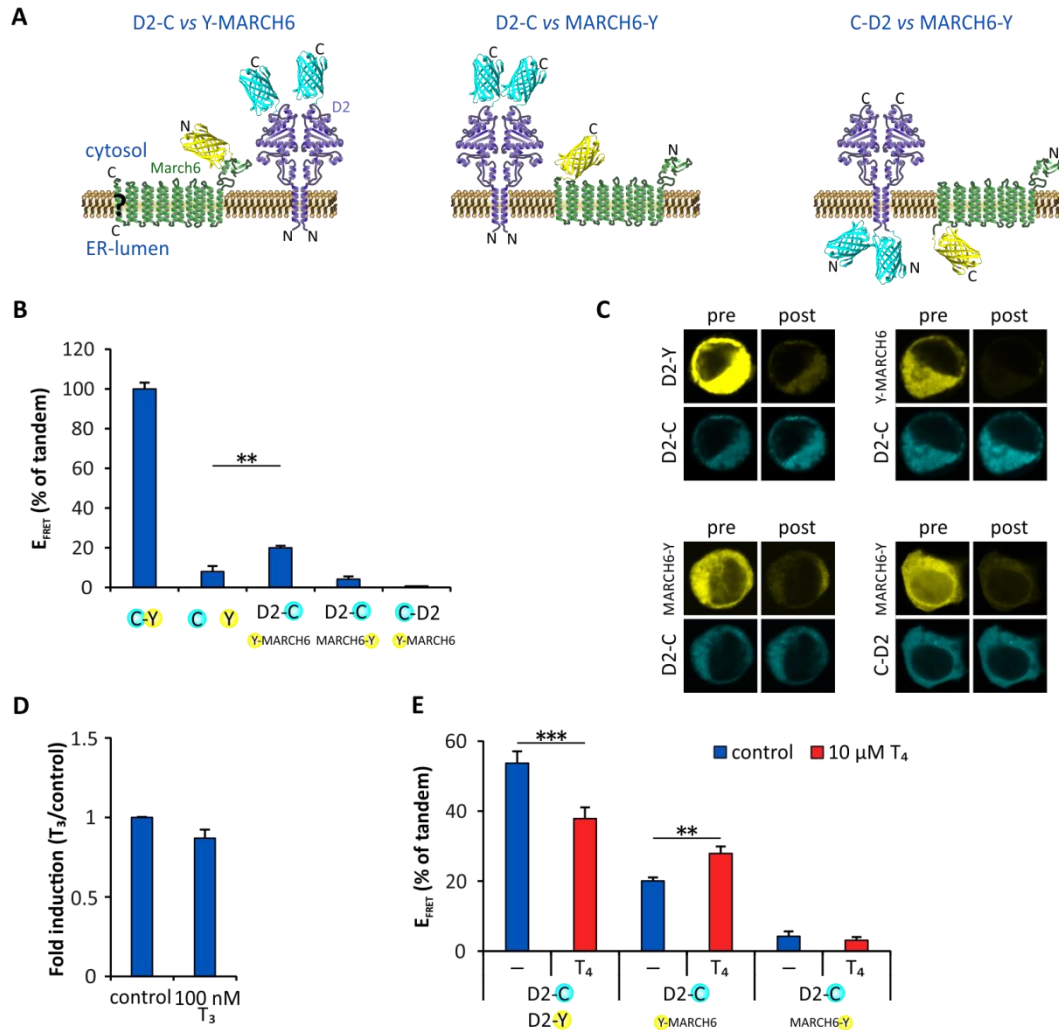


**Figure 25. N-terminus of MARCH6 interacts with D2 on T4-dependent manner**

(A) Design of FRET pairs used to reveal and map the topology of MARCH6 and D2 interaction, the C-terminus of MARCH6 was measured in pair with both the C- and N-terminus of D2. (B) Results of FRET measurement of protein-protein interactions in HEK-293T cells, data are expressed as percentage of ECFP-EYFP tandem (C-Y) used as positive control while monomers of ECFP and EYFP (C Y) were applied to detect non-specific background. The order of C (ECFP) or Y (EYFP) in the name of constructs reflects the type of fusion (mean  $\pm$  SEM,  $n \geq 15$  per group) \*\*:  $p < 0.01$ , \*\*\*:  $p < 0.001$  by one-way ANOVA followed by Tukey *post hoc* test vs monomer. (C) Photomicrographs of HEK-293T cells demonstrating the acceptor photobleaching method used for detection of MARCH6 and D2 interactions. Left-top: prebleach (pre) acceptor; right-top: postbleach (post) acceptor; left-bottom: prebleach donor; right-bottom: postbleach donor. (D) Results of dual luciferase assay demonstrating that the promoter activity 3.5 kb 5' FR of human MARCH6 gene is not regulated by 100 nM  $T_3$ . (E) Effect of 10  $\mu\text{M}$   $T_4$  on MARCH6-D2 interaction. D2 homodimers were used as positive control of treatment (mean  $\pm$  SEM,  $n \geq 15$  per group). \*\*:  $p < 0.01$ , \*\*\*:  $p < 0.001$  by t-test.

of MARCH6 and either the cytosolic C-terminus of D2 (MARCH6-EYFP vs D2-ECFP;  $E_{\text{FRET}} = 4.26 \pm 1.38 \%$ ) or the ER-lumen localized N-terminus of D2 (MARCH6-EYFP vs ECFP-D2;  $E_{\text{FRET}} = 0.73 \pm 1.11 \%$ ) (Fig. 25B). These data suggest that the structural properties responsible for the recognition of D2 as substrate are localized in close

proximity to the N-terminus of MARCH6 protein. Moreover this FRET study directly proved the existence of protein-protein interaction between MARCH6 and D2 in living cell and identified MARCH6 as functional ubiquitin ligase of D2.

#### **6.2.5. Thyroid hormone-dependence of MARCH6-mediated regulation of D2**

First, the involvement of THs in the regulation of MARCH6 action was investigated on transcriptional level using a dual luciferase promoter assay as described above. Therefore the response of 5' FR of human *MARCH6* gene was measured by 100 nM T<sub>3</sub> treatment for 4-hours. These data demonstrate that *MARCH6* expression is not regulated by THs at transcriptional level (**Fig. 25D**).

However, THs regulates D2 activity most effectively via increasing its ubiquitination directly. This mechanism is governed by the D2 substrate, T<sub>4</sub>, and not subjected to the more typical product driven (i.e. T<sub>3</sub>-mediated) regulation. However it was not clarified whether the MARCH6 – similarly to WSB1 – is involved in this regulatory process. FRET studies were applied to target this question. HEK-293T cells were transfected with the previously described constructs and on the second day after transfection and treated with 10 μM T<sub>4</sub> in charcoal-stripped serum for 4-hours. The FRET signal between the N-terminus of MARCH6 and C-terminus of D2 (EYFP-MARCH6 *vs* D2-ECFP) was significantly increased by 39.17 % upon T<sub>4</sub>-treatment (**Fig. 25E**). In contrast, measurable FRET signal still could not be detected between the C-terminus of MARCH6 and C-terminus of D2 (MARCH6-EYFP *vs* D2-ECFP) in presence of T<sub>4</sub>. The D2-D2 homodimer (D2-ECFP *vs* D2-EYFP) used as positive control of treatment showed a 29.41 % decrease in FRET signal (**Fig. 25E**). These data demonstrate the involvement of MARCH6 in the substrate-induced downregulation of TH activation via the ubiquitination of D2.

#### **6.2.6. Construction of a 3-FRET approach to study parallel the interactions of D2 with the two E3-ligases**

FRET experiments proved the direct protein-protein interaction of MARCH6 with D2 during D2 ubiquitination and revealed the involvement of MARCH6 in the substrate-mediated inactivation of D2 by ubiquitination. However, it was not known whether

MARCH6 cooperates or competes with WSB1 – the substrate-recognition subunit of the other described ubiquitin ligase of D2 – whether both of them are coexpressed with D2 as the case in hypothalamic tanycytes. Therefore we established a 3-FRET approach based on the combination ECFP-EYFP and EYFP-mCherry FRET-pairs within one system. Based on their properties the EYFP could be both a FRET acceptor for ECFP and at the same time representing a donor for mCherry. To achieve this, the following constructs were generated: ECFP was fused to the N-terminus of MARCH6 (ECFP-MARCH6) and mCherry was added to the C-terminus of WSB1 followed by additional SOCS-box cassette (WSB1-mCherry) (**Fig. 26A**). These constructs were used in combination with the previously described D2-EYFP allowing the parallel detection of D2-MARCH6 and D2-WSB1 interactions within living cells (**Fig. 26B**). Using this 3-FRET system allowed the investigation of ligase preference of the T<sub>4</sub>-mediated ubiquitination. 10 μM T<sub>4</sub>-treatment resulted in 55.55 % increase of D2-MARCH6 and 49.99 % increase of D2-WSB1 FRET signal interaction demonstrating that the T<sub>4</sub>-mediated ubiquitination is carried out by both ubiquitin ligases at a very similar level (**Fig. 26C**).

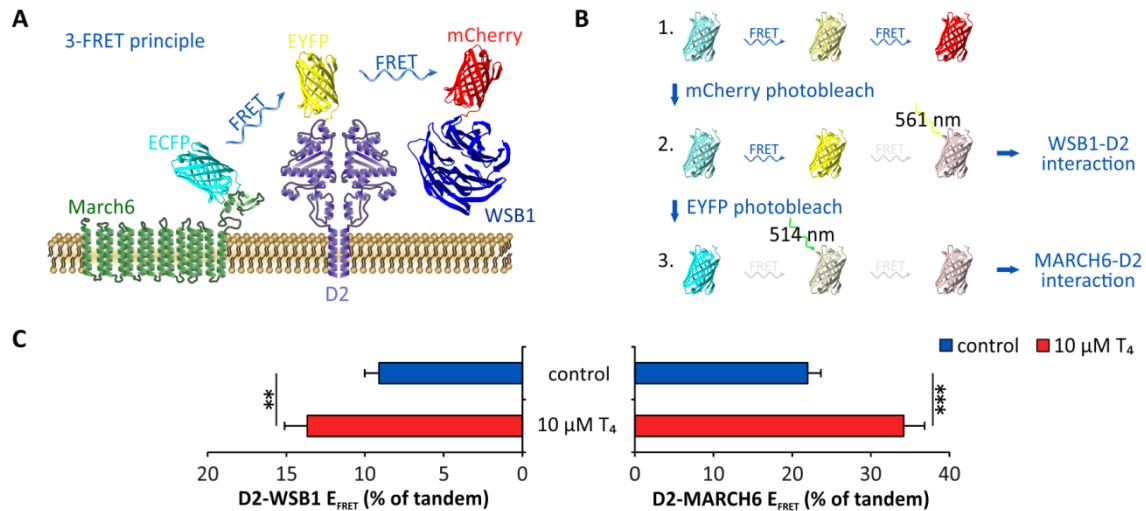


**Figure 26. 3-FRET assisted detection of the interaction between D2 and MARCH6 and WSB1 ligases**

(A) Schematic depiction of the 3-FRET system. (B) Flowchart of detection based on sequential bleaching of FRET donors. In the first cycle mCherry was bleached and EYFP intensity measured followed by the bleaching of EYFP and measuring ECFP intensity. (C) Effect of 10 μM T<sub>4</sub> on the protein-protein interactions between D2 and ligases. Data are expressed as percentage of ECFP-EYFP or EYP-mCherry tandem (mean ± SEM, n≥25). \*\*: p<0.01, \*\*\*: p<0.001 by t-test.

### 6.3. STRUCTURAL BACKGROUND OF THE UBIQUITINATION OF DEIODINASES

#### 6.3.1. Molecular background of stability and ubiquitination of deiodinases

Previous studies identified critical structural elements and properties involved in the control of D2 activity by the ubiquitin-proteasome system. However the minimal requirements of a deiodinase protein sufficient to be processed by ubiquitination are unresolved. To address this question we constructed D1-D2 chimeras using the stable, non-ubiquitinated D1 protein as backbone and inserted ubiquitination-related D2 structural elements into original D1 sequence resulted in chimeric deiodinase proteins. The following D2-specific properties were investigated: the ubiquitin chain carrier lysines (K237 and K244 in human D2 protein), instability-loop (aa. 92-97 in human D2) and ER-localization. Structural elements were inserted into the homologue regions of rat D1: arginine was changed to lysine at position 223 and proline was mutated to lysine at position 230. The instability-loop (-TEGGDN- sequence in human D2) was inserted between amino acids 102 and 103 (**Fig. 27A**). ER localization was carried out by N-terminal SEC62 fusion. These mutations were combined to reveal their importance in the ubiquitination of deiodinases. Therefore the following chimeras were constructed and the abbreviations used in the text were indicated in parenthesis: P230K (D1-K); R223K and P230K (D1-2K); instability-loop- and P230K-containing (D1-K-loop); instability-loop-, R223K- and P230K-containing (D1-2K-loop); SEC62-fusion, instability-loop-, R223K- and P230K-containing (SEC62-D1-2K-loop). Structures of chimeras were depicted on **Fig. 27B**. Constructs were cloned into the mammalian Tet-off D10 expression system allowing the capability of tetracycline-mediated selective suppression of recombinant protein expression.

A subset of these chimeras were fused to the N-terminus of EYFP allowing protein-protein interaction studies to reveal the importance of these properties in the recognition of D2 by its ubiquitin ligases.

The chimeras were expressed in HEK-293T cells and their stability and susceptibility to ubiquitination were studied by Western blot. To assess the half-life of chimeric deiodinases their transcription was stopped by tetracycline in 1 µg/ml as final concentration for 12-hours using a Tet-repressible promoter system (**Fig. 28A**). In case of the lysine-containing chimeras (D1-K and D1-2K) no high molecular mass

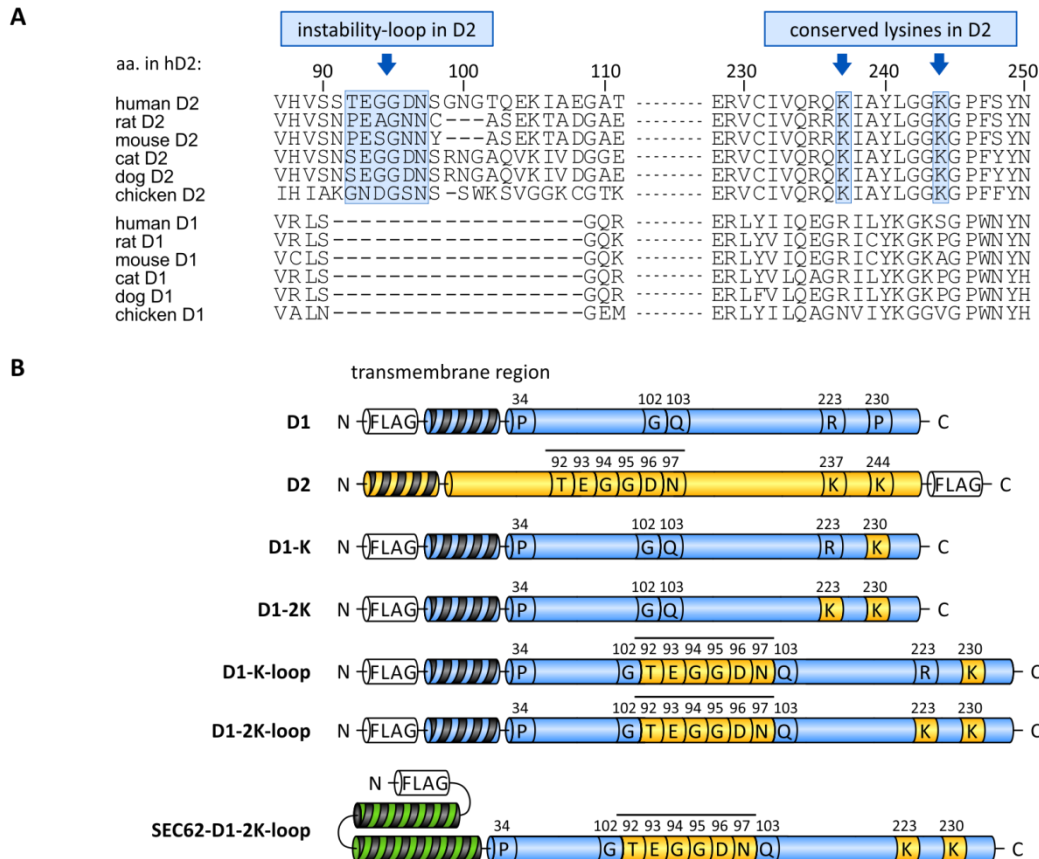


**Figure 27. Design of D1-D2 chimeras**

(A) Alignment of D1 and D2 proteins of different species. Amino acid positions were indicated according to the homologue positions in human D2. Specific elements of D2 involved in ubiquitination are boxed and indicated by arrows. (B) Schematic drawing about the constructed chimeric D1-D2 proteins applied in the study. All constructs are tagged with FLAG-epitope and selenocysteine was mutated to cysteine in order to avoid the requirement of selenocysteine incorporating apparatus.

ubiquitinated forms were present and the stability was not affected compared to wild-type D1 (**Fig. 28B**). Insertion of the instability-loop of D2 to the lysine-containing chimera (D1-K-loop and D1-2K-loop) remarkably reduced the stability of the proteins although high molecular mass ubiquitinated forms could not be revealed by Western blot (**Fig. 28B**). A lysine- and loop-containing chimera was directed into the ER (SEC62-D1-2K-loop) to test the protein in the compartment where the wild-type D2 is located. In this case a shorter half-life and high molecular mass forms could be observed indicating this mutant undergoes ubiquitination (**Fig. 28B**).

Ubiquitination of chimeras was also tested by an independent approach based on the inhibition of the proteasome. Loss of the catalytic activity of the proteasome impacts UPS-targeted substrate proteins in two ways. As a direct consequence the degradation of these proteins is blocked and due increased half-life this leads to elevated biological

activity of proteins that remain in active form after ubiquitin conjugation. As an indirect effect on protein turnover the impaired processing of ubiquitinated proteins results in blocked recycling of ubiquitin originating from the ubiquitin chain on these proteins that leads to ubiquitin-depletion within the cell that consequently interferes with ubiquitin-conjugation. Therefore transfected cells were treated by 2  $\mu$ M MG132 a commonly used proteasome inhibitor and the deiodinase activity of cell lysates was measured (**Fig. 28A**).

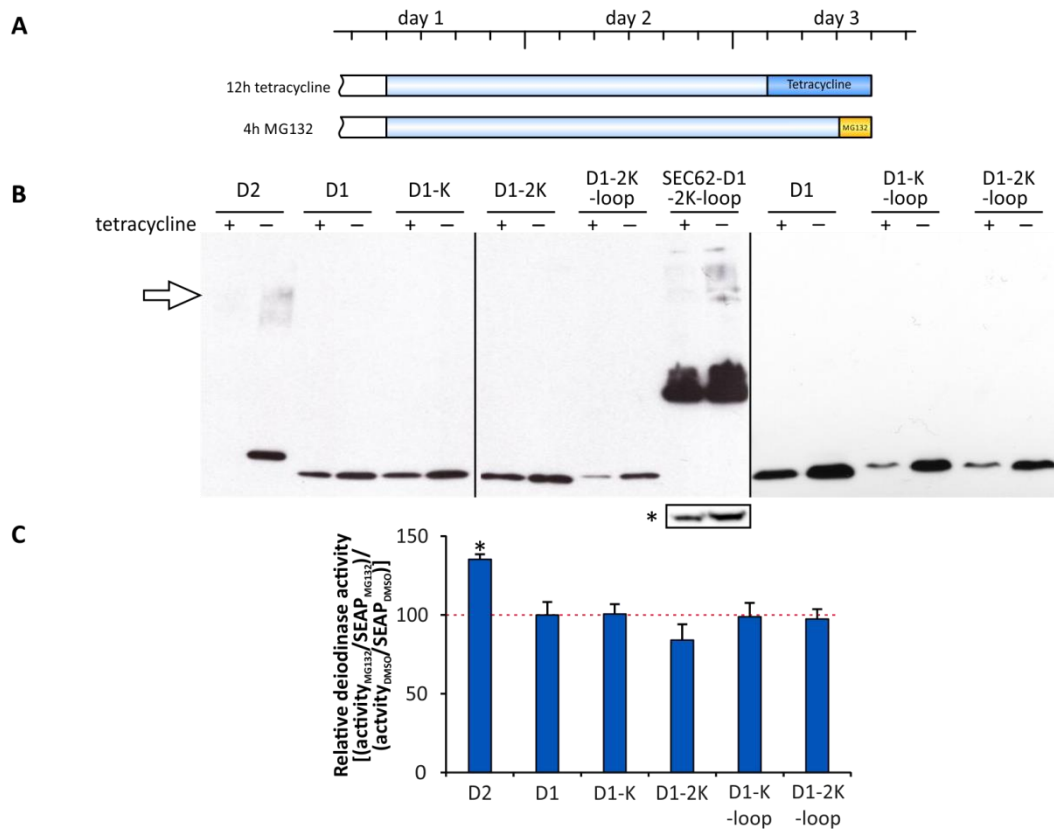


**Figure 28. Assessment of the stability and ubiquitination of D1-D2 chimeras**  
**(A)** Experimental design. **(B)** Testing the stability and ubiquitination of chimeras by Western blot. HEK-293T cells expressing chimeras were treated by 1 mg/l tetracycline for 12 hours to selectively abort *de novo* synthesis and samples were run in 4-20% gradient gel followed by the detection using FLAG-tag. Open arrow indicates the high molecular mass ubiquitinated deiodinase forms, asterisk indicates the SEC62-D1-2K-loop construct run in 10% gel and detected by shorter exposure. **(C)** Testing the ubiquitination of chimeras by 2  $\mu$ M MG132 proteasome inhibitor treatment for 4-hours. D1 activities were normalized by cotransfected secreted alkaline phosphatase (SEAP). Data represented as fold change of MG132/DMSO vehicle. D2 was used as positive control of MG132 treatment (mean  $\pm$  SEM, n=3). \*: p<0.05 by t-test.

The activities of the lysine- and loop-containing chimeras were not increased by the inhibition of proteasome supporting the results of stability studies that these mutants are

not targeted by ubiquitin-mediated regulation (**Fig. 28C**). The ER directed mutants could not be tested this way due to the known loss of enzymatic activity by the fusion to SEC62.

### 6.3.2. Importance of D2-specific elements in the recognition by ubiquitin ligases

Protein-protein interactions were measured to exclude aspecific ubiquitination of the chimeras and test the structural basis of the recognition of D2 as substrate for its ubiquitin ligases. Therefore FRET experiments were performed using C-terminal EYFP-tagged chimeras containing lysines and loop-region (D1-2K-loop-EYFP), directed to ER (SEC62-D1-EYFP) and containing these properties together (SEC62-D1-2K-loop-EYFP) combined with ECFP-tagged WSB1 (WSB1-ECFP) or MARCH6 (ECFP-MARCH6). Measurable FRET signal was not observed either for the lysine- and loop-containing (D1-2K-loop-EYFP) or the ER-localized (SEC62-D1-EYFP) mutants indicating these chimeras could not be recognized by the WSB1 or MARCH6 proteins (**Fig. 29A and B**).

However intense FRET signal ( $E_{\text{FRET}} = 53.14 \pm 2.5 \%$ ) could be detected between the lysine- and loop-containing ER-targeted chimera (SEC62-D1-2K-loop-EYFP) and WSB1 demonstrating these elements in combination allow the recognition by one of the known D2 ligases (**Fig. 29A and B**). Interestingly, this chimera did not interact with MARCH6 suggesting different structural background of the recognition of D2 by its ubiquitin ligases (**Fig. 29A and C**). Our data also demonstrate that the ubiquitination of SEC62-D1-2K-loop chimera is carried out by one of the ubiquitin ligases of D2 the ECS<sup>WSB1</sup> complex.

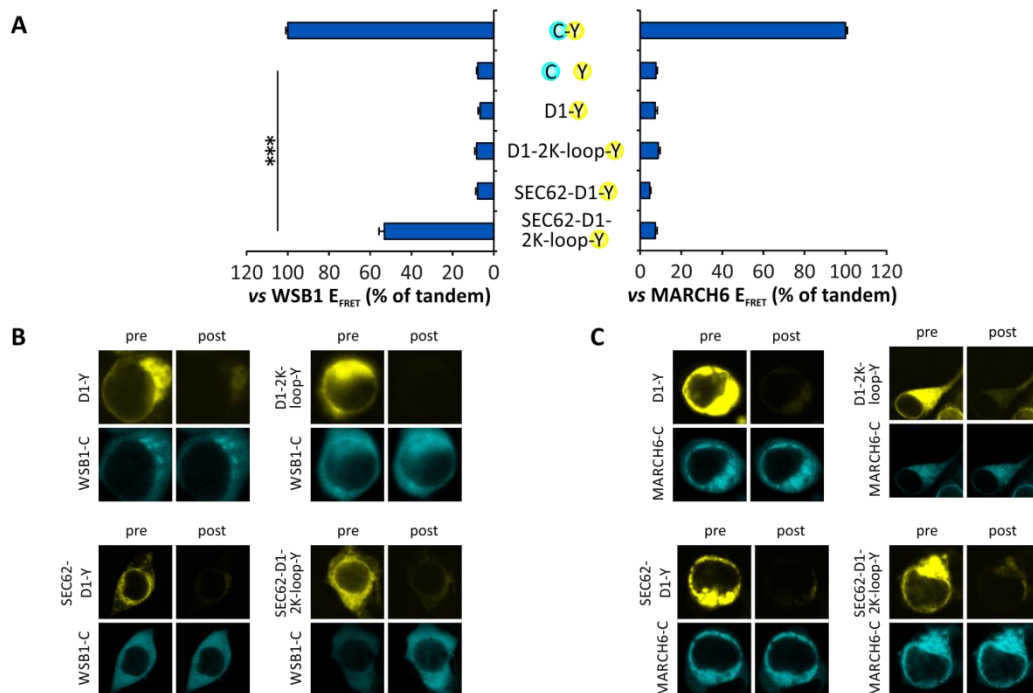


**Figure 29. Processing of chimeric D1-D2 chimeric proteins by the ubiquitin-proteasome system**  
 (A) Importance of D2-specific elements in the recognition by ubiquitin ligases assessed by FRET in HEK-293T cells. Data are expressed as percentage of ECFP-EYFP tandem (C-Y) used as positive control while monomer ECFP and EYFP (C Y) were applied to detect non-specific background (mean  $\pm$  SEM,  $n \geq 30$  per group). \*\*\*:  $p < 0.001$  by one-way ANOVA followed by Tukey *post hoc* test vs monomer (B) Photomicrograph Photomicrography of individual HEK-293T cells demonstrating FRET between deiodinase chimeras and WSB1. (C) Same as C with MARCH6. Each panel contains the following pictures: left-top: prebleach (pre) acceptor; right-top: postbleach (post) acceptor; left-bottom: prebleach donor; right-bottom: postbleach donor. The order of the fluorescent protein (C or Y) and the tagged protein in the name of the constructs reflects their position in the fusion protein.

### 6.3.3. Effect of threonine/alanine polymorphism in D2 on the interaction with ubiquitin ligases

The threonine/alanine polymorphism in the position of 92th amino acid of human D2 was suggested to affect glucose metabolism and HPT axis therefore the polymorphism of D2 could have importance in diabetes and diseases associated with impaired TH metabolism. Despite the clinical data suggesting elevated insulin level, increased risk of type 2 diabetes, osteoarthritis and mental deficits in polymorphic *DIO2* allele carriers the impact of the polymorphism on the properties of D2 protein has not been adequately resolved. Taking into account that this amino acid position belongs to the D2-specific loop-region involved in the inherent instability of D2 protein the mutation of threonine to alanine could potentially affect D2 degradation via ubiquitination. Therefore using the previously established 3-FRET approach we studied whether the amino acid change

affects the recognition of D2 by its ubiquitin-conjugating apparatus. FRET signal was similar in case of interaction with WSB1 and allele variants of D2:  $E_{\text{FRET}}(\text{WSB1-D2-92T}) = 44.60 \pm 4.84 \%$  and  $E_{\text{FRET}}(\text{WSB1-D2-92A}) = 42.29 \pm 4.95 \%$  (**Fig. 30**). The induction of D2-WSB1 interaction by 10  $\mu\text{M}$   $\text{T}_4$  treatment was also unaffected in case of allele variants:  $E_{\text{FRET}}(\text{WSB1-D2-92T} \bullet \text{T}_4) = 68.86 \pm 7.82 \%$  and  $E_{\text{FRET}}(\text{WSB1-D2-92A} \bullet \text{T}_4) = 68.64 \pm 9.03 \%$  resulting 54.38 % increase for D2-92T and 62.31 % for D2-92A (**Fig. 30**). Interestingly, the  $\text{T}_4$ -induction of D2-MARCH6 interaction was slightly altered by the substitution of 92th threonine to alanine. While the basal interaction was similar on wild-type and polymorphic D2  $E_{\text{FRET}}(\text{MARCH6-D2-92T}) = 24.39 \pm 2.57 \%$  and  $E_{\text{FRET}}(\text{MARCH6-D2-92A}) = 29.33 \pm 3.32 \%$  the  $\text{T}_4$  treatment did not result significant increase of D2-MARCH6 interaction in case of D2-92A allele:  $E_{\text{FRET}}(\text{MARCH6-D2-92T} \bullet \text{T}_4) = 37.43 \pm 3.68 \%$   $E_{\text{FRET}}(\text{MARCH6-D2-92A} \bullet \text{T}_4) = 36.43 \pm 3.22 \%$  resulting 53.44 % induction for D2-92T while for D2-92A that was not statistically significant indicating that posttranslational regulation could be affected by the common polymorphism of D2 (**Fig. 30**).

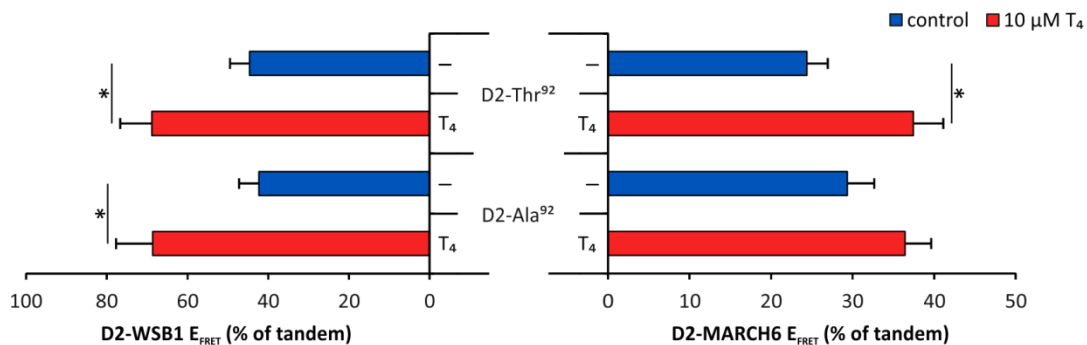


**Figure 30. Effect of the T92A D2 polymorphism on the recognition of D2 by ubiquitin ligases**  
 FRET efficiencies between the wild-type (D2-Thr<sup>92</sup>) and polymorphic (D2-Ala<sup>92</sup>) D2 assessed by 3-FRET. Data are expressed as percentage of ECFP-EYFP or EYFP-mCherry tandem (mean  $\pm$  SEM,  $n \geq 25$ ). \*:  $p < 0.05$  by two-way factorial ANOVA followed by Newman-Keuls *post hoc* test.

#### 6.3.4. Relationship between deubiquitination and extraction of D2 from the ER

D2 is a type I transmembrane protein and is processed by the endoplasmic reticulum associated degradation (ERAD) [211]. As a consequence D2 needs to be extracted from the ER membrane to reach the cytosolic proteasome. This process is carried out by the p97/VCP complex. However the inhibition of this machinery by Eeyarestatin I (EERI) did not result an increase in D2 activity. To target this question, we used FRET to measure protein-protein interactions between the D2-D2 homodimers and between the D2 and its

deubiquitinase enzyme the USP33. D2-EYFP/D2-ECFP or ECFP-USP33/D2-EYFP fusion constructs were expressed in HEK-293T cells which were treated by 10  $\mu$ M EERI and/or 10  $\mu$ M T<sub>4</sub>. The FRET signal between the globular domains of D2-D2 homodimers was significantly decreased by 30.30 % compared to the absence of T<sub>4</sub> (**Fig. 31A**). Presence of 10  $\mu$ M EERI alone resulted in decreased interaction between monomers of D2-D2 homodimers and the rate of reduction was similar to that achieved with T<sub>4</sub>-treatment (**Fig. 31A**). Interestingly, the addition of 10  $\mu$ M T<sub>4</sub> beside EERI did not result in further decrease in the interaction between the globular domains of D2 (**Fig. 31A**).

These findings suggested an impaired deubiquitination capacity and as a consequence the enrichment of the inactive ubiquitinated D2. To target this proposed mechanism the alterations of interaction between the D2 and USP33 was measured. Inhibition of D2 export by EERI treatment significantly reduced the FRET signal between D2 and USP33 by 51.89 % (**Fig. 31B**). This effect was independent of D2 substrate since in presence of 10  $\mu$ M T<sub>4</sub> the EERI-driven decrease was very similar, 52.20 % (**Fig. 31B**). In contrast the inhibition of proteasomal activity by 1  $\mu$ M MG132 resulting the ablation of the final processing of ubiquitinated D2 did not result detectable alteration in the D2-USP33 interaction (**Fig. 31B**).

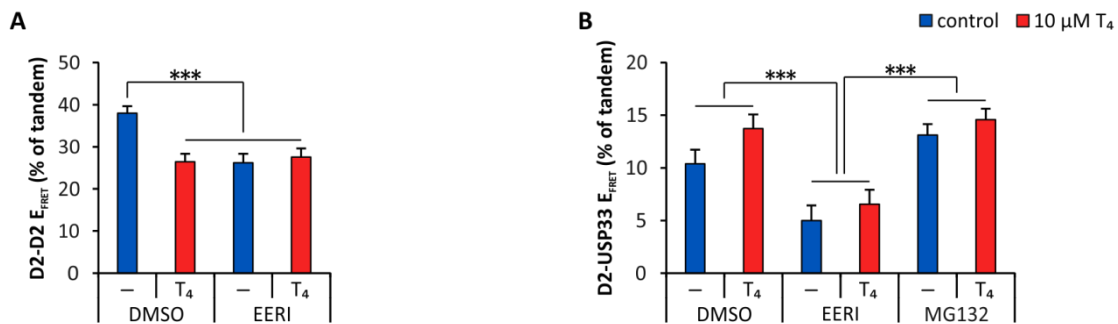


**Figure 31. Inhibition of p97/VCP complex affects the deubiquitination of D2**  
**(A)** Interaction between globular domains of a D2 homodimer in the presence of p97/VCP inhibitor 10  $\mu$ M Eeyarestatin I (EERI) and/or 10  $\mu$ M T<sub>4</sub>. Data are represented as percentage of ECFP-EYFP tandem (mean  $\pm$  SEM, n $\geq$ 40). \*\*\*: p<0.001 by two-way factorial ANOVA followed by Tukey *post hoc* test. **(B)** Interaction between globular domain of D2 and USP33 deubiquitinase in presence of 10  $\mu$ M Eeyarestatin I (EERI) or 2  $\mu$ M MG132 proteasome inhibitor in combination with 10  $\mu$ M T<sub>4</sub> (mean  $\pm$  SEM, n $\geq$ 20). \*\*\*: p<0.001 by two-way factorial ANOVA followed by Tukey *post hoc* test revealing effect of drugs and T<sub>4</sub> without interaction.

## 7. DISCUSSION

### 7.1. INTERACTION BETWEEN PACAP AND THYROID HORMONE SIGNALING

#### 7.1.1. PACAP induces D2 expression via cAMP/PKA pathway

The inductive effect of PACAP on the 5' FR of human *DIO2* gene was demonstrated in HEK-293T cells showed endogenous PAC1R receptor expression. Importantly, PAC1R – in contrast with the other group of PACAP receptors including VPAC1 and VPAC2 – is selective for PACAP over vasoactive intestinal polypeptide (VIP). PACAP action via PAC1R receptor is transmitted by two major intracellular signalization cascades: the cAMP/PKA and PLC/Ca<sup>2+</sup>. To dissect between intracellular pathways involved in the induction *DIO2* by PACAP, cAMP response element (CRE) mutant 5' FR of *DIO2* was generated. The efficiency and specificity of mutation was demonstrated by its unresponsiveness to PKA overexpression and retained activation by a well-documented positive regulator of D2, the NF-κB cascade mimicked by p65 coexpression [155]. The induction of *DIO2* promoter by PACAP was completely abolished by the mutation of CRE suggesting that PACAP action on *DIO2* promoter is carried out exclusively by the cAMP/PKA second messenger system. Transcriptional regulation of *DIO2* includes several identified intracellular signals however the upstream factors activating these cascades are poorly resolved. The cAMP/PKA pathway is involved in the adrenergic stimulation of TH activation in BAT by cold stimulus and in the pineal gland by photoperiodic response [150, 151]. In birds, TSH – derived from pars tuberalis – is also suggested to act via cAMP to induce D2 in mediobasal hypothalamus [153]. Our results suggest PACAP as a novel cAMP-dependent mediator of D2 activity.

#### 7.1.2. Tanycytes express the PAC1R PACAP receptor

Having established *in vitro* that PACAP is able to activate *DIO2* transcription we aimed to identify D2 expressing cell types and brain regions where PACAP-mediated regulation of TH activation could be relevant *in vivo*. We demonstrated by immunohistochemistry that tanycytes express the PAC1R receptor. Tanycytes have exclusive D2-expression in hypothalamus therefore these cells have critical role in the regulation of HPT axis providing the main T<sub>3</sub>-source. Alterations in tanycytic D2 activity

is known to exert major impact on the feedback of the HPT axis demonstrated in bacterial infection model of non-thyroidal illness syndrome [81]. In contrast to tanycytes PAC1R expression could not be detected in cortical and hippocampal D2-expressing astrocytes however it should be noted that PAC1R expression was demonstrated in reactive astrocytes and these cells could express VPAC1 or VPAC2 receptors showing similar affinity for PACAP and VIP. Thus under certain conditions PACAP could act on TH activation within these regions [212, 213].

### **7.1.3. PACAP affects the feedback and development of HPT axis**

To test, whether PACAP mediated modulation of D2 expression and HPT function is functional *in vivo*, we performed acute intracerebroventricular PACAP administration. PACAP resulted in remarkable alterations in the HPT axis of CD1 mice. The increased mediobasal hypothalamic D2 activity confirms the presence of functional receptors – identified by immunohistochemistry – on tanycytes because D2 expression is confined to these cells within this region. The elevated T<sub>3</sub> generation resulted in suppressed TRH in the paraventricular nucleus despite the putative stimulatory effect of PACAP on the TRH neurons which was overwritten by the increased negative feedback. The decreased *Trh* was manifested in decreased *Tshb* transcription demonstrating that PACAP suppressed the HPT axis via tanycytic D2. The serum TSH bioactivity and free T<sub>4</sub> level were unaffected however taking into account the series of required transcriptional events and the stability of circulating T<sub>4</sub> this parameter was unlike to be affected within 4-hours after treatment. Our data established PACAP as a novel modulator of hypothalamic TH economy. The hypothalamus is densely innervated by PACAP-containing fibers and several nuclei of hypothalamus express PACAP. [214-217]. Interestingly, a subdivision of TRH neurons was found to express PACAP and exerted a reverse, orexigenic effect on energy homeostasis [88]. Additionally, taking into account the localization of tanycytes in the wall of third ventricle the PACAP-mediated modulation of hypothalamic TH activation could be affected by external sources via the cerebrospinal fluid. In contrast with hypothalamus in the cortex and hippocampus significant difference was not observed however – especially in case of hippocampus – D2 activity showed a tendency for increase. Taken together with the immunohistochemical results these data raise the

possibility that D2 could be targeted in this region by PACAP via VPAC1 and VPAC2 receptors or indirectly.

The TH status and TH activation of heterozygous PACAP-deficient (PACAP<sup>+/-</sup>) mice were tested to reveal long-term effects of PACAP on TH economy and HPT axis. The decreased serum free T<sub>3</sub> and T<sub>4</sub> levels together with suppressed TSH bioactivity suggested central hypothyroidism. As a consequence, the cortical and hippocampal D2 activities were elevated compensating the decreased TH availability while in regions with crucial impact on HPT axis – in the mediobasal hypothalamus and in the pituitary – D2 activity was not affected. Similar signs of central hypothyroidism are known to exist in the infection model of non-thyroidal illness [81]. Taken together with the potent antiinflammatory effect of PACAP raised the possibility that an altered immune state could result the observed phenotype [218]. However measuring serum inflammatory and antiinflammatory cytokine concentrations did not indicate difference in the immunological state of genotypes.

Therefore we hypothesized that the maturation – rather than the adult state – of the HPT axis could be affected in PACAP-deficient mice. HPT axis is highly sensitive for the alterations in TH availability within the postnatal period when the set point of the axis is established as demonstrated in *Dio3* knock-out mice where the local hyperthyroidism results in decreased activity of the HPT axis and consequent long-term suppression of HPT axis manifested in hypothyroidism persisting also in adult mice [143]. Measuring the expression of genes involved in TH metabolism, transport and reception revealed increased *Dio3* expression in PACAP-deficient mice. The elevated TH inactivation during this critical period of HPT axis could lead to altered set point formation to lower TH availability and results the lack of compensation of hypothyroid periphery. Further studies are required to clarify how *Dio3* transcription is modulated by PACAP in hypothalamus, especially within this critical window of the maturation of HPT axis.

The revealed complex involvement of PACAP in the regulation and development of HPT axis and the proposed underlying mechanisms are depicted in **Fig. 32**.

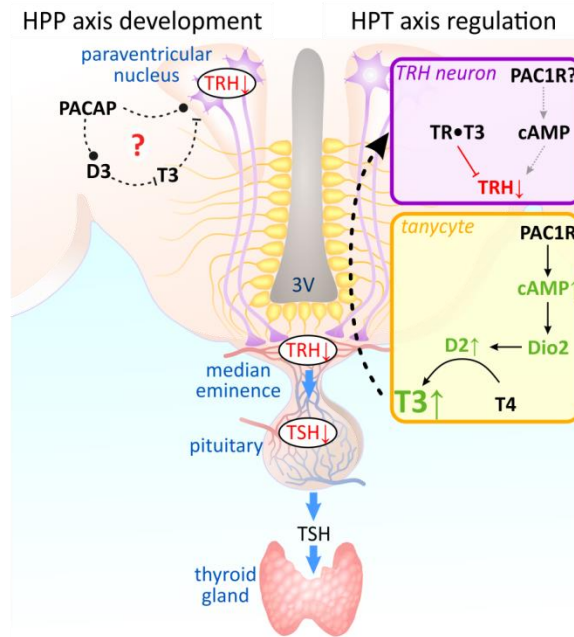


**Figure 32. Schematic depiction of PACAP-mediated regulation of the HPT axis**  
 PACAP interacts with hypothalamic thyroid hormone signaling at multiple levels. Dotted lines represent suggested processes still need to be conformed directly. PACAP upregulates D2 in tanycytes via PAC1R as the expression of this PACAP-specific receptor is demonstrated but the additional involvement of VPAC1/2 cannot be presently ruled out. D2-generated T<sub>3</sub> downregulates TRH expression in the PVN and counteracts the suggested direct stimulatory effect of PACAP on TRH neurons. T<sub>3</sub> can downregulate TRH expression directly and by interfering with cAMP induced TRH upregulation and this second mechanism can also impact PACAP expression. PACAP also plays a hypothetic role in HPT set point formation during development.

#### 7.1.4. Thyroid hormones modulate *Adcyap1* (PACAP) gene transcription

In order to test whether the interaction between TH and PACAP signaling is bidirectional the responsiveness of *Adcyap1* gene – encoding PACAP – to THs was studied. The 3 kb 5' flanking region of mouse *Adcyap1* gene was found to be insensitive for different T<sub>3</sub> concentrations indicating PACAP synthesis – at least on transcriptional level – is not targeted by THs. However, we found that the cAMP/PKA pathway-mediated induction of *Adcyap1* promoter is interfered by liganded TR suggesting that THs are able to modulate the *Adcyap1* gene transcription indirectly. The proposed mechanism could be the interfered CREB phosphorylation by ligand-bound TR based on the protein-protein interaction between TR and CREB [219, 220]. Hypo- and hyperthyroid mice were generated to test the *in vivo* significance of the altered TH levels on *Adcyap1* gene transcription. In general, *Adcyap1* transcript was found to be unaffected in various brain regions but it was decreased by hyperthyroidism in the parabrachial nucleus. Importantly,

this region is in bidirectional connection with hypothalamic areas involved in the central regulation of feeding and energy homeostasis. The parabrachial nucleus receives inhibitory input from orexigenic AgRP neurons of arcuate nucleus [221] and sends inputs into PVN, ventromedial nucleus [214] and lateral hypothalamus [222]. *Adcyap1* level was also altered in the pituitary, a major target of PACAP action affecting the hypothalamo-pituitary-gonadal axis by modulating LH and FSH secretion [223, 224] and hypothalamo-pituitary-adrenal axis [225] via affecting ACTH production. Further studies are required to elucidate the significance of these findings.

## **7.2. CHARACTERIZATION OF MARCH6 AS D2 UBIQUITIN LIGASE**

### **7.2.1. Expression profile of *March6***

It has been demonstrated, that tanycytes coexpress the MARCH6 ubiquitin ligase with D2 [164]. We also aimed to identify extrahypothalamic brain regions and tissues where *March6* is expressed therefore its expression profile was studied in adult Wistar rats with semi-quantitative RT-PCR. *March6* expression was compared with *Wsb1* focusing predominantly tissues where the D2 is the preferred activating deiodinase. *March6* showed strong expression in kidney, skeletal muscle, cortex, heart and hypophysis where the subunit of the other D2-specific ubiquitin ligase, *Wsb1* is also expressed. A striking difference in ligase expression was observed in brown adipose tissue (BAT) where *March6* was poorly expressed while strong *Wsb1* expression was found. BAT is one of the best characterized targets of TH action. The induction and maintenance of UCP1-mediated thermogenesis requires a tight regulation of D2 activity [226]. Recently it is not fully understood how this process is affected by the ubiquitination of D2. Reduced ubiquitination and the increased deubiquitination of D2 could increase local T<sub>3</sub> generation however further studies are required to clarify the involvement of this machinery in thermogenesis. Interestingly, we did not detect D2 specific ubiquitin ligase expression in the thyroid gland, suggesting that D2 regulation could be independent from UPS in this tissue. However it is important to note that other, recently unknown, ubiquitin ligases for D2 could exist while on the other hand D2 is not the exclusive substrate of WSB1 and MARCH6. WSB1 was reported as ubiquitin ligase of HIPK2 kinase involved in hypoxia response [227]. MARCH6 was found to target squalene monooxygenase (SM)

for proteasomal degradation [208] and MARCH6 is also important member of quality control system of ER.

### **7.2.2. Characterization of the human *MARCH6* promoter**

While the involvement of MARCH6 in ERAD machinery is well documented however the regulation of *MARCH6* gene is poorly characterized. Therefore the 5' FR of human *MARCH6* was cloned and analyzed by *in silico* transcription factor binding site prediction using the TRANSFAC database and the TESS algorithm. Focusing primarily on regulators involved in the transcriptional control of human *DIO2* gene we identified several potential CREB and NF- $\kappa$ B binding sites in the 5' FR of human *MARCH6* gene. Canonical TRE could not be detected however TRE-half sites were predicted and in the close proximity of TSS and SP1 binding site rich region was identified. The effectivity of these putative sites was tested on the 3.5 kb fragment of human *MARCH6* gene.

The results of luciferase promoter assay suggest an opposite regulation between *MARCH6* and *DIO2* gene while *MARCH6* promoter activity is suppressed by NF- $\kappa$ B and cAMP-CREB intracellular signals that are strong activators of *DIO2* transcription [119, 155]. Therefore MARCH6-assisted ubiquitination provides an indirect mechanism acting on the post-translational level to affect D2 activity in presence of active NF- $\kappa$ B and cAMP/PKA signaling pathways. The *in vivo* relevance of these signals in TH activation is well documented. The NF- $\kappa$ B pathway is affected by numerous receptors involved in immune system-related signalizations [228] and it was previously shown that acute inflammation evoked by LPS administration induces D2 expression in tanycytes [81]. It is not completely understood whether LPS is directly sensed by tanycytes via Toll-like receptor 4 (TLR) or inflammatory signals produced by the immune system (e.g. interleukins, tumor necrosis factor etc.) are involved in NF- $\kappa$ B-mediated alterations in gene expression. However, it was clearly demonstrated that the induction of D2 in tanycytes by acute inflammation has a major impact on thyroid axis offering a mechanistic model for the molecular pathogenesis of non-thyroidal illness [8, 81]. According to this concept the increased T<sub>3</sub> generation via elevated D2 levels in tanycytes results in local hypothalamic hyperthyroidism and as a consequence leads to the suppression of the HPT axis. Since *March6* expression was found in tanycytes [164] and

our recent data demonstrated the negative regulation of *March6* expression by the NF- $\kappa$ B pathway, it can be suggested, that the local increase of D2 activity – beside *de novo* protein synthesis – could be further supported by the decreased inactivation capacity via the ubiquitin-proteasome system.

The cAMP/CREB intracellular signalization has central role in transducing the noradrenergic-stimulation to TH activation in brown adipose tissue and pineal gland and MARCH6 could provide an additional, posttranslational mechanism to support increased T<sub>3</sub> generation.

The *MARCH6* gene promoter belongs to the GC-rich promoters and SP1 is usually an important factor involved in the regulation of this type of promoters. Additionally, the transcription factor binding site analysis of *MARCH6* 5' FR region revealed several putative SP1 sites. To test the importance of SP1 in the regulation of *MARCH6* expression the region contains these sites was deleted and promoter activity was measured revealing significant decrease in basal promoter activity that confirmed the involvement of SP1 in the regulation of *MARCH6* transcription.

We revealed an important difference in the SHH responsiveness of *MARCH6* and the subunit of other D2 ubiquitin ligase, the *WSB1* demonstrating a functional difference between the two ligases of D2. WSB1 has the ability to transduce the antagonistic effect of proliferative SHH on T<sub>3</sub> a known inducer of differentiation [161] while our data indicate that MARCH6 is not regulated by the effector transcription factor of SHH signalization, Gli2. These data suggest a distinct role in the posttranslational control of D2 enzyme while MARCH6 could refer for short half-life and instability; additionally WSB1 interlinks two major morphogenetic signaling pathways, governed by Sonic hedgehog and THs. This putative role of WSB1 could be important during development and also in adulthood, especially in cell types like tanycytes where all members required for the SHH-mediated regulation of TH activation are expressed. Tanycytes due their abundant D2 expression are the major source of hypothalamic T<sub>3</sub> therefore the signals affecting tanycytic D2 activity have a systemic role via the HPT axis as it was shown in the pathogenesis of LPS-induced acute inflammation [81]. Additionally, tanycytes are recently identified as the potential source of newborn neurons in the adult hypothalamus [229, 230]. In this process a precise balance is required between the proliferative signals like SHH and differentiative agents as THs. Therefore the SHH-driven downregulation

of T<sub>3</sub> generation could serve as important switch point in adult hypothalamic neurogenesis.

The Wnt pathway along with SHH acts as major regulator in the determination of dorsoventral axis and potent regulator of proliferation-differentiation balance. Similarly to SHH the Wnt can also support proliferation of progenitors promoting cell division and interfering with the exit from cell cycle [231]. This process was shown to be essential in the adult hippocampal neurogenesis [232]. The importance of Wnt pathway in the regulation of TH metabolism was shown in previous studies and revealed an antagonistic effect of Wnt on the T<sub>3</sub> level which acts both on the TH activating and inactivating enzymes on transcriptional level [202]. However it was not clarified whether Wnt affects the post-translational control of T<sub>3</sub> generation. We demonstrated that the *MARCH6* promoter was suppressed by  $\beta$ -catenin, the effector of Wnt signaling. Importantly, the molecular elements of Wnt signalization are expressed in tanycytes therefore the Wnt could be involved in the fine-tuning of proliferation-differentiation equilibrium via *MARCH6* mediated ubiquitination of D2 and consequently the T<sub>3</sub> generation.

The regulation of *MARCH6* expression and involvement in the posttranslational control of D2 is summarized in **Fig. 33**.

### **7.2.3. Contribution of ubiquitination to the regulation of D2 in brown adipose tissue (BAT)**

Local induction of TH activation is critical in the cold response of BAT [226]. It was demonstrated that the activation of cAMP/PKA pathway by adrenergic stimuli induces *de novo* D2 synthesis however it remained to be elucidated how the posttranslational regulation of D2 enzyme is affected during BAT thermogenesis. To target this question the expression of genes involved in the ubiquitin-mediated regulation of D2 were monitored during and after the cold induction of BAT. Our *in vitro* data indicated that *March6* could be targeted by the cAMP/PKA pathway activated in BAT by cold stimulus. However *March6* mRNA level during cold stress was found to be stable. In contrast to *March6* the *Wsb1* ligase subunit expression showed a remarkable temperature-sensitivity. Transferring mice to 4 °C *Wsb1* expression is rapidly increased

by 2-fold and remained constantly upregulated during cold induction. After returning to room temperature *Wsb1* mRNA fell to the level of non-induced control after the first hour.

Taken together these data suggest that cold-induced alterations in the ubiquitination of D2 do not contribute directly to the increased  $T_3$  production in BAT. *March6* was shown to be insensitive for cold induction of BAT. In contrast, *Wsb1* showed an opposite pattern than it was expected however the precise function of this phenomenon should be addressed by further investigations. Presently precise structural data are not available that would explain the intramolecular conformational changes and intermediates during catalytic cycle in D2. However a selenenyl-sulfide intermediate state is suggested in D3 by studies based on the structural analysis of D3 protein. Comparison of homologies between D2 and D3 revealed that D2 lacks a critical cysteine proposed to be important in the reduction of deiodinases therefore D2 could be trapped in this inactive state and could be facilitated for ubiquitination [142]. This hypothesis should be clarified by further investigation however the presence of one of this inactive intermediate D2 could affect the active conformation of the interacting partner in D2 homodimers. Therefore its clearance could be beneficial in the achievement and maintenance of elevated D2 activity.

#### **7.2.4. Topology of D2-MARCH6 interaction**

The involvement of MARCH6 protein in the posttranslational regulation of D2 has been previously demonstrated but its precise action is remained to be clarified. Using FRET method we documented direct protein-protein interaction between MARCH6 and D2 in living mammalian cells. We have also shown that this interaction is realized between the N-terminus of MARCH6 protein and the C-terminal globular domain of D2. Taking into account the ambiguous membrane topology of MARCH6 [233, 234] our interaction study also addressed the potential localization of the MARCH6 C-terminus but we observed that this part of the protein is not involved in the recognition of D2 directly. It is important to note that the N-terminus of MARCH6 carries RING-domain a common structural unit of the vast majority of E3 ubiquitin ligases or ligase complexes. Therefore the N-terminus of MARCH6 protein incorporates both of the most important function of an E3 ligase – at least in case of D2 – the facility of substrate recognition and the ubiquitin-conjugation catalytic activity.

### 7.2.5. Thyroid hormone-dependence of MARCH6-mediated regulation of D2

Promoter analysis did not revealed canonical positive TRE consensus sequence in the 3.5 kb 5' FR of human *MARCH6* gene but several TRE half-sites were predicted. Taking into account the numerous genes known to be regulated by THs in the absence of a classical TRE (e.g. DR4) sequence, we tested the effect of T<sub>3</sub> on *MARCH6* promoter activity with dual luciferase promoter assay. However, 3.5 kb FR of human *MARCH6* did not respond to T<sub>3</sub> indicating the D2 ubiquitination via *MARCH6* is not regulated by THs on transcriptional level.

The product- or intermediate compound-driven feedback is an important and common mechanism of the regulation of enzyme activity allowing the rapid control of biological processes. Usually this regulation is carried out by the allosteric action of a product (or another downstream metabolite) of the enzyme. However, as an untypical example of enzyme regulation D2 is regulated by its substrate, T<sub>4</sub>. In this case, T<sub>4</sub> serves as a feedforward regulator inhibiting the activity of the enzyme by increasing the accessibility of D2 by its ubiquitin-conjugating apparatus. The accurate mechanism is still remained to be elucidated whether this phenomenon is originated from the catalytic cycle of D2 or is related to a region located outside of the active center. The increased ubiquitination of D2 by T<sub>4</sub> results an inactive enzyme conformation or leads to its degradation in the 26S proteasome. Previous studies showed the importance of WSB1 ligase subunit within this process. Using FRET studies we found that the D2- *MARCH6* interaction is also positively controlled by T<sub>4</sub> that clearly indicates the involvement of *MARCH6* in the substrate-mediated ubiquitination of D2. Therefore both known E3 ligases of D2 are involved in substrate-mediated downregulation of TH activating capacity.

The regulation of *MARCH6* expression and involvement in the posttranslational control of D2 is summarized in **Fig. 33**.

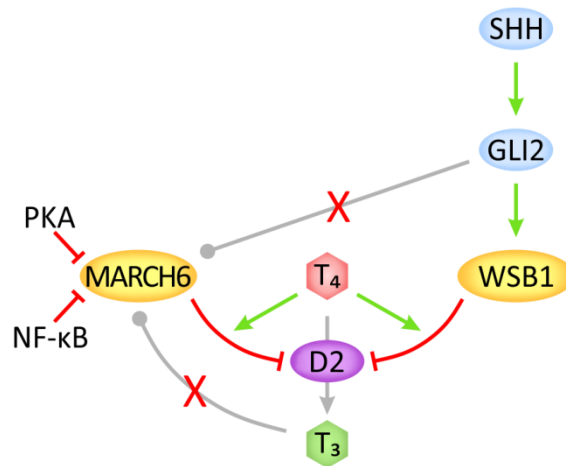


**Figure 33. Schematic depiction of the regulation and involvement of MARCH6 in D2 ubiquitination**

### **7.2.6. Construction of a 3-FRET approach to study parallel the interactions of D2 with the two E3-ligases**

The previously revealed T<sub>4</sub>-mediated action of MARCH6 raised the question whether ligase preference exists in the substrate-mediated ubiquitination of D2. Importantly, tanyocytes are the only cell type in the brain where D2 could be regulated by both of its E3 ligases therefore the coordinated action of WSB1 and MARCH6 regulating the T<sub>3</sub> generation could have a role in the regulation of HPT axis. Standard FRET design is restricted to the investigation of interaction between two proteins therefore it cannot be used to study the interaction between D2 and its two E3 ligases at the same time. To overcome this limitation we aimed to set-up a 3-FRET approach by taking advantage of the properties of EYFP. The EYFP is able to serve both as an acceptor and a donor in appropriate FRET pairs. In this application the D2 was fused to EYFP therefore it can be a FRET acceptor for ECFP-fused MARCH6 while acts as a donor for mCherry-fused WSB1. This system was capable to monitor the interactions between the D2 and its ubiquitin ligases within the same living cell. Using this approach we demonstrated that both E3 ligases has associated with D2-dimers in the lack of T<sub>4</sub> and both of them are involved at a similar level in T<sub>4</sub>-dependent D2 inactivation and the process did not demonstrate ligase preference. These data suggest that the substrate-mediated inhibition is based on a conformational change within the D2 allowing the availability of the recognition surface for the ubiquitin ligases. It is important to note that this recognition surface of D2 is not yet identified due lacking structural data. However, these results

indicate that significant interference does not exist between the two E3 ligases that suggest the existence of different recognition motifs. It was previously shown that the subunits of ECF<sup>WSB1</sup> ligase complex are closely associated to D2 dimers in the ER [162]. These results also indicate that MARCH6 has high affinity to D2 although it is not incorporated of the ECF<sup>WSB1</sup> ligase complex.

### **7.3. STRUCTURAL BACKGROUND OF THE UBIQUITINATION OF DEIODINASES**

#### **7.3.1. Molecular background of stability and ubiquitination of deiodinases**

Ubiquitination mediated processing of D2 is presently the most sensitive and quickest way to regulate TH activation. In order to better understand the mechanism of regulation of TH metabolism by ubiquitination, we aimed to identify the minimal requirements of ubiquitination of deiodinases. Previous studies were based on deletion and mutation of D2-specific motifs and targeted the identification of elements and motifs involved in the ubiquitination of the D2 protein [161, 162, 203]. We applied a reverse strategy incorporating D2-specific elements into D1 a non-ubiquitinated and stable deiodinase backbone resulting a D1-D2 chimeric protein. The previously used approach was capable to predict structural elements – or the parts of these elements – with important role in ubiquitination by detecting the interfered ubiquitination in absence of these regions. However, this strategy is unable to dissect precisely whether a specific element is an independent degradation unit or only part of such an element without the capacity to induce ubiquitin-mediated instability alone. For example this approach could not be used to resolve whether the identified element composes a discrete motif or represents a portion of a larger interaction surface, or alternatively, its function is the scaffolding of recognition epitope for ubiquitin ligases. The last case could result altered ubiquitination by misfolded epitope in deletion studies. Therefore we applied a reversed strategy to try to convert a non-ubiquitinated deiodinase into ubiquitination-susceptible form by the incorporation of the complete and functional element. Using this approach combinations of D2-specific elements were tested to reveal the sufficient and required set of molecular elements needed to turn the stable D1 protein to a destabilized D2-like protein that is sensitive to ubiquitination.

We found that the incorporation of one or two ubiquitin-carrier lysines of D2 did not result in significant alteration in the half-life of the chimera and no ubiquitinated forms could be revealed. In contrast, simultaneous mutations of these lysines within the D2 stabilized the protein and led to loss of T<sub>4</sub>-mediated downregulation via ubiquitination [162]. Together these data directly prove that other D2-specific elements that are not present in D1 are required to the recognition of the protein by the ubiquitin-conjugating apparatus, since the insertion of ubiquitin-carrier lysines without additional motifs was unable to target the chimeric protein for the UPS. We then studied the impact of the insertion of the D2-specific instability-loop into the chimera carrying lysine mutation(s) in the homologue position compared to D2 protein. Alignment of D1 and D2 proteins revealed an 18 amino acid-length sequence which is unique in D2 proteins and its existence but not its sequence is conserved among species. A previous study focused on the characterization of the effect of this region on the ubiquitin-mediated regulation of D2 showed that the critical region of this loop is the N-terminal 6 amino acids. The deletion of this region – similarly to the deletion of the whole loop – stabilized the D2 protein while the deletion of the C-terminal 12 amino acids has little effect on the protein half-life [203]. Therefore in this study we applied the incorporation of this 6 amino acid-length loop into chimeric deiodinases. Chimeras containing ubiquitin-carrier lysines and the loop sequence showed decreased half-life without detectable signs of the involvement of the ubiquitin-proteasomal system since no high molecular mass forms could be identified and inhibition of proteasome did not increase the activity of the enzyme. It is unlikely that this short region could interact directly with ubiquitin ligases of D2. However this flexible loop may have an important role in T<sub>4</sub>-induced conformational changes underlying the acceptability of D2 by the E3 ligases. These findings raise the possibility that the inherent instability of D2 is not exclusively derived from the UPS but other non-proteasomal mechanisms could be involved as shown for iron regulatory protein 2 and IKBA [235, 236]. The combined insertion of lysine residues and the loop-sequence was accompanied by the addition of a SEC62 domain to allow sorting of the protein to the ER, the cellular compartment where D2 – uniquely among deiodinases – is located in the cells. Interestingly, these properties resulted high molecular mass ubiquitinated forms and decreased stability of the chimera indicating that the applied elements were sufficient and required to induce the ubiquitination of the chimera. It was

previously shown that the SEC62-fusion used for the direction of the chimera to the ER abolished deiodinase activity [203]. As a consequence the effect of proteasome inhibitors on the activity of the ER directed D1-D2 chimera could not be tested by activity assay. Therefore to prove the specificity of this ubiquitination carried out by D2 ubiquitin ligases we tested the interaction between chimeras and WSB1 ligase subunit and MARCH6 ligase as discussed in the following section. The effect of the investigated structural elements on the stability and ubiquitination of deiodinases are summarized in **Fig.34**.

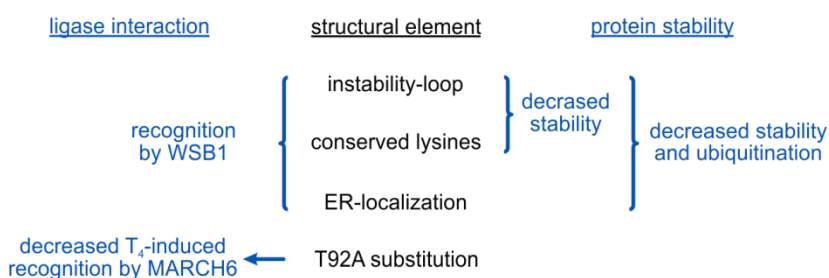


**Figure 34. Summary of the effects of structural elements on D2 stability and ubiquitination**

### 7.3.2. Importance of D2-specific elements in the recognition by ubiquitin ligases

We also studied the recognition criteria of D2-specific E3 ligases to exclude that ubiquitination of the generated chimera was a result of unspecific mechanisms triggered by either the cytotoxic levels of overexpressed proteins or non-specific interaction due to their high concentration or by misfolding. We also aimed to identify the required elements for D2 ligases to recognize a deiodinase protein as a substrate. These measurements revealed that the lysine residues in combination with instability-loop or the ER-localization alone are insufficient to allow an interaction between deiodinases and WSB1 or MARCH6 E3 ligases. These data are in accordance with our above demonstrated findings on testing the stability of chimeric deiodinases that the chimeras contained separately or in combination the lysine residues and instability-loop were not ubiquitinated. However the insertion of these elements into ER-directed D1 backbone (SEC62-D1-2K-loop) resulted in detectable interaction with the WSB1 ligase subunit while MARCH6 was still unable to recognize this chimera. These data together indicates that a specific D2 ligase can catalyze the ubiquitination of the lysine- and loop-containing, ER-targeted chimera. Additionally, the difference in binding of this chimera by the two known D2 E3 ligases suggests the different structural background and mechanism of

action of WSB1 and MARCH6 on D2. The anticipated difference in ubiquitin-conjugation raises the possibility of different function of D2-specific E3 ligases in the regulation of TH activation.

The ubiquitin-code – defining the downstream processing of proteins tagged by ubiquitin or multiple ubiquitin moieties – is under intensive examination. However, it has been poorly understood how the quality of the polyubiquitin chain determines the further processing of protein. A subset of these ubiquitin signals has well characterized functions – e.g. K48-linked and K63-linked polyubiquitin chains as canonical degradative and non-degradative signals, respectively. In combination with UBC6 E2 ubiquitin conjugating enzyme (yeast orthologue of UBE2J) the Doa10 ubiquitin ligase (yeast orthologue of MARCH6) was shown to be involved in the synthesis of the relatively rare K11-linked polyubiquitin chain formation that function is poorly understood [182]. The involvement of UBE2J and MARCH6 in the ubiquitination of D2 was shown in previous studies [160, 211] raising the possibility that this non-canonical, K11-linked polyubiquitin chain could play a role in the regulation of TH activation. Therefore further studies are required to target the characterization of the precise architecture of the ubiquitin signal built on D2 focusing on the occurrence of chain-types and their function in the regulation of the D2 enzyme. It is also remains to be clarified whether the equilibrium between reversible ubiquitination and degradation of D2 is determined by the capacity and efficiency of ubiquitination, deubiquitination and membrane extraction or these pathways are controlled by different ubiquitin motifs.

The effect of the investigated structural elements on recognition by D2 ubiquitin ligases are summarized in **Fig.34**.

### **7.3.3. Effect of threonine/alanine polymorphism in D2 on the interaction with its ubiquitin ligases**

Previous studies based on statistical correlations suggested linkage between genetic variant of human D2 and obesity, insulin secretion, risk of type 2 diabetes [237-239] and altered response for TH replacement therapy [240]. However, the importance of T92A substitution in D2 protein and how this single amino acid change affects the enzyme properties are poorly understood. Previous results indicated decreased  $V_{max}$  and

unaffected  $K_M$  and stability [126]. Importantly, the 92th amino acid is the first residue of the instability-loop of D2. Therefore 3-FRET measurements were applied to understand whether the ubiquitin-mediated processing of polymorphic Ala<sup>92</sup> D2 is altered compared to the wild-type Thr<sup>92</sup> D2. We demonstrated that the interactions with WSB1 and MARCH6 were unaffected by the polymorphism. Interestingly, the T<sub>4</sub>-mediated increase in association with MARCH6 was interfered by T92A mutation while the induction of WSB1-D2 interaction was similar between wild-type and polymorphic D2. Since polymorphic D2 is suggested to have longer half-life compared to wild-type, our findings revealed a mechanism that could contribute to this phenomenon [128]. These results also support our previous findings that WSB1 and MARCH6 could recognize different interaction surface on D2 (**Fig. 34**).

#### **7.3.4. Relationship between deubiquitination and extraction of D2 from the ER**

Cytosolic soluble ubiquitinated proteins can be directly processed by the proteasome. However, ER-resident proteins need to be extracted from the ER before their degradation can occur. This step includes ATP-dependent processes carried out by multiprotein-complex organized by the p97 hexamer [241] and Atx3 deubiquitinase [242]. In ERAD, this is a critically important step in the degradation of misfolded proteins however for specific targets, e.g. D2 this process has an additional feature. The ubiquitination of D2 enzyme leads to abolished enzyme activity however this process does not result in obligatory protein degradation, active D2 conformation could be recovered by deubiquitination allowing reversible ubiquitin-mediated regulation. Therefore this mechanism provides a rapid and economic way to control the T<sub>3</sub> generating capacity. D2 deubiquitination was suggested to play a role in the generation of different responsiveness of D2 activity to T<sub>4</sub> in specific brain regions. For example in the cortex, D2 activity in astrocytes responds to T<sub>4</sub> in a homeostatic manner while tanycytes in the hypothalamus do not and in accordance, not astrocytes, only tanycytes express the D2 deubiquitinase USP33 that could allow a rescue from T<sub>4</sub> induced downregulation of D2 activity [243]. However, regaining D2 activity by deubiquitination can occur only before membrane-extraction. Therefore the membrane extraction of ubiquitinated D2 could be a rate limiting step regulating the equilibrium between reversible inactivation of D2 and its

irreversible degradation. Consequently, this system is a key factor determining the amount of ubiquitinated D2 available for its deubiquitinases USP33 and USP20 [163]. However the inhibition of p97/Atx3 complex did not lead to increased D2 activity. Therefore we dissected with FRET the protein-protein interactions underlying this phenomenon. We observed a decreased interaction between the globular domains of the D2 homodimer in presence of p97 inhibitor, EERI and the interaction gained insensitivity to T<sub>4</sub> in the presence of EERI. Since ubiquitination is known to destabilize D2 homodimers we concluded that the equilibrium in the ubiquitination state of D2 shifted to the inactive, ubiquitin-conjugated state providing mechanistic explanation for the observed unchanged D2 activity in preliminary studies. However it remains to be answered how the abolished ER membrane extraction affects the ubiquitination or deubiquitination. Therefore we also measured the interaction between the USP33 deubiquitinase and D2 revealing decreased recognition of the D2 by its deubiquitinase enzyme upon the inhibition of p97/Atx3 complex. These data suggest that the enrichment of ubiquitinated D2 in the ER due to the loss of extraction capacity is compensated by decreased deubiquitination. Importantly, the action of USP33 is not restricted to D2 therefore the alteration of ubiquitination state of its other substrates could affect the amount of available deubiquitinase enzyme for D2. Our data indicate strong link between USP33-mediated deubiquitination and p97 membrane extraction complex. This finding is in accordance with previous observations revealing the USP33 itself as a target of ubiquitination and interestingly this process is depends on the presence and activity of p97 [244].

## 8. CONCLUSIONS

The performed studies aimed to better understand the impact of thyroid hormone activation on the HPT axis along with molecular mechanisms underlying the regulation of type 2 deiodinase, the key player of thyroid hormone activation.

Our data demonstrated that cAMP-mediated activation of *Dio2* gene by PACAP in tanycytes has a striking effect on the HPT axis by suppressing TRH neurons of the hypothalamic paraventricular nucleus via elevated local T<sub>3</sub> production, despite the earlier proposed stimulatory effect of PACAP on TRH. We also found that PACAP affects the maturation of the HPT axis. A bidirectional interaction was found between thyroid hormones and PACAP since the liganded thyroid hormone receptor interferes with the cAMP-mediated induction of the PACAP encoding *Adcyap1* promoter although the consequences of this mechanism was region-specific *in vivo*.

D2 ubiquitination represent the most efficient way to regulate D2 activity. To better understand the mechanism of D2 ubiquitination, we characterized the MARCH6 ubiquitin ligase in comparison with the WSB1 ligase subunit. Both of these D2 ubiquitin ligases are widely expressed with alterations in expression level. Major differences were found in the regulation of the two ubiquitin ligases. In contrast to WSB1, MARCH6 was found unresponsive to important regulators of thyroid hormone metabolism like Sonic hedgehog, and cold stress. These findings suggested that MARCH6 could be responsible for basal instability of D2 while WSB1 represent the inducible component of the D2 ubiquitination machinery.

We clarified the topology of the D2-MARCH6 interaction by demonstrating direct protein-protein interaction between the D2 globular domain and the N-terminal RING-domain of MARCH6 in living cells. We proved that the interaction is increased upon T<sub>4</sub> exposure as an underlying mechanism of substrate induced downregulation of the D2 protein. In contrast, the expression of *MARCH6* was not affected by thyroid hormones.

Using chimeric recombinant deiodinases we identified the minimal combination of structural elements required and sufficient for the instability and targeting of deiodinase proteins for ubiquitination. Additionally, our data revealed differences in the structural background of the recognition of D2 by its ubiquitin ligases. Differences were also observed between wild-type and T92A polymorphic D2 protein with respect to MARCH6

ligase binding since the polymorphism abolished the T<sub>4</sub>-sensitivity of D2-MARCH6 interaction, while did not alter WSB1 binding under this conditions.

Our data indicated a strong functional link between D2 deubiquitination and its extraction from the ER membrane indicating this step could be rate-limiting during reversible ubiquitination.

## 9. SUMMARY

The major secretory product of the thyroid gland is the thyroxine ( $T_4$ ), a stable prohormone with low affinity to thyroid hormone nuclear receptors.  $T_4$  needs to undergo local activation to  $T_3$  via type 2 deiodinase (D2) to evoke thyroid hormone action. This process is crucial in the brain where  $T_4$  has poor access to the brain parenchyma via the blood-brain and CSF-brain barriers. Therefore D2 is under tight control including transcriptional elements and the posttranslational ubiquitin-proteasome system. We aimed to better understand the molecular regulation of D2 and its impact on the HPT axis.

We described that PACAP affects the activity of the HPT axis via cAMP-mediated activation of D2 encoding *Dio2* in tanycytes of the mediobasal hypothalamus. The increased  $T_3$  generation suppresses TRH expression in the hypothalamic paraventricular nucleus despite the earlier proposed stimulatory effect of PACAP on TRH expression. PACAP was also found to play a role in the maturation of HPT axis by affecting the local thyroid hormone metabolism during the establishment of the set point of HPT axis.

D2 is targeted by two ubiquitin ligases, the WSB1 complex and MARCH6. We demonstrated that similarly to *Wsb1* the *March6* gene is widely expressed in different brain regions and tissues while both were absent in thyroid gland. We demonstrated the role of MARCH6 in the regulation of D2 based on protein-protein interaction in living cells. This interaction occurs between the globular domain of D2 and N-terminus of MARCH6 and sensitive for  $T_4$  – similarly to D2-WSB1 interaction – indicating the contribution of both ligases in the substrate-mediated inactivation of D2.

Constructing chimeric deiodinases we identified the minimal structural elements required for the instability and ubiquitination of a deiodinase protein and demonstrated differences between the recognition of D2 by the two ubiquitin ligases. Using a protein-protein interaction approach we observed intense connection between ER-extraction of D2 and its deubiquitination suggesting that this process represents a rate limiting step in the reversible ubiquitination of D2.

As conclusion our data contribute to the better understanding of the complex regulation of D2 enzyme the crucial element of thyroid hormone action in the brain.

## 10. ÖSSZEFOGLALÁS

A pajzsmirigy fő szekretoros terméke a stabil prohormon tiroxin ( $T_4$ ), alacsony affinitással a pajzsmirigyhormon magi receptorok felé. A  $T_4$ -nek lokálisan  $T_3$ -má kell alakulnia a kettes-típusú dejodáz (D2) enzim által a szöveti pajzsmirigyhormon hatás kifejtéséhez. E folyamat az agyban kiemelt jelentőségű, mivel a  $T_3$  rendkívül alacsony mértékben jut át a vér-agy és az CSF-agy gáton. Ezért a D2 komplex transzkripcionális és poszttranszlációs szabályozás alatt áll. Célunk a D2 molekuláris szabályozásának jobb megértése és annak jelentőségének feltárása a HHP tengely működésében.

Leírtuk a HHP tengely PACAP-általi szabályozását a D2-t kódoló *Dio2* gén cAMP-általi aktiválásán keresztül tunicitákban, a mediobasalis hypothalamusban. Az így megemelkedett  $T_3$  előállítás gátolja a TRH expressziót a hypothalamus paraventricularis magjában a PACAP korábban feltételezett TRH-t stimuláló hatása ellenére. A PACAP fontos szerepet játszhat a HHP tengely fejlődésében a helyi pajzsmirigyhormon metabolizmus szabályozásával a tengely egyensúlyi pontjának kialakulása során.

A D2-t szabályozásában két ubikvitin ligáz vesz részt: a WSB1 komplex és a MARCH6. Azonban a MARCH6 tulajdonságai és szabályozása kevésbé feltárt. Eredményeink a *March6* széleskörű szöveti expressziójára mutatnak rá, hasonlóan a *Wsb1*-hez, beleértve mindkét ligáz hiányát a pajzsmirigyben. Igazoltuk, hogy a MARCH6 szerepe a D2 szabályozásában fehérje-fehérje interakción alapul. Ezen interakció a MARCH6 N-terminusa és a D2 globuláris doménje között jön létre és – a WSB1-hez hasonlóan –  $T_4$ -re érzékeny, vagyis mindkét ligáz részt vesz a D2 szubsztrát-közvetítette inaktiválásában.

Kiméra dejodázok létrehozásával azonosítottuk a szerkezeti elemek azon minimális kombinációját, amely szükséges és elégséges egy dejodáz enzim instabilizálásához és ubikvitinációjához. E mellett a két ligáz kötőhelyében különbségeket találtunk. Fehérje-fehérje interakciós vizsgálatokkal szoros kapcsolatot tártunk fel a D2 ER membránextrakciója és deubikvitinációja között, amely a folyamat sebesség-meghatározó szerepére utal a D2 reverzibilis ubikvitinációjában. Összefoglalásként az eredményeink hozzájárulnak az agyi pajzsmirigyhormon hatás kiemelt eleme, a D2 enzim összetett szabályozásának jobb megértéséhez az agyban.

## 11. REFERENCES

1. Bernal, J. and J. Nunez. (1995) Thyroid hormones and brain development. *Eur J Endocrinol.* 133(4): 390-8.
2. Fekete, C. and R.M. Lechan. (2014) Central regulation of hypothalamic-pituitary-thyroid axis under physiological and pathophysiological conditions. *Endocr Rev.* 35(2): 159-94.
3. Laurberg, P. (1984) Mechanisms governing the relative proportions of thyroxine and 3,5,3'-triiodothyronine in thyroid secretion. *Metabolism.* 33(4): 379-92.
4. Zhang, J. and M.A. Lazar. (2000) The mechanism of action of thyroid hormones. *Annu Rev Physiol.* 62: 439-66.
5. Schweizer, U., J. Johannes, D. Bayer and D. Braun. (2014) Structure and function of thyroid hormone plasma membrane transporters. *Eur Thyroid J.* 3(3): 143-53.
6. Crantz, F.R., J.E. Silva and P.R. Larsen. (1982) An analysis of the sources and quantity of 3,5,3'-triiodothyronine specifically bound to nuclear receptors in rat cerebral cortex and cerebellum. *Endocrinology.* 110(2): 367-75.
7. Campos-Barros, A., T. Hoell, A. Musa, S. Sampaolo, G. Stoltenburg, G. Pinna, M. Eravci, H. Meinhold and A. Baumgartner. (1996) Phenolic and tyrosyl ring iodothyronine deiodination and thyroid hormone concentrations in the human central nervous system. *J Clin Endocrinol Metab.* 81(6): 2179-85.
8. Freitas, B.C., B. Gereben, M. Castillo, I. Kallo, A. Zeold, P. Egri, Z. Liposits, A.M. Zavacki, R.M. Maciel, S. Jo, P. Singru, E. Sanchez, R.M. Lechan and A.C. Bianco. (2010) Paracrine signaling by glial cell-derived triiodothyronine activates neuronal gene expression in the rodent brain and human cells. *J Clin Invest.* 120(6): 2206-17.
9. Dayan, C.M. and V. Panicker. (2009) Novel insights into thyroid hormones from the study of common genetic variation. *Nat Rev Endocrinol.* 5(4): 211-8.
10. Abe, T., M. Kakyo, T. Tokui, R. Nakagomi, T. Nishio, D. Nakai, H. Nomura, M. Unno, M. Suzuki, T. Naitoh, S. Matsuno and H. Yawo. (1999) Identification of a novel gene family encoding human liver-specific organic anion transporter LST-1. *J Biol Chem.* 274(24): 17159-63.
11. Friesema, E.C., S. Ganguly, A. Abdalla, J.E. Manning Fox, A.P. Halestrap and T.J. Visser. (2003) Identification of monocarboxylate transporter 8 as a specific thyroid hormone transporter. *J Biol Chem.* 278(41): 40128-35.

12. Visser, T.J. (2013) Thyroid hormone transporters and resistance. *Endocr Dev.* 24: 1-10.
13. van der Deure, W.M., R.P. Peeters and T.J. Visser. (2010) Molecular aspects of thyroid hormone transporters, including MCT8, MCT10, and OATPs, and the effects of genetic variation in these transporters. *J Mol Endocrinol.* 44(1): 1-11.
14. Mayerl, S., T.J. Visser, V.M. Darras, S. Horn and H. Heuer. (2012) Impact of Oatp1c1 deficiency on thyroid hormone metabolism and action in the mouse brain. *Endocrinology.* 153(3): 1528-37.
15. Mayerl, S., J. Muller, R. Bauer, S. Richert, C.M. Kassmann, V.M. Darras, K. Buder, A. Boelen, T.J. Visser and H. Heuer. (2014) Transporters MCT8 and OATP1C1 maintain murine brain thyroid hormone homeostasis. *J Clin Invest.* 124(5): 1987-99.
16. Bassett, J.H. and G.R. Williams. (2009) The skeletal phenotypes of TR $\alpha$  and TR $\beta$  mutant mice. *J Mol Endocrinol.* 42(4): 269-82.
17. Ortiga-Carvalho, T.M., A.R. Sidhaye and F.E. Wondisford. (2014) Thyroid hormone receptors and resistance to thyroid hormone disorders. *Nat Rev Endocrinol.* 10(10): 582-91.
18. Katz, D., M.J. Reginato and M.A. Lazar. (1995) Functional regulation of thyroid hormone receptor variant TR  $\alpha$  2 by phosphorylation. *Mol Cell Biol.* 15(5): 2341-8.
19. Souza, P.C., A.C. Puhl, L. Martinez, R. Aparicio, A.S. Nascimento, A.C. Figueira, P. Nguyen, P. Webb, M.S. Skaf and I. Polikarpov. (2014) Identification of a new hormone-binding site on the surface of thyroid hormone receptor. *Mol Endocrinol.* 28(4): 534-45.
20. Borngraeber, S., M.J. Budny, G. Chiellini, S.T. Cunha-Lima, M. Togashi, P. Webb, J.D. Baxter, T.S. Scanlan and R.J. Fletterick. (2003) Ligand selectivity by seeking hydrophobicity in thyroid hormone receptor. *Proc Natl Acad Sci U S A.* 100(26): 15358-63.
21. Horlein, A.J., A.M. Naar, T. Heinzl, J. Torchia, B. Gloss, R. Kurokawa, A. Ryan, Y. Kamei, M. Soderstrom, C.K. Glass and M.G. Rosenfeld. (1995) Ligand-independent repression by the thyroid hormone receptor mediated by a nuclear receptor co-repressor. *Nature.* 377(6548): 397-404.
22. Perissi, V., K. Jepsen, C.K. Glass and M.G. Rosenfeld. (2010) Deconstructing repression: evolving models of co-repressor action. *Nat Rev Genet.* 11(2): 109-23.

23. Cheng, S.Y., J.L. Leonard and P.J. Davis. (2010) Molecular aspects of thyroid hormone actions. *Endocr Rev.* 31(2): 139-70.
24. Refetoff, S., L.T. DeWind and L.J. DeGroot. (1967) Familial syndrome combining deaf-mutism, stunted epiphyses, goiter and abnormally high PBI: possible target organ refractoriness to thyroid hormone. *J Clin Endocrinol Metab.* 27(2): 279-94.
25. Bochukova, E., N. Schoenmakers, M. Agostini, E. Schoenmakers, O. Rajanayagam, J.M. Keogh, E. Henning, J. Reinemund, E. Gevers, M. Sarri, K. Downes, A. Offiah, A. Albanese, D. Halsall, J.W. Schwabe, M. Bain, K. Lindley, F. Muntoni, F. Vargha-Khadem, M. Dattani, I.S. Farooqi, M. Gurnell and K. Chatterjee. (2012) A mutation in the thyroid hormone receptor alpha gene. *N Engl J Med.* 366(3): 243-9.
26. Moran, C., M. Agostini, W.E. Visser, E. Schoenmakers, N. Schoenmakers, A.C. Offiah, K. Poole, O. Rajanayagam, G. Lyons, D. Halsall, M. Gurnell, D. Chrysis, A. Efthymiadou, C. Buchanan, S. Aylwin and K.K. Chatterjee. (2014) Resistance to thyroid hormone caused by a mutation in thyroid hormone receptor (TR)alpha1 and TRalpha2: clinical, biochemical, and genetic analyses of three related patients. *Lancet Diabetes Endocrinol.* 2(8): 619-26.
27. van Mullem, A.A., D. Chrysis, A. Efthymiadou, E. Chroni, A. Tsatsoulis, Y.B. de Rijke, W.E. Visser, T.J. Visser and R.P. Peeters. (2013) Clinical phenotype of a new type of thyroid hormone resistance caused by a mutation of the TRalpha1 receptor: consequences of LT4 treatment. *J Clin Endocrinol Metab.* 98(7): 3029-38.
28. Wrutniak, C., I. Cassar-Malek, S. Marchal, A. Rascle, S. Heusser, J.M. Keller, J. Flechon, M. Dauca, J. Samarut, J. Ghysdael and G. Cabello. (1995) A 43-kDa protein related to c-Erb A alpha 1 is located in the mitochondrial matrix of rat liver. *J Biol Chem.* 270(27): 16347-54.
29. Pessemeesse, L., A. Schlernitzauer, C. Sar, J. Levin, S. Grandemange, P. Seyer, F.B. Favier, S. Kaminski, G. Cabello, C. Wrutniak-Cabello and F. Casas. (2012) Depletion of the p43 mitochondrial T3 receptor in mice affects skeletal muscle development and activity. *FASEB J.* 26(2): 748-56.
30. Bergh, J.J., H.Y. Lin, L. Lansing, S.N. Mohamed, F.B. Davis, S. Mousa and P.J. Davis. (2005) Integrin alphaVbeta3 contains a cell surface receptor site for thyroid hormone that is linked to activation of mitogen-activated protein kinase and induction of angiogenesis. *Endocrinology.* 146(7): 2864-71.
31. Davis, P.J., A. Shih, H.Y. Lin, L.J. Martino and F.B. Davis. (2000) Thyroxine promotes association of mitogen-activated protein kinase and nuclear thyroid

- hormone receptor (TR) and causes serine phosphorylation of TR. *J Biol Chem.* 275(48): 38032-9.
32. Smith, J.W., A.T. Evans, B. Costall and J.W. Smythe. (2002) Thyroid hormones, brain function and cognition: a brief review. *Neurosci Biobehav Rev.* 26(1): 45-60.
  33. Alvarez-Dolado, M., M. Ruiz, J.A. Del Rio, S. Alcantara, F. Burgaya, M. Sheldon, K. Nakajima, J. Bernal, B.W. Howell, T. Curran, E. Soriano and A. Munoz. (1999) Thyroid hormone regulates reelin and *dab1* expression during brain development. *J Neurosci.* 19(16): 6979-93.
  34. Koibuchi, N., H. Fukuda and W.W. Chin. (1999) Promoter-specific regulation of the brain-derived neurotropic factor gene by thyroid hormone in the developing rat cerebellum. *Endocrinology.* 140(9): 3955-61.
  35. Calza, L., M. Fernandez, A. Giuliani, L. Aloe and L. Giardino. (2002) Thyroid hormone activates oligodendrocyte precursors and increases a myelin-forming protein and NGF content in the spinal cord during experimental allergic encephalomyelitis. *Proc Natl Acad Sci U S A.* 99(5): 3258-63.
  36. Farsetti, A., T. Mitsuhashi, B. Desvergne, J. Robbins and V.M. Nikodem. (1991) Molecular basis of thyroid hormone regulation of myelin basic protein gene expression in rodent brain. *J Biol Chem.* 266(34): 23226-32.
  37. Farsetti, A., B. Desvergne, P. Hallenbeck, J. Robbins and V.M. Nikodem. (1992) Characterization of myelin basic protein thyroid hormone response element and its function in the context of native and heterologous promoter. *J Biol Chem.* 267(22): 15784-8.
  38. Potter, G.B., F. Facchinetti, G.M. Beaudoin, 3rd and C.C. Thompson. (2001) Neuronal expression of synaptotagmin-related gene 1 is regulated by thyroid hormone during cerebellar development. *J Neurosci.* 21(12): 4373-80.
  39. Heuer, H. and C.A. Mason. (2003) Thyroid hormone induces cerebellar Purkinje cell dendritic development via the thyroid hormone receptor alpha1. *J Neurosci.* 23(33): 10604-12.
  40. Faustino, L.C. and T.M. Ortiga-Carvalho. (2014) Thyroid hormone role on cerebellar development and maintenance: a perspective based on transgenic mouse models. *Front Endocrinol (Lausanne).* 5: 75.
  41. Fauquier, T., E. Romero, F. Picou, F. Chatonnet, X.N. Nguyen, L. Quignodon and F. Flamant. (2011) Severe impairment of cerebellum development in mice expressing a dominant-negative mutation inactivating thyroid hormone receptor alpha1 isoform. *Dev Biol.* 356(2): 350-8.

42. Fernandez-Lamo, I., A. Montero-Pedrazuela, J.M. Delgado-Garcia, A. Guadano-Ferraz and A. Gruart. (2009) Effects of thyroid hormone replacement on associative learning and hippocampal synaptic plasticity in adult hypothyroid rats. *Eur J Neurosci.* 30(4): 679-92.
43. Desouza, L.A., U. Ladiwala, S.M. Daniel, S. Agashe, R.A. Vaidya and V.A. Vaidya. (2005) Thyroid hormone regulates hippocampal neurogenesis in the adult rat brain. *Mol Cell Neurosci.* 29(3): 414-26.
44. Bauer, M., A. Heinz and P.C. Whybrow. (2002) Thyroid hormones, serotonin and mood: of synergy and significance in the adult brain. *Mol Psychiatry.* 7(2): 140-56.
45. Viguie, C., D.F. Battaglia, H.B. Krasa, L.A. Thrun and F.J. Karsch. (1999) Thyroid hormones act primarily within the brain to promote the seasonal inhibition of luteinizing hormone secretion in the ewe. *Endocrinology.* 140(3): 1111-7.
46. Shinomiya, A., T. Shimmura, T. Nishiwaki-Ohkawa and T. Yoshimura. (2014) Regulation of seasonal reproduction by hypothalamic activation of thyroid hormone. *Front Endocrinol (Lausanne).* 5: 12.
47. Pernasetti, F., L. Caccavelli, C. Van de Weerd, J.A. Martial and M. Muller. (1997) Thyroid hormone inhibits the human prolactin gene promoter by interfering with activating protein-1 and estrogen stimulations. *Mol Endocrinol.* 11(7): 986-96.
48. Castillo, A.I., R. Sanchez-Martinez, J.L. Moreno, O.A. Martinez-Iglesias, D. Palacios and A. Aranda. (2004) A permissive retinoid X receptor/thyroid hormone receptor heterodimer allows stimulation of prolactin gene transcription by thyroid hormone and 9-cis-retinoic acid. *Mol Cell Biol.* 24(2): 502-13.
49. Shi, Z.X., A. Levy and S.L. Lightman. (1994) Thyroid hormone-mediated regulation of corticotropin-releasing hormone messenger ribonucleic acid in the rat. *Endocrinology.* 134(3): 1577-80.
50. Johnson, E.O., A.E. Calogero, M. Konstandi, T.C. Kamilaris, S. La Vignera and G.P. Chrousos. (2012) Effects of short- and long-duration hypothyroidism on hypothalamic-pituitary-adrenal axis function in rats: in vitro and in situ studies. *Endocrine.* 42(3): 684-93.
51. Buras, A., L. Battle, E. Landers, T. Nguyen and N. Vasudevan. (2014) Thyroid hormones regulate anxiety in the male mouse. *Horm Behav.* 65(2): 88-96.
52. Weber, T., U. Zimmermann, H. Winter, A. Mack, I. Kopschall, K. Rohbock, H.P. Zenner and M. Knipper. (2002) Thyroid hormone is a critical determinant for the

- regulation of the cochlear motor protein prestin. *Proc Natl Acad Sci U S A.* 99(5): 2901-6.
53. Sharlin, D.S., T.J. Visser and D. Forrest. (2011) Developmental and cell-specific expression of thyroid hormone transporters in the mouse cochlea. *Endocrinology.* 152(12): 5053-64.
  54. Ng, L., R.J. Goodyear, C.A. Woods, M.J. Schneider, E. Diamond, G.P. Richardson, M.W. Kelley, D.L. Germain, V.A. Galton and D. Forrest. (2004) Hearing loss and retarded cochlear development in mice lacking type 2 iodothyronine deiodinase. *Proc Natl Acad Sci U S A.* 101(10): 3474-9.
  55. Ng, L., A. Hernandez, W. He, T. Ren, M. Srinivas, M. Ma, V.A. Galton, D.L. St Germain and D. Forrest. (2009) A protective role for type 3 deiodinase, a thyroid hormone-inactivating enzyme, in cochlear development and auditory function. *Endocrinology.* 150(4): 1952-60.
  56. Gamborino, M.J., E. Sevilla-Romero, A. Munoz, J. Hernandez-Yago, J. Renau-Piqueras and M.D. Pinazo-Duran. (2001) Role of thyroid hormone in craniofacial and eye development using a rat model. *Ophthalmic Res.* 33(5): 283-91.
  57. Ng, L., J.B. Hurley, B. Dierks, M. Srinivas, C. Salto, B. Vennstrom, T.A. Reh and D. Forrest. (2001) A thyroid hormone receptor that is required for the development of green cone photoreceptors. *Nat Genet.* 27(1): 94-8.
  58. Ma, H., A. Thapa, L. Morris, T.M. Redmond, W. Baehr and X.Q. Ding. (2014) Suppressing thyroid hormone signaling preserves cone photoreceptors in mouse models of retinal degeneration. *Proc Natl Acad Sci U S A.* 111(9): 3602-7.
  59. Cioffi, F., R. Senese, A. Lanni and F. Goglia. (2013) Thyroid hormones and mitochondria: with a brief look at derivatives and analogues. *Mol Cell Endocrinol.* 379(1-2): 51-61.
  60. Martinez-Sanchez, N., C.V. Alvarez, J. Ferno, R. Nogueiras, C. Dieguez and M. Lopez. (2014) Hypothalamic effects of thyroid hormones on metabolism. *Best Pract Res Clin Endocrinol Metab.* 28(5): 703-12.
  61. Sinha, R.A., B.K. Singh and P.M. Yen. (2014) Thyroid hormone regulation of hepatic lipid and carbohydrate metabolism. *Trends Endocrinol Metab.* 25(10): 538-45.
  62. de Lange, P., R. Senese, F. Cioffi, M. Moreno, A. Lombardi, E. Silvestri, F. Goglia and A. Lanni. (2008) Rapid activation by 3,5,3'-L-triiodothyronine of adenosine 5'-monophosphate-activated protein kinase/acetyl-coenzyme a carboxylase and akt/protein kinase B signaling pathways: relation to changes in

- fuel metabolism and myosin heavy-chain protein content in rat gastrocnemius muscle in vivo. *Endocrinology*. 149(12): 6462-70.
63. Cannon, B. and J. Nedergaard. (2004) Brown adipose tissue: function and physiological significance. *Physiol Rev*. 84(1): 277-359.
  64. van der Lans, A.A., R. Wierdsma, M.J. Vosselman, P. Schrauwen, B. Brans and W.D. van Marken Lichtenbelt. (2014) Cold-activated brown adipose tissue in human adults: methodological issues. *Am J Physiol Regul Integr Comp Physiol*. 307(2): R103-113.
  65. van Marken Lichtenbelt, W.D., J.W. Vanhommerig, N.M. Smulders, J.M. Drossaerts, G.J. Kemerink, N.D. Bouvy, P. Schrauwen and G.J. Teule. (2009) Cold-activated brown adipose tissue in healthy men. *N Engl J Med*. 360(15): 1500-8.
  66. Saito, M., Y. Okamatsu-Ogura, M. Matsushita, K. Watanabe, T. Yoneshiro, J. Nio-Kobayashi, T. Iwanaga, M. Miyagawa, T. Kameya, K. Nakada, Y. Kawai and M. Tsujisaki. (2009) High incidence of metabolically active brown adipose tissue in healthy adult humans: effects of cold exposure and adiposity. *Diabetes*. 58(7): 1526-31.
  67. Harms, M. and P. Seale. (2013) Brown and beige fat: development, function and therapeutic potential. *Nat Med*. 19(10): 1252-63.
  68. Wu, J., P. Bostrom, L.M. Sparks, L. Ye, J.H. Choi, A.H. Giang, M. Khandekar, K.A. Virtanen, P. Nuutila, G. Schaart, K. Huang, H. Tu, W.D. van Marken Lichtenbelt, J. Hoeks, S. Enerback, P. Schrauwen and B.M. Spiegelman. (2012) Beige adipocytes are a distinct type of thermogenic fat cell in mouse and human. *Cell*. 150(2): 366-76.
  69. Sharp, L.Z., K. Shinoda, H. Ohno, D.W. Scheel, E. Tomoda, L. Ruiz, H. Hu, L. Wang, Z. Pavlova, V. Gilsanz and S. Kajimura. (2012) Human BAT possesses molecular signatures that resemble beige/brite cells. *PLoS One*. 7(11): e49452.
  70. Tupone, D., C.J. Madden and S.F. Morrison. (2014) Autonomic regulation of brown adipose tissue thermogenesis in health and disease: potential clinical applications for altering BAT thermogenesis. *Front Neurosci*. 8: 14.
  71. Grujic, D., V.S. Susulic, M.E. Harper, J. Himms-Hagen, B.A. Cunningham, B.E. Corkey and B.B. Lowell. (1997) Beta3-adrenergic receptors on white and brown adipocytes mediate beta3-selective agonist-induced effects on energy expenditure, insulin secretion, and food intake. A study using transgenic and gene knockout mice. *J Biol Chem*. 272(28): 17686-93.

72. Martinez de Mena, R., T.S. Scanlan and M.J. Obregon. (2010) The T3 receptor beta1 isoform regulates UCP1 and D2 deiodinase in rat brown adipocytes. *Endocrinology*. 151(10): 5074-83.
73. Shen, X., Q.L. Li, G.A. Brent and T.C. Friedman. (2004) Thyroid hormone regulation of prohormone convertase 1 (PC1): regional expression in rat brain and in vitro characterization of negative thyroid hormone response elements. *J Mol Endocrinol*. 33(1): 21-33.
74. Li, Q.L., E. Jansen, G.A. Brent and T.C. Friedman. (2001) Regulation of prohormone convertase 1 (PC1) by thyroid hormone. *Am J Physiol Endocrinol Metab*. 280(1): E160-70.
75. Sanchez, E., M.A. Vargas, P.S. Singru, I. Pascual, F. Romero, C. Fekete, J.L. Charli and R.M. Lechan. (2009) Tanycyte pyroglutamyl peptidase II contributes to regulation of the hypothalamic-pituitary-thyroid axis through glial-axonal associations in the median eminence. *Endocrinology*. 150(5): 2283-91.
76. Lazcano, I., A. Cabral, R.M. Uribe, L. Jaimes-Hoy, M. Perello, P. Joseph-Bravo, E. Sanchez-Jaramillo and J.L. Charli. (2015) Fasting Enhances Pyroglutamyl Peptidase II Activity in Tanycytes of the Mediobasal Hypothalamus of Male Adult Rats. *Endocrinology*. 156(7): 2713-23.
77. Segerson, T.P., J. Kauer, H.C. Wolfe, H. Mobtaker, P. Wu, I.M. Jackson and R.M. Lechan. (1987) Thyroid hormone regulates TRH biosynthesis in the paraventricular nucleus of the rat hypothalamus. *Science*. 238(4823): 78-80.
78. Sugrue, M.L., K.R. Vella, C. Morales, M.E. Lopez and A.N. Hollenberg. (2010) The thyrotropin-releasing hormone gene is regulated by thyroid hormone at the level of transcription in vivo. *Endocrinology*. 151(2): 793-801.
79. Nillni, E.A. and K.A. Sevarino. (1999) The biology of pro-thyrotropin-releasing hormone-derived peptides. *Endocr Rev*. 20(5): 599-648.
80. Abel, E.D., R.S. Ahima, M.E. Boers, J.K. Elmquist and F.E. Wondisford. (2001) Critical role for thyroid hormone receptor beta2 in the regulation of paraventricular thyrotropin-releasing hormone neurons. *J Clin Invest*. 107(8): 1017-23.
81. Fekete, C., B. Gereben, M. Doleschall, J.W. Harney, J.M. Dora, A.C. Bianco, S. Sarkar, Z. Liposits, W. Rand, C. Emerson, I. Kacs Kovics, P.R. Larsen and R.M. Lechan. (2004) Lipopolysaccharide induces type 2 iodothyronine deiodinase in the mediobasal hypothalamus: implications for the nonthyroidal illness syndrome. *Endocrinology*. 145(4): 1649-55.

82. Gereben, B., E.A. McAninch, M.O. Ribeiro and A.C. Bianco. (2015) Scope and limitations of iodothyronine deiodinases in hypothyroidism. *Nat Rev Endocrinol.* 11(11): 642-52.
83. Yamamura, T., S. Yasuo, K. Hirunagi, S. Ebihara and T. Yoshimura. (2006) T(3) implantation mimics photoperiodically reduced encasement of nerve terminals by glial processes in the median eminence of Japanese quail. *Cell Tissue Res.* 324(1): 175-9.
84. Prevot, V., D. Croix, S. Bouret, S. Dutoit, G. Tramu, G.B. Stefano and J.C. Beauvillain. (1999) Definitive evidence for the existence of morphological plasticity in the external zone of the median eminence during the rat estrous cycle: implication of neuro-glio-endothelial interactions in gonadotropin-releasing hormone release. *Neuroscience.* 94(3): 809-19.
85. Harris, M., C. Aschkenasi, C.F. Elias, A. Chandrankunnel, E.A. Nillni, C. Bjoorbaek, J.K. Elmquist, J.S. Flier and A.N. Hollenberg. (2001) Transcriptional regulation of the thyrotropin-releasing hormone gene by leptin and melanocortin signaling. *J Clin Invest.* 107(1): 111-20.
86. Diaz-Gallardo, M.Y., A. Cote-Velez, A. Carreon-Rodriguez, J.L. Charli and P. Joseph-Bravo. (2010) Phosphorylated cyclic-AMP-response element-binding protein and thyroid hormone receptor have independent response elements in the rat thyrotropin-releasing hormone promoter: an analysis in hypothalamic cells. *Neuroendocrinology.* 91(1): 64-76.
87. Fekete, C. and R.M. Lechan. (2007) Negative feedback regulation of hypophysiotropic thyrotropin-releasing hormone (TRH) synthesizing neurons: role of neuronal afferents and type 2 deiodinase. *Front Neuroendocrinol.* 28(2-3): 97-114.
88. Krashes, M.J., B.P. Shah, J.C. Madara, D.P. Olson, D.E. Storchlic, A.S. Garfield, L. Vong, H. Pei, M. Watabe-Uchida, N. Uchida, S.D. Liberles and B.B. Lowell. (2014) An excitatory paraventricular nucleus to AgRP neuron circuit that drives hunger. *Nature.* 507(7491): 238-42.
89. Wittmann, G., Z. Liposits, R.M. Lechan and C. Fekete. (2004) Medullary adrenergic neurons contribute to the cocaine- and amphetamine-regulated transcript-immunoreactive innervation of thyrotropin-releasing hormone synthesizing neurons in the hypothalamic paraventricular nucleus. *Brain Res.* 1006(1): 1-7.
90. Wittmann, G., Z. Liposits, R.M. Lechan and C. Fekete. (2002) Medullary adrenergic neurons contribute to the neuropeptide Y-ergic innervation of

- hypophysiotropic thyrotropin-releasing hormone-synthesizing neurons in the rat. *Neurosci Lett.* 324(1): 69-73.
91. Legradi, G., J. Hannibal and R.M. Lechan. (1997) Association between pituitary adenylate cyclase-activating polypeptide and thyrotropin-releasing hormone in the rat hypothalamus. *J Chem Neuroanat.* 13(4): 265-79.
  92. Rabeler, R., J. Mittag, L. Geffers, U. Ruther, M. Leitges, A.F. Parlow, T.J. Visser and K. Bauer. (2004) Generation of thyrotropin-releasing hormone receptor 1-deficient mice as an animal model of central hypothyroidism. *Mol Endocrinol.* 18(6): 1450-60.
  93. Sun, Y., X. Lu and M.C. Gershengorn. (2003) Thyrotropin-releasing hormone receptors -- similarities and differences. *J Mol Endocrinol.* 30(2): 87-97.
  94. Hashimoto, K., K. Zanger, A.N. Hollenberg, L.E. Cohen, S. Radovick and F.E. Wondisford. (2000) cAMP response element-binding protein-binding protein mediates thyrotropin-releasing hormone signaling on thyrotropin subunit genes. *J Biol Chem.* 275(43): 33365-72.
  95. Shibusawa, N., A.N. Hollenberg and F.E. Wondisford. (2003) Thyroid hormone receptor DNA binding is required for both positive and negative gene regulation. *J Biol Chem.* 278(2): 732-8.
  96. Szkudlinski, M.W., V. Fremont, C. Ronin and B.D. Weintraub. (2002) Thyroid-stimulating hormone and thyroid-stimulating hormone receptor structure-function relationships. *Physiol Rev.* 82(2): 473-502.
  97. Ikegami, K., X.H. Liao, Y. Hoshino, H. Ono, W. Ota, Y. Ito, T. Nishiwaki-Ohkawa, C. Sato, K. Kitajima, M. Iigo, Y. Shigeyoshi, M. Yamada, Y. Murata, S. Refetoff and T. Yoshimura. (2014) Tissue-specific posttranslational modification allows functional targeting of thyrotropin. *Cell Rep.* 9(3): 801-10.
  98. Schneider, M.J., S.N. Fiering, S.E. Pallud, A.F. Parlow, D.L. St Germain and V.A. Galton. (2001) Targeted disruption of the type 2 selenodeiodinase gene (DIO2) results in a phenotype of pituitary resistance to T4. *Mol Endocrinol.* 15(12): 2137-48.
  99. Fonseca, T.L., M. Correa-Medina, M.P. Campos, G. Wittmann, J.P. Werneck-de-Castro, R. Arrojo e Drigo, M. Mora-Garzon, C.B. Ueta, A. Caicedo, C. Fekete, B. Gereben, R.M. Lechan and A.C. Bianco. (2013) Coordination of hypothalamic and pituitary T3 production regulates TSH expression. *J Clin Invest.* 123(4): 1492-500.
  100. Vassart, G. and J.E. Dumont. (1992) The thyrotropin receptor and the regulation of thyrocyte function and growth. *Endocr Rev.* 13(3): 596-611.

101. Zaballos, M.A., B. Garcia and P. Santisteban. (2008) Gbetagamma dimers released in response to thyrotropin activate phosphoinositide 3-kinase and regulate gene expression in thyroid cells. *Mol Endocrinol.* 22(5): 1183-99.
102. Weiss, S.J., N.J. Philp, F.S. Ambesi-Impiombato and E.F. Grollman. (1984) Thyrotropin-stimulated iodide transport mediated by adenosine 3',5'-monophosphate and dependent on protein synthesis. *Endocrinology.* 114(4): 1099-107.
103. Christophe, D., C. Gerard, G. Juvenal, A. Bacolla, E. Teugels, C. Ledent, C. Christophe-Hobertus, J.E. Dumont and G. Vassart. (1989) Identification of a cAMP-responsive region in thyroglobulin gene promoter. *Mol Cell Endocrinol.* 64(1): 5-18.
104. Nagayama, Y., S. Yamashita, H. Hirayu, M. Izumi, T. Uga, N. Ishikawa, K. Ito and S. Nagataki. (1989) Regulation of thyroid peroxidase and thyroglobulin gene expression by thyrotropin in cultured human thyroid cells. *J Clin Endocrinol Metab.* 68(6): 1155-9.
105. Gnidehou, S., B. Caillou, M. Talbot, R. Ohayon, J. Kaniewski, M.S. Noel-Hudson, S. Morand, D. Agnangji, A. Sezan, F. Courtin, A. Virion and C. Dupuy. (2004) Iodotyrosine dehalogenase 1 (DEHAL1) is a transmembrane protein involved in the recycling of iodide close to the thyroglobulin iodination site. *FASEB J.* 18(13): 1574-6.
106. Buettner, C., J.W. Harney and P.R. Larsen. (2000) The role of selenocysteine 133 in catalysis by the human type 2 iodothyronine deiodinase. *Endocrinology.* 141(12): 4606-12.
107. Hoffmann, P.R. and M.J. Berry. (2005) Selenoprotein synthesis: a unique translational mechanism used by a diverse family of proteins. *Thyroid.* 15(8): 769-75.
108. Turanov, A.A., X.M. Xu, B.A. Carlson, M.H. Yoo, V.N. Gladyshev and D.L. Hatfield. (2011) Biosynthesis of selenocysteine, the 21st amino acid in the genetic code, and a novel pathway for cysteine biosynthesis. *Adv Nutr.* 2(2): 122-8.
109. Dumitrescu, A.M. and S. Refetoff. (2013) The syndromes of reduced sensitivity to thyroid hormone. *Biochim Biophys Acta.* 1830(7): 3987-4003.
110. Bianco, A.C., D. Salvatore, B. Gereben, M.J. Berry and P.R. Larsen. (2002) Biochemistry, cellular and molecular biology, and physiological roles of the iodothyronine selenodeiodinases. *Endocr Rev.* 23(1): 38-89.
111. Darras, V.M. and S.L. Van Herck. (2012) Iodothyronine deiodinase structure and function: from ascidians to humans. *J Endocrinol.* 215(2): 189-206.

112. Kuiper, G.G., F. Wassen, W. Klootwijk, H. Van Toor, E. Kaptein and T.J. Visser. (2003) Molecular basis for the substrate selectivity of cat type I iodothyronine deiodinase. *Endocrinology*. 144(12): 5411-21.
113. Foster, D.J., K.L. Thoday and G.J. Beckett. (2000) Thyroid hormone deiodination in the domestic cat. *J Mol Endocrinol*. 24(1): 119-26.
114. Schneider, M.J., S.N. Fiering, B. Thai, S.Y. Wu, E. St Germain, A.F. Parlow, D.L. St Germain and V.A. Galton. (2006) Targeted disruption of the type 1 selenodeiodinase gene (*Dio1*) results in marked changes in thyroid hormone economy in mice. *Endocrinology*. 147(1): 580-9.
115. Berry, M.J., A.L. Kates and P.R. Larsen. (1990) Thyroid hormone regulates type I deiodinase messenger RNA in rat liver. *Mol Endocrinol*. 4(5): 743-8.
116. Erickson, V.J., R.R. Cavalieri and L.L. Rosenberg. (1982) Thyroxine-5'-deiodinase of rat thyroid, but not that of liver, is dependent on thyrotropin. *Endocrinology*. 111(2): 434-40.
117. Koenig, R.J. (2005) Regulation of type 1 iodothyronine deiodinase in health and disease. *Thyroid*. 15(8): 835-40.
118. Gereben, B., C. Goncalves, J.W. Harney, P.R. Larsen and A.C. Bianco. (2000) Selective proteolysis of human type 2 deiodinase: a novel ubiquitin-proteasomal mediated mechanism for regulation of hormone activation. *Mol Endocrinol*. 14(11): 1697-708.
119. Bartha, T., S.W. Kim, D. Salvatore, B. Gereben, H.M. Tu, J.W. Harney, P. Rudas and P.R. Larsen. (2000) Characterization of the 5'-flanking and 5'-untranslated regions of the cyclic adenosine 3',5'-monophosphate-responsive human type 2 iodothyronine deiodinase gene. *Endocrinology*. 141(1): 229-37.
120. Ohba, K., T. Yoshioka and T. Muraki. (2001) Identification of two novel splicing variants of human type II iodothyronine deiodinase mRNA. *Mol Cell Endocrinol*. 172(1-2): 169-75.
121. Gereben, B., A. Kollar, J.W. Harney and P.R. Larsen. (2002) The mRNA structure has potent regulatory effects on type 2 iodothyronine deiodinase expression. *Mol Endocrinol*. 16(7): 1667-79.
122. Callebaut, I., C. Curcio-Morelli, J.P. Mornon, B. Gereben, C. Buettner, S. Huang, B. Castro, T.L. Fonseca, J.W. Harney, P.R. Larsen and A.C. Bianco. (2003) The iodothyronine selenodeiodinases are thioredoxin-fold family proteins containing a glycoside hydrolase clan GH-A-like structure. *J Biol Chem*. 278(38): 36887-96.

123. Salvatore, D., J.W. Harney and P.R. Larsen. (1999) Mutation of the Secys residue 266 in human type 2 selenodeiodinase alters <sup>75</sup>Se incorporation without affecting its biochemical properties. *Biochimie*. 81(5): 535-8.
124. Taylor, P.N., R. Peeters and C.M. Dayan. (2015) Genetic abnormalities in thyroid hormone deiodinases. *Curr Opin Endocrinol Diabetes Obes*.
125. Zevenbergen, C., W. Klootwijk, R.P. Peeters, M. Medici, Y.B. de Rijke, S.A. Huisman, H. Goeman, E. Boot, G. de Kuijper, K.H. de Waal, M.E. Meima, P.R. Larsen, T.J. Visser and W.E. Visser. (2014) Functional analysis of novel genetic variation in the thyroid hormone activating type 2 deiodinase. *J Clin Endocrinol Metab*. 99(11): E2429-36.
126. Canani, L.H., C. Capp, J.M. Dora, E.L. Meyer, M.S. Wagner, J.W. Harney, P.R. Larsen, J.L. Gross, A.C. Bianco and A.L. Maia. (2005) The type 2 deiodinase A/G (Thr92Ala) polymorphism is associated with decreased enzyme velocity and increased insulin resistance in patients with type 2 diabetes mellitus. *J Clin Endocrinol Metab*. 90(6): 3472-8.
127. Verloop, H., O.M. Dekkers, R.P. Peeters, J.W. Schoones and J.W. Smit. (2014) Genetics in endocrinology: genetic variation in deiodinases: a systematic review of potential clinical effects in humans. *Eur J Endocrinol*. 171(3): R123-35.
128. McAninch, E.A., S. Jo, N.Z. Preite, E. Farkas, P. Mohacsik, C. Fekete, P. Egri, B. Gereben, Y. Li, Y. Deng, M.E. Patti, C. Zevenbergen, R.P. Peeters, D.C. Mash and A.C. Bianco. (2015) Prevalent polymorphism in thyroid hormone-activating enzyme leaves a genetic fingerprint that underlies associated clinical syndromes. *J Clin Endocrinol Metab*. 100(3): 920-33.
129. Leiria, L.B., J.M. Dora, S.M. Wajner, A.A. Estivalet, D. Crispim and A.L. Maia. (2014) The rs225017 polymorphism in the 3'UTR of the human DIO2 gene is associated with increased insulin resistance. *PLoS One*. 9(8): e103960.
130. Bianco, A.C. and S. Casula. (2012) Thyroid hormone replacement therapy: three 'simple' questions, complex answers. *Eur Thyroid J*. 1(2): 88-98.
131. Berry, M.J., J.D. Kieffer, J.W. Harney and P.R. Larsen. (1991) Selenocysteine confers the biochemical properties characteristic of the type I iodothyronine deiodinase. *J Biol Chem*. 266(22): 14155-8.
132. Salvatore, D., H. Tu, J.W. Harney and P.R. Larsen. (1996) Type 2 iodothyronine deiodinase is highly expressed in human thyroid. *J Clin Invest*. 98(4): 962-8.
133. Dentice, M., A. Marsili, R. Ambrosio, O. Guardiola, A. Sibilio, J.H. Paik, G. Minchiotti, R.A. DePinho, G. Fenzi, P.R. Larsen and D. Salvatore. (2010) The

- FoxO3/type 2 deiodinase pathway is required for normal mouse myogenesis and muscle regeneration. *J Clin Invest.* 120(11): 4021-30.
134. Ma, S.F., L. Xie, M. Pino-Yanes, S. Sammani, M.S. Wade, E. Letsiou, J. Siegler, T. Wang, G. Infusino, R.A. Kittles, C. Flores, T. Zhou, B.S. Prabhakar, L. Moreno-Vinasco, J. Villar, J.R. Jacobson, S.M. Dudek and J.G. Garcia. (2011) Type 2 deiodinase and host responses of sepsis and acute lung injury. *Am J Respir Cell Mol Biol.* 45(6): 1203-11.
  135. Hernandez, A., S. Fiering, E. Martinez, V.A. Galton and D. St Germain. (2002) The gene locus encoding iodothyronine deiodinase type 3 (Dio3) is imprinted in the fetus and expresses antisense transcripts. *Endocrinology.* 143(11): 4483-6.
  136. Martinez, M.E., M. Charalambous, A. Saferali, S. Fiering, A.K. Naumova, D.S. Germain, A.C. Ferguson-Smith and A. Hernandez. (2014) Genomic Imprinting Variations in the Mouse Type 3 Deiodinase Gene Between Tissues and Brain Regions. *Mol Endocrinol:* me20141210.
  137. Hernandez, A., G.J. Lyon, M.J. Schneider and D.L. St Germain. (1999) Isolation and characterization of the mouse gene for the type 3 iodothyronine deiodinase. *Endocrinology.* 140(1): 124-30.
  138. Tu, H.M., G. Legradi, T. Bartha, D. Salvatore, R.M. Lechan and P.R. Larsen. (1999) Regional expression of the type 3 iodothyronine deiodinase messenger ribonucleic acid in the rat central nervous system and its regulation by thyroid hormone. *Endocrinology.* 140(2): 784-90.
  139. Hernandez, A., M.E. Martinez, W. Croteau and D.L. St Germain. (2004) Complex organization and structure of sense and antisense transcripts expressed from the DIO3 gene imprinted locus. *Genomics.* 83(3): 413-24.
  140. Baqui, M., D. Botero, B. Gereben, C. Curcio, J.W. Harney, D. Salvatore, K. Sorimachi, P.R. Larsen and A.C. Bianco. (2003) Human type 3 iodothyronine selenodeiodinase is located in the plasma membrane and undergoes rapid internalization to endosomes. *J Biol Chem.* 278(2): 1206-11.
  141. Kuiper, G.G., M.H. Kester, R.P. Peeters and T.J. Visser. (2005) Biochemical mechanisms of thyroid hormone deiodination. *Thyroid.* 15(8): 787-98.
  142. Schweizer, U., C. Schlicker, D. Braun, J. Kohrle and C. Steegborn. (2014) Crystal structure of mammalian selenocysteine-dependent iodothyronine deiodinase suggests a peroxiredoxin-like catalytic mechanism. *Proc Natl Acad Sci U S A.* 111(29): 10526-31.

143. Hernandez, A., M.E. Martinez, S. Fiering, V.A. Galton and D. St Germain. (2006) Type 3 deiodinase is critical for the maturation and function of the thyroid axis. *J Clin Invest.* 116(2): 476-84.
144. Galton, V.A., E. Martinez, A. Hernandez, E.A. St Germain, J.M. Bates and D.L. St Germain. (1999) Pregnant rat uterus expresses high levels of the type 3 iodothyronine deiodinase. *J Clin Invest.* 103(7): 979-87.
145. Bates, J.M., D.L. St Germain and V.A. Galton. (1999) Expression profiles of the three iodothyronine deiodinases, D1, D2, and D3, in the developing rat. *Endocrinology.* 140(2): 844-51.
146. Wasco, E.C., E. Martinez, K.S. Grant, E.A. St Germain, D.L. St Germain and V.A. Galton. (2003) Determinants of iodothyronine deiodinase activities in rodent uterus. *Endocrinology.* 144(10): 4253-61.
147. Simonides, W.S., M.A. Mulcahey, E.M. Redout, A. Muller, M.J. Zuidwijk, T.J. Visser, F.W. Wassen, A. Crescenzi, W.S. da-Silva, J. Harney, F.B. Engel, M.J. Obregon, P.R. Larsen, A.C. Bianco and S.A. Huang. (2008) Hypoxia-inducible factor induces local thyroid hormone inactivation during hypoxic-ischemic disease in rats. *J Clin Invest.* 118(3): 975-83.
148. Song, S., K. Adachi, M. Katsuyama, K. Sorimachi and T. Oka. (2000) Isolation and characterization of the 5'-upstream and untranslated regions of the mouse type II iodothyronine deiodinase gene. *Mol Cell Endocrinol.* 165(1-2): 189-98.
149. Gereben, B., D. Salvatore, J.W. Harney, H.M. Tu and P.R. Larsen. (2001) The human, but not rat, *dio2* gene is stimulated by thyroid transcription factor-1 (TTF-1). *Mol Endocrinol.* 15(1): 112-24.
150. Silva, J.E. and P.R. Larsen. (1983) Adrenergic activation of triiodothyronine production in brown adipose tissue. *Nature.* 305(5936): 712-3.
151. Chik, C.L., M.T. Wloka, D.M. Price and A.K. Ho. (2007) The role of repressor proteins in the adrenergic induction of type II iodothyronine deiodinase in rat pinealocytes. *Endocrinology.* 148(7): 3523-31.
152. Nakao, N., H. Ono, T. Yamamura, T. Anraku, T. Takagi, K. Higashi, S. Yasuo, Y. Katou, S. Kageyama, Y. Uno, T. Kasukawa, M. Iigo, P.J. Sharp, A. Iwasawa, Y. Suzuki, S. Sugano, T. Niimi, M. Mizutani, T. Namikawa, S. Ebihara, H.R. Ueda and T. Yoshimura. (2008) Thyrotrophin in the pars tuberalis triggers photoperiodic response. *Nature.* 452(7185): 317-22.
153. Yoshimura, T., S. Yasuo, M. Watanabe, M. Iigo, T. Yamamura, K. Hirunagi and S. Ebihara. (2003) Light-induced hormone conversion of T4 to T3 regulates photoperiodic response of gonads in birds. *Nature.* 426(6963): 178-81.

154. Ono, H., Y. Hoshino, S. Yasuo, M. Watanabe, Y. Nakane, A. Murai, S. Ebihara, H.W. Korf and T. Yoshimura. (2008) Involvement of thyrotropin in photoperiodic signal transduction in mice. *Proc Natl Acad Sci U S A.* 105(47): 18238-42.
155. Zeold, A., M. Doleschall, M.C. Haffner, L.P. Capelo, J. Menyhart, Z. Liposits, W.S. da Silva, A.C. Bianco, I. Kacs Kovics, C. Fekete and B. Gereben. (2006) Characterization of the nuclear factor-kappa B responsiveness of the human dio2 gene. *Endocrinology.* 147(9): 4419-29.
156. Boelen, A., J. Kwakkel, D.C. Thijssen-Timmer, A. Alkemade, E. Fliers and W.M. Wiersinga. (2004) Simultaneous changes in central and peripheral components of the hypothalamus-pituitary-thyroid axis in lipopolysaccharide-induced acute illness in mice. *J Endocrinol.* 182(2): 315-23.
157. de Vries, E.M., J. Kwakkel, L. Eggels, A. Kalsbeek, P. Barrett, E. Fliers and A. Boelen. (2014) NFkappaB signaling is essential for the lipopolysaccharide-induced increase of type 2 deiodinase in tanycytes. *Endocrinology.* 155(5): 2000-8.
158. Dentice, M., C. Morisco, M. Vitale, G. Rossi, G. Fenzi and D. Salvatore. (2003) The different cardiac expression of the type 2 iodothyronine deiodinase gene between human and rat is related to the differential response of the Dio2 genes to Nkx-2.5 and GATA-4 transcription factors. *Mol Endocrinol.* 17(8): 1508-21.
159. Burmeister, L.A., J. Pachucki and D.L. St Germain. (1997) Thyroid hormones inhibit type 2 iodothyronine deiodinase in the rat cerebral cortex by both pre- and posttranslational mechanisms. *Endocrinology.* 138(12): 5231-7.
160. Botero, D., B. Gereben, C. Goncalves, L.A. De Jesus, J.W. Harney and A.C. Bianco. (2002) Ubc6p and ubc7p are required for normal and substrate-induced endoplasmic reticulum-associated degradation of the human selenoprotein type 2 iodothyronine monodeiodinase. *Mol Endocrinol.* 16(9): 1999-2007.
161. Dentice, M., A. Bandyopadhyay, B. Gereben, I. Callebaut, M.A. Christoffolete, B.W. Kim, S. Nissim, J.P. Mornon, A.M. Zavacki, A. Zeold, L.P. Capelo, C. Curcio-Morelli, R. Ribeiro, J.W. Harney, C.J. Tabin and A.C. Bianco. (2005) The Hedgehog-inducible ubiquitin ligase subunit WSB-1 modulates thyroid hormone activation and PTHrP secretion in the developing growth plate. *Nat Cell Biol.* 7(7): 698-705.
162. Sagar, G.D., B. Gereben, I. Callebaut, J.P. Mornon, A. Zeold, W.S. da Silva, C. Luongo, M. Dentice, S.M. Tente, B.C. Freitas, J.W. Harney, A.M. Zavacki and A.C. Bianco. (2007) Ubiquitination-induced conformational change within the deiodinase dimer is a switch regulating enzyme activity. *Mol Cell Biol.* 27(13): 4774-83.

163. Curcio-Morelli, C., A.M. Zavacki, M. Christofollete, B. Gereben, B.C. de Freitas, J.W. Harney, Z. Li, G. Wu and A.C. Bianco. (2003) Deubiquitination of type 2 iodothyronine deiodinase by von Hippel-Lindau protein-interacting deubiquitinating enzymes regulates thyroid hormone activation. *J Clin Invest.* 112(2): 189-96.
164. Zavacki, A.M., E.D.R. Arrojo, B.C. Freitas, M. Chung, J.W. Harney, P. Egri, G. Wittmann, C. Fekete, B. Gereben and A.C. Bianco. (2009) The E3 ubiquitin ligase TEB4 mediates degradation of type 2 iodothyronine deiodinase. *Mol Cell Biol.* 29(19): 5339-47.
165. Werneck de Castro, J.P., T.L. Fonseca, C.B. Ueta, E.A. McAninch, S. Abdalla, G. Wittmann, R.M. Lechan, B. Gereben and A.C. Bianco. (2015) Differences in hypothalamic type 2 deiodinase ubiquitination explain localized sensitivity to thyroxine. *J Clin Invest.* 125(2): 769-81.
166. Hershko, A. and A. Ciechanover. (1998) The ubiquitin system. *Annu Rev Biochem.* 67: 425-79.
167. Dye, B.T. and B.A. Schulman. (2007) Structural mechanisms underlying posttranslational modification by ubiquitin-like proteins. *Annu Rev Biophys Biomol Struct.* 36: 131-50.
168. Hibbert, R.G., F. Mattioli and T.K. Sixma. (2009) Structural aspects of multi-domain RING/Ubox E3 ligases in DNA repair. *DNA Repair (Amst).* 8(4): 525-35.
169. Mahrouf, N., W.B. Redwine, L. Florens, S.K. Swanson, S. Martin-Brown, W.D. Bradford, K. Staehling-Hampton, M.P. Washburn, R.C. Conaway and J.W. Conaway. (2008) Characterization of Cullin-box sequences that direct recruitment of Cul2-Rbx1 and Cul5-Rbx2 modules to Elongin BC-based ubiquitin ligases. *J Biol Chem.* 283(12): 8005-13.
170. Tenno, T., K. Fujiwara, H. Tochio, K. Iwai, E.H. Morita, H. Hayashi, S. Murata, H. Hiroaki, M. Sato, K. Tanaka and M. Shirakawa. (2004) Structural basis for distinct roles of Lys63- and Lys48-linked polyubiquitin chains. *Genes Cells.* 9(10): 865-75.
171. Wang, Q., L. Li and Y. Ye. (2008) Inhibition of p97-dependent protein degradation by Eeyarestatin I. *J Biol Chem.* 283(12): 7445-54.
172. Melikova, M.S., K.A. Kondratov and E.S. Kornilova. (2006) Two different stages of epidermal growth factor (EGF) receptor endocytosis are sensitive to free ubiquitin depletion produced by proteasome inhibitor MG132. *Cell Biol Int.* 30(1): 31-43.

173. Grou, C.P., M.P. Pinto, A.V. Mendes, P. Domingues and J.E. Azevedo. (2015) The de novo synthesis of ubiquitin: identification of deubiquitinases acting on ubiquitin precursors. *Sci Rep.* 5: 12836.
174. Park, C.W. and K.Y. Ryu. (2014) Cellular ubiquitin pool dynamics and homeostasis. *BMB Rep.* 47(9): 475-82.
175. Komander, D., M.J. Clague and S. Urbe. (2009) Breaking the chains: structure and function of the deubiquitinases. *Nat Rev Mol Cell Biol.* 10(8): 550-63.
176. Bish, R.A. and M.P. Myers. (2007) Werner helicase-interacting protein 1 binds polyubiquitin via its zinc finger domain. *J Biol Chem.* 282(32): 23184-93.
177. Wu-Baer, F., K. Lagrazon, W. Yuan and R. Baer. (2003) The BRCA1/BARD1 heterodimer assembles polyubiquitin chains through an unconventional linkage involving lysine residue K6 of ubiquitin. *J Biol Chem.* 278(37): 34743-6.
178. Srivastava, D. and O. Chakrabarti. (2014) Mahogunin-mediated alpha-tubulin ubiquitination via noncanonical K6 linkage regulates microtubule stability and mitotic spindle orientation. *Cell Death Dis.* 5: e1064.
179. Qin, Y., M.T. Zhou, M.M. Hu, Y.H. Hu, J. Zhang, L. Guo, B. Zhong and H.B. Shu. (2014) RNF26 temporally regulates virus-triggered type I interferon induction by two distinct mechanisms. *PLoS Pathog.* 10(9): e1004358.
180. Jin, L., A. Williamson, S. Banerjee, I. Philipp and M. Rape. (2008) Mechanism of ubiquitin-chain formation by the human anaphase-promoting complex. *Cell.* 133(4): 653-65.
181. Kirkpatrick, D.S., N.A. Hathaway, J. Hanna, S. Elsassner, J. Rush, D. Finley, R.W. King and S.P. Gygi. (2006) Quantitative analysis of in vitro ubiquitinated cyclin B1 reveals complex chain topology. *Nat Cell Biol.* 8(7): 700-10.
182. Xu, P., D.M. Duong, N.T. Seyfried, D. Cheng, Y. Xie, J. Robert, J. Rush, M. Hochstrasser, D. Finley and J. Peng. (2009) Quantitative proteomics reveals the function of unconventional ubiquitin chains in proteasomal degradation. *Cell.* 137(1): 133-45.
183. Gatti, M., S. Pinato, A. Maiolica, F. Rocchio, M.G. Prato, R. Aebersold and L. Penengo. (2015) RNF168 Promotes Noncanonical K27 Ubiquitination to Signal DNA Damage. *Cell Rep.*
184. Geisler, S., K.M. Holmstrom, D. Skujat, F.C. Fiesel, O.C. Rothfuss, P.J. Kahle and W. Springer. (2010) PINK1/Parkin-mediated mitophagy is dependent on VDAC1 and p62/SQSTM1. *Nat Cell Biol.* 12(2): 119-31.

185. Fei, C., Z. Li, C. Li, Y. Chen, Z. Chen, X. He, L. Mao, X. Wang, R. Zeng and L. Li. (2013) Smurf1-mediated Lys29-linked nonproteolytic polyubiquitination of axin negatively regulates Wnt/beta-catenin signaling. *Mol Cell Biol.* 33(20): 4095-105.
186. Hay-Koren, A., M. Caspi, A. Zilberberg and R. Rosin-Arbesfeld. (2011) The EDD E3 ubiquitin ligase ubiquitinates and up-regulates beta-catenin. *Mol Biol Cell.* 22(3): 399-411.
187. Yuan, W.C., Y.R. Lee, S.Y. Lin, L.Y. Chang, Y.P. Tan, C.C. Hung, J.C. Kuo, C.H. Liu, M.Y. Lin, M. Xu, Z.J. Chen and R.H. Chen. (2014) K33-Linked Polyubiquitination of Coronin 7 by Cul3-KLHL20 Ubiquitin E3 Ligase Regulates Protein Trafficking. *Mol Cell.* 54(4): 586-600.
188. Huang, H., M.S. Jeon, L. Liao, C. Yang, C. Elly, J.R. Yates, 3rd and Y.C. Liu. (2010) K33-linked polyubiquitination of T cell receptor-zeta regulates proteolysis-independent T cell signaling. *Immunity.* 33(1): 60-70.
189. Pickart, C.M. (1997) Targeting of substrates to the 26S proteasome. *FASEB J.* 11(13): 1055-66.
190. Wang, C., L. Deng, M. Hong, G.R. Akkaraju, J. Inoue and Z.J. Chen. (2001) TAK1 is a ubiquitin-dependent kinase of MKK and IKK. *Nature.* 412(6844): 346-51.
191. Chen, Z.J. and L.J. Sun. (2009) Nonproteolytic functions of ubiquitin in cell signaling. *Mol Cell.* 33(3): 275-86.
192. Metcalf, J.L., P.S. Bradshaw, M. Komosa, S.N. Greer, M. Stephen Meyn and M. Ohh. (2014) K63-ubiquitylation of VHL by SOCS1 mediates DNA double-strand break repair. *Oncogene.* 33(8): 1055-65.
193. Mukhopadhyay, D. and H. Riezman. (2007) Proteasome-independent functions of ubiquitin in endocytosis and signaling. *Science.* 315(5809): 201-5.
194. Bochtler, M., C. Hartmann, H.K. Song, G.P. Bourenkov, H.D. Bartunik and R. Huber. (2000) The structures of HsIU and the ATP-dependent protease HsIU-HsIV. *Nature.* 403(6771): 800-5.
195. Matyskiela, M.E. and A. Martin. (2013) Design principles of a universal protein degradation machine. *J Mol Biol.* 425(2): 199-213.
196. Jung, T., B. Catalgol and T. Grune. (2009) The proteasomal system. *Mol Aspects Med.* 30(4): 191-296.
197. Spaapen, R.M. and J. Neefjes. (2012) Immuno-waste exposure and further management. *Nat Immunol.* 13(2): 109-11.

198. Kincaid, E.Z., J.W. Che, I. York, H. Escobar, E. Reyes-Vargas, J.C. Delgado, R.M. Welsh, M.L. Karow, A.J. Murphy, D.M. Valenzuela, G.D. Yancopoulos and K.L. Rock. (2012) Mice completely lacking immunoproteasomes show major changes in antigen presentation. *Nat Immunol.* 13(2): 129-35.
199. Kollar, A., Z. Kvartha-Papp, P. Egri and B. Gereben. (2015) Different Types of Luciferase Reporters Show Distinct Susceptibility to T3-Evoked Downregulation. *Thyroid.*
200. Yamamoto, K., H. Hashimoto, N. Hagihara, A. Nishino, T. Fujita, T. Matsuda and A. Baba. (1998) Cloning and characterization of the mouse pituitary adenylate cyclase-activating polypeptide (PACAP) gene. *Gene.* 211(1): 63-9.
201. Sasaki, H., Y. Nishizaki, C. Hui, M. Nakafuku and H. Kondoh. (1999) Regulation of Gli2 and Gli3 activities by an amino-terminal repression domain: implication of Gli2 and Gli3 as primary mediators of Shh signaling. *Development.* 126(17): 3915-24.
202. Dentice, M., C. Luongo, R. Ambrosio, A. Sibilio, A. Casillo, A. Iaccarino, G. Troncone, G. Fenzi, P.R. Larsen and D. Salvatore. (2012) beta-Catenin regulates deiodinase levels and thyroid hormone signaling in colon cancer cells. *Gastroenterology.* 143(4): 1037-47.
203. Zeold, A., L. Pormuller, M. Dentice, J.W. Harney, C. Curcio-Morelli, S.M. Tente, A.C. Bianco and B. Gereben. (2006) Metabolic instability of type 2 deiodinase is transferable to stable proteins independently of subcellular localization. *J Biol Chem.* 281(42): 31538-43.
204. Gossen, M. and H. Bujard. (1992) Tight control of gene expression in mammalian cells by tetracycline-responsive promoters. *Proc Natl Acad Sci U S A.* 89(12): 5547-51.
205. Vandesompele, J., K. De Preter, F. Pattyn, B. Poppe, N. Van Roy, A. De Paepe and F. Speleman. (2002) Accurate normalization of real-time quantitative RT-PCR data by geometric averaging of multiple internal control genes. *Genome Biol.* 3(7): RESEARCH0034.
206. Weiss, R.E., D. Forrest, J. Pohlenz, K. Cua, T. Curran and S. Refetoff. (1997) Thyrotropin regulation by thyroid hormone in thyroid hormone receptor beta-deficient mice. *Endocrinology.* 138(9): 3624-9.
207. Nagayama, Y., K.D. Kaufman, P. Seto and B. Rapoport. (1989) Molecular cloning, sequence and functional expression of the cDNA for the human thyrotropin receptor. *Biochem Biophys Res Commun.* 165(3): 1184-90.

208. Zelcer, N., L.J. Sharpe, A. Loregger, I. Kristiana, E.C. Cook, L. Phan, J. Stevenson and A.J. Brown. (2014) The E3 ubiquitin ligase MARCH6 degrades squalene monooxygenase and affects 3-hydroxy-3-methyl-glutaryl coenzyme A reductase and the cholesterol synthesis pathway. *Mol Cell Biol.* 34(7): 1262-70.
209. Loregger, A., E.C. Cook, J.K. Nelson, M. Moeton, L.J. Sharpe, S. Engberg, M. Karimova, G. Lambert, A.J. Brown and N. Zelcer. (2015) A MARCH6 and IDOL E3 Ubiquitin Ligase Circuit Uncouples Cholesterol Synthesis from Lipoprotein Uptake in Hepatocytes. *Mol Cell Biol.* 36(2): 285-94.
210. Park, S.E., J.M. Kim, O.H. Seok, H. Cho, B. Wadas, S.Y. Kim, A. Varshavsky and C.S. Hwang. (2015) Control of mammalian G protein signaling by N-terminal acetylation and the N-end rule pathway. *Science.* 347(6227): 1249-52.
211. Kim, B.W., A.M. Zavacki, C. Curcio-Morelli, M. Dentice, J.W. Harney, P.R. Larsen and A.C. Bianco. (2003) Endoplasmic reticulum-associated degradation of the human type 2 iodothyronine deiodinase (D2) is mediated via an association between mammalian UBC7 and the carboxyl region of D2. *Mol Endocrinol.* 17(12): 2603-12.
212. Suzuki, R., S. Arata, S. Nakajo, K. Ikenaka, S. Kikuyama and S. Shioda. (2003) Expression of the receptor for pituitary adenylate cyclase-activating polypeptide (PAC1-R) in reactive astrocytes. *Brain Res Mol Brain Res.* 115(1): 10-20.
213. Nakamachi, T., J. Farkas, N. Kagami, Y. Wada, M. Hori, D. Tsuchikawa, M. Tsuchida, A. Yoshikawa, N. Imai, T. Hosono, S. Arata and S. Shioda. (2013) Expression and distribution of pituitary adenylate cyclase-activating polypeptide receptor in reactive astrocytes induced by global brain ischemia in mice. *Acta Neurochir Suppl.* 118: 55-9.
214. Resch, J.M., B. Maunze, A.K. Gerhardt, S.K. Magnuson, K.A. Phillips and S. Choi. (2013) Intrahypothalamic pituitary adenylate cyclase-activating polypeptide regulates energy balance via site-specific actions on feeding and metabolism. *Am J Physiol Endocrinol Metab.* 305(12): E1452-63.
215. Hannibal, J., J.D. Mikkelsen, J. Fahrenkrug and P.J. Larsen. (1995) Pituitary adenylate cyclase-activating peptide gene expression in corticotropin-releasing factor-containing parvicellular neurons of the rat hypothalamic paraventricular nucleus is induced by colchicine, but not by adrenalectomy, acute osmotic, ether, or restraint stress. *Endocrinology.* 136(9): 4116-24.
216. Koves, K., A. Arimura, T.G. Gorcs and A. Somogyvari-Vigh. (1991) Comparative distribution of immunoreactive pituitary adenylate cyclase activating polypeptide and vasoactive intestinal polypeptide in rat forebrain. *Neuroendocrinology.* 54(2): 159-69.

217. Vaudry, D., B.J. Gonzalez, M. Basille, L. Yon, A. Fournier and H. Vaudry. (2000) Pituitary adenylate cyclase-activating polypeptide and its receptors: from structure to functions. *Pharmacol Rev.* 52(2): 269-324.
218. Delgado, M., C. Abad, C. Martinez, M.G. Juarranz, J. Leceta, D. Ganea and R.P. Gomariz. (2003) PACAP in immunity and inflammation. *Ann N Y Acad Sci.* 992: 141-57.
219. Lo, M.J., M.M. Kau, Y.H. Chen, S.C. Tsai, Y.C. Chiao, J.J. Chen, C. Liaw, C.C. Lu, B.P. Lee, S.C. Chen, V.S. Fang, L.T. Ho and P.S. Wang. (1998) Acute effects of thyroid hormones on the production of adrenal cAMP and corticosterone in male rats. *Am J Physiol.* 274(2 Pt 1): E238-45.
220. Mendez-Pertuz, M., A. Sanchez-Pacheco and A. Aranda. (2003) The thyroid hormone receptor antagonizes CREB-mediated transcription. *EMBO J.* 22(12): 3102-12.
221. Wu, Q., M.P. Boyle and R.D. Palmiter. (2009) Loss of GABAergic signaling by AgRP neurons to the parabrachial nucleus leads to starvation. *Cell.* 137(7): 1225-34.
222. Tokita, K., W.E. Armstrong, S.J. St John and J.D. Boughter, Jr. (2014) Activation of lateral hypothalamus-projecting parabrachial neurons by intraorally delivered gustatory stimuli. *Front Neural Circuits.* 8: 86.
223. Grafer, C.M., R. Thomas, L. Lambrakos, I. Montoya, S. White and L.M. Halvorson. (2009) GnRH stimulates expression of PACAP in the pituitary gonadotropes via both the PKA and PKC signaling systems. *Mol Endocrinol.* 23(7): 1022-32.
224. Halvorson, L.M. (2014) PACAP modulates GnRH signaling in gonadotropes. *Mol Cell Endocrinol.* 385(1-2): 45-55.
225. Propato-Mussafiri, R., S.M. Kanse, M.A. Ghatei and S.R. Bloom. (1992) Pituitary adenylate cyclase-activating polypeptide releases 7B2, adrenocorticotrophin, growth hormone and prolactin from the mouse and rat clonal pituitary cell lines AtT-20 and GH3. *J Endocrinol.* 132(1): 107-13.
226. de Jesus, L.A., S.D. Carvalho, M.O. Ribeiro, M. Schneider, S.W. Kim, J.W. Harney, P.R. Larsen and A.C. Bianco. (2001) The type 2 iodothyronine deiodinase is essential for adaptive thermogenesis in brown adipose tissue. *J Clin Invest.* 108(9): 1379-85.
227. Choi, D.W., Y.M. Seo, E.A. Kim, K.S. Sung, J.W. Ahn, S.J. Park, S.R. Lee and C.Y. Choi. (2008) Ubiquitination and degradation of homeodomain-interacting

- protein kinase 2 by WD40 repeat/SOCS box protein WSB-1. *J Biol Chem.* 283(8): 4682-9.
228. Newton, K. and V.M. Dixit. (2012) Signaling in innate immunity and inflammation. *Cold Spring Harb Perspect Biol.* 4(3).
  229. Lee, D.A., J.L. Bedont, T. Pak, H. Wang, J. Song, A. Miranda-Angulo, V. Takiar, V. Charubhumi, F. Balordi, H. Takebayashi, S. Aja, E. Ford, G. Fishell and S. Blackshaw. (2012) Tanycytes of the hypothalamic median eminence form a diet-responsive neurogenic niche. *Nat Neurosci.* 15(5): 700-2.
  230. Robins, S.C., I. Stewart, D.E. McNay, V. Taylor, C. Giachino, M. Goetz, J. Ninkovic, N. Briancon, E. Maratos-Flier, J.S. Flier, M.V. Kokoeva and M. Placzek. (2013) alpha-Tanycytes of the adult hypothalamic third ventricle include distinct populations of FGF-responsive neural progenitors. *Nat Commun.* 4: 2049.
  231. Chenn, A. and C.A. Walsh. (2002) Regulation of cerebral cortical size by control of cell cycle exit in neural precursors. *Science.* 297(5580): 365-9.
  232. Lie, D.C., S.A. Colamarino, H.J. Song, L. Desire, H. Mira, A. Consiglio, E.S. Lein, S. Jessberger, H. Lansford, A.R. Dearie and F.H. Gage. (2005) Wnt signalling regulates adult hippocampal neurogenesis. *Nature.* 437(7063): 1370-5.
  233. Kreft, S.G., M. Wang L Fau - Hochstrasser and M. Hochstrasser. Membrane topology of the yeast endoplasmic reticulum-localized ubiquitin ligase Doa10 and comparison with its human ortholog TEB4 (MARCH-VI). (0021-9258 (Print)).
  234. Hassink, G., M. Kikkert, S. van Voorden, S.J. Lee, R. Spaapen, T. van Laar, C.S. Coleman, E. Bartee, K. Fruh, V. Chau and E. Wiertz. (2005) TEB4 is a C4HC3 RING finger-containing ubiquitin ligase of the endoplasmic reticulum. *Biochem J.* 388(Pt 2): 647-55.
  235. Shumway, S.D. and S. Miyamoto. (2004) A mechanistic insight into a proteasome-independent constitutive inhibitor kappaBalpha (IkappaBalpha) degradation and nuclear factor kappaB (NF-kappaB) activation pathway in WEHI-231 B-cells. *Biochem J.* 380(Pt 1): 173-80.
  236. Chang, A.H., J. Jeong and R.L. Levine. (2011) Iron regulatory protein 2 turnover through a nonproteasomal pathway. *J Biol Chem.* 286(27): 23698-707.
  237. Grarup, N., M.K. Andersen, C.H. Andreasen, A. Albrechtsen, K. Borch-Johnsen, T. Jorgensen, J. Auwerx, O. Schmitz, T. Hansen and O. Pedersen. (2007) Studies of the common DIO2 Thr92Ala polymorphism and metabolic phenotypes in 7342 Danish white subjects. *J Clin Endocrinol Metab.* 92(1): 363-6.

238. Mentuccia, D., M.J. Thomas, G. Coppotelli, L.J. Reinhart, B.D. Mitchell, A.R. Shuldiner and F.S. Celi. (2005) The Thr92Ala deiodinase type 2 (DIO2) variant is not associated with type 2 diabetes or indices of insulin resistance in the old order of Amish. *Thyroid*. 15(11): 1223-7.
239. Dora, J.M., W.E. Machado, J. Rheinheimer, D. Crispim and A.L. Maia. (2010) Association of the type 2 deiodinase Thr92Ala polymorphism with type 2 diabetes: case-control study and meta-analysis. *Eur J Endocrinol*. 163(3): 427-34.
240. Panicker, V., P. Saravanan, B. Vaidya, J. Evans, A.T. Hattersley, T.M. Frayling and C.M. Dayan. (2009) Common variation in the DIO2 gene predicts baseline psychological well-being and response to combination thyroxine plus triiodothyronine therapy in hypothyroid patients. *J Clin Endocrinol Metab*. 94(5): 1623-9.
241. Madsen, L., M. Seeger, C.A. Semple and R. Hartmann-Petersen. (2009) New ATPase regulators--p97 goes to the PUB. *Int J Biochem Cell Biol*. 41(12): 2380-8.
242. Mao, Y., F. Senic-Matuglia, P.P. Di Fiore, S. Polo, M.E. Hodsdon and P. De Camilli. (2005) Deubiquitinating function of ataxin-3: insights from the solution structure of the Josephin domain. *Proc Natl Acad Sci U S A*. 102(36): 12700-5.
243. Fekete, C., B.C. Freitas, A. Zeold, G. Wittmann, A. Kadar, Z. Liposits, M.A. Christoffolete, P. Singru, R.M. Lechan, A.C. Bianco and B. Gereben. (2007) Expression patterns of WSB-1 and USP-33 underlie cell-specific posttranslational control of type 2 deiodinase in the rat brain. *Endocrinology*. 148(10): 4865-74.
244. Chan, N.C., W. den Besten, M.J. Sweredoski, S. Hess, R.J. Deshaies and D.C. Chan. (2014) Degradation of the deubiquitinating enzyme USP33 is mediated by p97 and the ubiquitin ligase HERC2. *J Biol Chem*. 289(28): 19789-98.

## 12. PUBLICATION LIST

### 12.1. LIST OF PUBLICATIONS THE THESIS IS BASED ON

1. Zavacki AM, Arrojo E Drigo R, Freitas BC, Chung M, Harney JW, **Egri P**, Wittmann G, Fekete C, Gereben B, Bianco AC. (2009) The E3 ubiquitin ligase TEB4 mediates degradation of type 2 iodothyronine deiodinase. *Mol Cell Biol* 29(19):5339-47.
2. Arrojo E Drigo R\*, **Egri P\***, Jo S, Gereben B, Bianco AC. (2013) The type II deiodinase is retrotranslocated to the cytoplasm and proteasomes via p97/Atx3 complex. *Mol Endocrinol* 27(12):2105-15.  
\*equally contributed
3. **Egri P** and Gereben B. (2014) Minimal requirements for ubiquitination-mediated regulation of thyroid hormone activation. *J Mol Endocrinol* 53(2):217-26.
4. **Egri P**, Fekete C, Dénes Á, Reglődi D, Hashimoto H, Fülöp BD and Gereben B. (2016) Pituitary adenylate cyclase-activating polypeptide (PACAP) regulates the hypothalamo-pituitary-thyroid (HPT) axis via type 2 deiodinase in male mice. *Endocrinology* Epub 2016 Apr 5:en20161043.

### 12.2. OTHER PUBLICATIONS

1. Christoffolete MA, Doleschall M, **Egri P**, Liposits Z, Zavacki AM, Bianco AC, Gereben B. (2010) Regulation of thyroid hormone activation via the liver X-receptor/retinoid X-receptor pathway. *J Endocrinol* 205(2):179-86.
2. Freitas BC, Gereben B, Castillo M, Kalló I, Zeöld A, **Egri P**, Liposits Z, Zavacki AM, Maciel RM, Jo S, Singru P, Sanchez E, Lechan RM, Bianco AC. (2010) Paracrine signaling by glial cell-derived triiodothyronine activates neuronal gene expression in the rodent brain and human cells. *J Clin Invest* 120(6):2206-17.
3. Schéle E, Fekete C, **Egri P**, Füzesi T, Palkovits M, Keller É, Liposits Z, Gereben B, Karlsson-Lindahl L, Shao R, Jansson JO. (2012) Interleukin-6 receptor  $\alpha$  is co-localised with melanin-concentrating hormone in human and mouse hypothalamus. *J Neuroendocrinol* 24(6):930-43.
4. McAninch EA, Jo S, Preite NZ, Farkas E, Mohácsik P, Fekete C, **Egri P**, Gereben B, Li Y, Deng Y, Patti ME, Zevenbergen C, Peeters RP, Mash DC, Bianco AC. (2015) Prevalent polymorphism in thyroid hormone-activating enzyme leaves a genetic fingerprint that underlies associated clinical syndromes. *J Clin Endocrinol Metab* 100(3):920-33.

5. Jansen SW, Akintola AA, Roelfsema F, van der Spoel E, Cobbaert CM, Ballieux BE, **Egri P**, Kvarta-Papp Z, Gereben B, Fekete C, Slagboom PE, van der Grond J, Demeneix BA, Pijl H, Westendorp RG, van Heemst D. (2015) Human longevity is characterised by high thyroid stimulating hormone secretion without altered energy metabolism. *Sci Rep.* 19;5:11525.
6. Kollár A, Kvarta-Papp Z, **Egri P**, Gereben B. (2016) Different Types of Luciferase Reporters Show Distinct Susceptibility to T3-Evoked Downregulation. *Thyroid* 26(1):179-82.

### 13. ACKNOWLEDGMENTS

I would like to thank my tutor, Dr. Balázs Gereben for his support and the opportunity to perform my doctoral work in his laboratory.

I am very grateful to Professor Zsolt Liposits, Head of the Laboratory of Endocrine Neurobiology.

Special thanks to Professor Dóra Reglődi for the support of collaborative work. I wish to thank to Dr. Seiji Shioda providing anti-PAC1R serum and Dr. Attila Patócs for his help with thyroid hormone measurements.

I am very thankful to László Barna, Dr. Márton Doleschall, Dr. Csaba Fekete, Dr. Miklós Sárvári and Dr. Anikó Zeöld for their valuable methodological and technical advices.

I wish to thank to Vivien Hársfalvi and Andrea Juhász for their excellent technical help.